Validation of the ITU-R P Series Radio Wave Propagation Model for Millimetre Wave V-Band (60GHz) Line-of-Sight Point-to-Point Short Distance Link

The University of Salford

School of Computing, Science & Engineering

ODUM ROWANI

Submitted in Partial Fulfilment of the Requirement for the Degree of

Doctor of Philosophy (PhD) in Computer Networks and

Telecommunications

November 2019

CONTENTS

List of Figures

List of Tables

Abbreviations

5G	**Fifth Generation of Mobile Communications**
ACM	**Adaptive Coding and Modulation**
ACMA	**Australian Communications and Media Authority**
ARQ	**Automatic Repeat Query**
ATCP	**Automatic Transmit Power Control**
BER	**Bit Error Rate**
bps	**Bytes per Second**
BPSK	**Differential phase shift keying**
BT	**British Telecommunications**
CEPT	**European Conference of Postal and Telecommunications**
C/n	**Carrier to Noise Ratio**
CMOS	**Complementary Metal-Oxide-Semiconductor**
dB	**Decibels**
dBi	**Decibels Relative to Isotropic**
DVD	**Digital Video Disc**
ECMA	**European Computer Manufacturers Association**
EHF	**Extremely High Frequency**
EIRP	**Equivalent Isotropic Radiated Power**
ETSI	**European Telecommunication Standards Institute**
Eb	**Energy per bit**
Es/No	**Energy per Modulation Symbol to Noise Spectral Density**
FEC	**Forward Error Correction**
FCC	**Federal Communications Commission**
FSO	**Free Space Optic**
FSPL	**Free Space Path Loss**
FWHM	**Full Width Half Maximum**
GaAs	**Gallium Arsenide**
GaN	**Gallium Nitride**
Gbps	**Gigabits per second**
GHz	**Gigahertz**
GigE/GbE	**Gigabits Ethernet**

HD	**High Definition**
HDMI	**High-Definition Multimedia Interface**
HDTV	**High Definition TV**
HD-SDI	**High-Definition Serial Digital Interface**
IC	**Integrated Circuits**
ICSMT	**Industry Canada Spectrum Management and Telecommunications**
IEEE	**Institute of Electrical Electronics Engineers**
InP	**Indium Phosphide**
IP	**Internet Protocol**
ISPs	**Internet Service Providers**
ITU	**International Telecommunications Union**
LAN	**Local Area Network**
LTE	**Long Term Evolution**
LOS	**Line of Sight**
MAC	**Media Access Control**
mbar	**Millibars**
MHz	**Mega Hertz**
MiWaveS	**Millimetre-Wave Small Cell Access and Backhauling**
MMW	**Millimetre Wave**
MIMO	**Multiple Input Multiple Output**
mm/hr	**Millimetre per Hour**
MPM	**Millimetre-wave Propagation Model**
MTPC	**Multiple Transmit Power Control**
NLOS	**Non-Line of Sight**
nLOS	**near Line of Sight**
O_2	**Oxygen**
ODU	**Outdoor Unit**
OFCOM	**Office of Communications**
PC	**Personal Computer**
PDH	**Plesiochronous Digital Hierarchy**
PoE+	**Power over Ethernet**
QAM	**Quadrature Amplitude Modulation**

QoE	Quality of Experience
QoS	Quality of Service
QPSK	Quadrature Phase Shift Keying
RPL	Residual Path Loss
RF	Radio Frequency
RLANs	Radio Local Area Networks
ROI	Return on Investment
STB	Set Top Box
SiGe	Silicon Germanium
SNR	Signal to Noise Ratio
S1/P1	Slot1/Port1
SMPTE	Society of Motion Picture & Television Engineers
STM-1, STM-4	Synchronous Transport Module level-1, 4 etc.
TCO	Total Cost of Ownership
Wi-Fi	Wireless Fidelity
WISPs	Wireless Internet Service Providers
WiMAX	Worldwide Interoperability for Microwave Access
WLAN	Wireless Local Area Network
XPIC	Cross Polar Interference Cancellation

Acknowledgements

I wish to express my profound gratitude to my supervisor Dr STEVE HILL and Prof. NIGEL LINGE for their guidance, support and advice during this research work. Dr STEVE and Prof NIGEL have provided me with fatherly advice, love and encouragement during my time at this University. I am privileged to learn from STEVE and NIGEL. My appreciation goes to Professor Andy Sutton from BT for his continuous support. Special thanks to Patrick Linnebank and NEC Europe for the equipment. Thank you Sabine Von-Hunerbein and Dave Townend for the support. A big thank you to all the people involved in this project.

I wish to say thank you to the entire ODUM's family and my friends who have in one way or the other contributed to the successful completion of my studies.

Special thanks to the school of Computing, Science and Engineering, University of Salford, Manchester for their support and encouragement throughout my studies.

Dedication

This project is dedicated to

UDI ODUM

This is for U

Thank U for everything.

MADIGHI

Спасибо

Abstract

Millimetre-wave communication systems have a very high potential to become mobile technology of choice for future 4G and 5G network architectures, which has led to many researchers carrying out studies regarding the effects of the atmosphere on radio propagation. There is growing interest in the use of millimetre-wave spectrum as a potential candidate for the provision of high capacity, short range, and backhaul solutions within future 5G ultra-dense network infrastructures. However, these frequencies are highly susceptible to atmospheric conditions and therefore a more detailed understanding of such behaviour is required. This research presents results from a one-year trial of a 60GHz short-range point-to-point link test between two building rooftops at the University of Salford, UK. In this research, a short-range 60GHz radio link measures power attenuations in millimetre-wave ranges with simultaneous measurement of weather parameters.

The results obtained confirm a strong correlation between path-loss and the impact of rain and atmospheric gases as predicted by the ITU path-loss model but also highlight a discrepancy. Further analysis revealed that rain duration appears to be having a detrimental effect on link performance. The experimental data from this trial is presented as evidence of the potential impact of rain at 60GHz.

The results also confirm the attenuation due to atmospheric gases (Oxygen absorption and water vapour) agree with the attenuation calculations from ITU recommendation for atmospheric gases. The results having considered impacts due to atmospheric gases and rain as per the ITU recommendations, there is a general residue of between 1dB and 2dB path loss throughout the month, interspersed by definite larger peaks ranging from 3dB to 9dB. The extra 3dB to 9dB of residual path loss, is unaccounted for by the ITU path-loss model. The analysis

and discussion of measurement results are presented. The results also confirm that the link throughput can be maintained except in the most extreme weather conditions.

1   INTRODUCTION

1.1   Introduction

The high system capacity and end-user data rates demanded of 5G will see the emergence of ultra-dense network infrastructures based on a small cell architecture (Baldemair et al., 2015; Ge et al., 2016). However, such architectures will bring new challenges in the provision of backhaul and create significant interest in the adoption of millimetre-wave solutions (30GHz to 300GHz).

The millimetre-wave spectrum offers high-speed wireless communications but suffers from attenuation loss caused by atmospheric and moisture absorption that greatly limits its effective range. The major impairments to radio signals at millimetre waves are oxygen absorption, water vapour absorption and rain. These impairments, especially rain and oxygen absorption, greatly influence the behaviour of radio signals and lead to errors in transmission. Attenuations due to rainfall and absorptions by atmospheric gases greatly affect signals above 10GHz frequency (Marcus & Pattan, 2005). These impairments from rain and atmospheric gases lead to a reduction in radio link Quality of Service (QoS). It is essential for engineers and service providers to model these effects to properly plan radio links at millimetre wave frequencies. This will enable the engineers to select the appropriate power level as well as modulation schemes to maximize link performance. Nevertheless, the 60GHz characteristics are precisely those required within ultra-dense networks. Short transmission paths coupled with high propagation losses limit the amount of interference between adjacent point-to-point backhaul links. Operating at extremely high frequencies also allows narrow beam technology, which in turn aids security. Additionally, operators need not pay for a license, because the frequencies within V-Band (57 to 66GHz) are often unlicensed or lightly licensed which makes

it an attractive proposition for network providers (European Telecommunications Standards Institute, 2015).

Consequently, the unlicensed 60GHz band is a potential candidate to provide backhaul in future 5G network architectures. However, there is a need to understand its reliability against varying weather conditions over an extended period. Hence, this thesis reports on and presents results from, a new project undertaken at the University of Salford, UK in partnership with both NEC, British Telecommunications BT and EE, to investigate atmospheric impacts on point-to-point links operating at 60GHz over a period of one year or more.

1.2   **Statement of the Problem**

Balancing the trade-offs between attenuation problems and bandwidth availability is one of the dominant issues faced by engineers working on millimetre waves. Although the ITU has made available propagation models that can predict attenuations and plan links at any radio frequencies, there are some unaccounted-for residual losses, especially in the 60GHz band.

In terms of rain attenuation, the ITU-R P.530 is the most widely used model for prediction but this model has a major drawback because it uses an extrapolation procedure. In addition, this model does not consider the duration of rainfall. The duration of rainfall is crucial to the amount of path loss observed at 60GHz. The other problem with this model is that the rainfall rate exceeded for 0.01% of the time is used for predicting the corresponding rain attenuation value for different regions with different rain characteristics. The mathematical calculations for the ITU-R P.530 use several approximations, which may be inaccurate with certain rain conditions. This method can only work accurately if rain can be described precisely along the path. Due to a lack of extensive meteorological data from all regions of the world, the models primarily rely on semi-empirical methods, which calculates the path length through the rain by assuming

the rain rate is constant. This assumption of constant rain rate leads to constant specific attenuation.

The ITU-R P.676 is widely used for the prediction and planning of links, but it takes into consideration attenuation issues that arise from oxygen absorption and water vapour absorptions only. Other factors that can affect radio signals are different combinations of humidity, temperature and pressure, wind speed, wind direction, as well as the rivers, trees, buildings shadow, roads etc. No recent work has taken into consideration the effect of rain duration at 60GHz.

For vendors to design radio equipment at 60GHz and operators to plan links, most factors that cause attenuations must be taken into consideration to maximise link availability and bandwidth usage. In addition, it is worth knowing how much of these parameters that cause signal attenuations can be compensated. Having experimental data can help answer these questions and help us build a better understanding of the 60GHz band as we move towards 5G. Our experimental data and result analysis will go a long way in answering most of these questions.

1.3 Research Motivation

With smaller cell sites set to play an integral role in meeting the capacity, latency and throughput requirements of future 4G and 5G networks, mobile backhaul is a growing challenge. To meet this challenge, it is important to test how these millimetre wave links can stand up to the rigorous weather conditions in an outdoor environment for a period of one-year.

This research is motivated towards presenting experimental data and analysing the effects of weather and the resilience of 60GHz in an urban area for more than one year. Specifically, this research will analyse using experimental data the effects and causes of path loss due to rain duration at rooftop levels.

1.4 Research Aim and Objectives

1.4.1 Aim

The aim of this research was to measure the performance of a 60GHz point-to-point data link against varying weather conditions for a period of 12 months using the (iPASOLINK SX 60GHz Packet Radio System) built by NEC, and to validate the ITU-R Path Loss Model for 60GHz millimetre-wave Band. The research was carried out at the University of Salford in partnership with NEC, EE and BT.

1.4.2 Objectives

The specific objectives of this research are to:

➢ Setup an experimental testbed to measure the performance of 60GHz link in Salford against different weather conditions over a long period.

➢ Study the propagation characteristics of 60GHz through the atmosphere in a line of sight link.

➢ Evaluate and analyse the atmospheric impact on the performance of a 60GHz point-to-point link for 5G infrastructures

➢ Verify and validate the operation of 60GHz V-band radio performance against rain rate and barometric pressure for more than one year.

➢ Gathering experimental propagation data in millimetre-wave (60GHz V-band) to give engineers additional information and tools in the design of communications systems for 5G infrastructure.

➢ Share experiment findings and data with equipment vendor NEC as well as BT

➢ Propose modification to the path loss model that will help networks operators and engineers plan links at 60GHz

1.5 Research Methodology

➢ *Review of existing related literature V-Band*

To understand a comprehensive study of millimetre wave at EHF such as V-Band, including advantages and disadvantages, resilience to weather impairments, licencing, availability etc. also to inquire in-depth knowledge of 5G networks. This thesis reviewed several previous types of research works on path loss models for millimetre waves. In addition, this thesis reviewed the ITU R recommendations for the design of terrestrial links to understand the constraints of the current path loss model widely used around the globe. The literature reviewed will provide the basis for this research work.

➢ *Research problem*

Based on the literature reviewed, there are some residual path loss still unaccounted for using the ITU R propagation model. The literature identified research problems related to path loss at 60GHz with specific attention to rain duration, (Oxygen absorptions) and the changes in barometric pressure. There is not much research on the measurement of barometric pressure and rain duration. In addition, there is limited knowledge of how rain duration affects radio signal attenuation at 60GHz in a real-world scenario. There are several papers on the attenuation due to water vapour and Oxygen absorption but there is no mention of the changes in barometric pressure, which causes spectral lines of Oxygen to broaden at 60GHz as well as rain duration.

➢ *Proposed Solution*

The experimental requirements and setup at the Salford University testbed studied the problem, the data has been collected, collated and analysed. The

results from data analysis show that rain duration causes residual path loss which is unaccounted for using the ITU models for 60GHz. This thesis proposes an update to the ITU path loss model to capture the effects of rain duration thereby eliminating the residual path loss that was unaccounted for using the popular ITU R model. This experimental data and results will help equipment vendors take rain duration into consideration when designing equipment at 60GHz. The research findings will also benefit network operators as they design links to maximise bandwidth usage at 60GHz.

➢ *Data collection*

Daily data collection of data is done for both the NEC radio and weather station from 2017 to 2019. The NEC equipment data is saved to a designated laptop. While weather data is collected from the University of Salford Manchester weather station archives monthly.

➢ *Data sorting, processing, interpretation and statistical analysis.*

Sorting and pre-processing of data from both the weather station and NEC Radio equipment. Both sets of data are converted to Microsoft Excel format and processed.

➢ *Comparing results to previous work and existing path loss models*

The results obtained from the experiments are analysed and compared with literature and a related experiment

➢ *Analysing the effects of rain duration changes in barometric pressure at 60GHz*

Further analysis to confirm the effect of rain duration and barometric pressure on the 60GHz radio link.

➢ *Writing PhD thesis.*

This marks the final part of the research study; it combines all parts and pieces of the research to form this thesis for submission. The theoretical analysis, the background studies, the review of the literature, the scientific methodology used to design this experiment, the process of data collection, presentation and analysis, the contributions of this research to the field of radio propagation at millimetre wave frequencies and conclusion are put together to complete the PhD thesis. There is a suggestion on future update and upgrade to this research work.

1.6   Contribution

This thesis is based on the 60GHz IPASOLINK-SX radio equipment supplied by NEC. This thesis addresses the experimental implementation to investigate climatic effects on long-term data transmission using high bandwidth 60GHz radio in a clear line of sight configuration.

This research involves the theoretical and experimental support for link path loss for rooftop levels at 60GHz radio frequencies.

➢ The key factors that affect radio signals at 60GHz communications are Attenuations due to Free Space Path Loss, Water Vapour Attenuations, Attenuations due to Oxygen Absorptions, and Attenuation due to Rain.

➢ The International Telecommunications Union ITU has built several models to enable engineers to plan links at different radio frequencies.

➢ Results are calculated according to Annex 1 of Recommendation ITU-R (International Telecommunication Union – Radio communication Sector)

➢ The ITU has recommended that the Total Attenuation at 60GHz are: Total path attenuation = Attenuation Free Space Path Loss + Attenuation caused by Oxygen + Attenuation due to Water vapour + Attenuation due to Rain.

Specifically, for 60GHz frequency, the major attenuation issues are because of Oxygen absorption and rain.

This thesis makes the following **CONTRIBUTION** in the field of millimetre wave propagations:

> - **There are about 3dB to 9dB of residual path-loss that occur during rain event, which is not accounted for in the ITU path loss model.**

> - **There is always a general residue of between 1dB and 2dB path-loss, which is consistent throughout the experiment and not captured by the ITU path loss model.**

> - **Total path attenuation = Attenuation Free Space Path Loss + Attenuation caused by Oxygen + Attenuation due to Water vapour + Attenuation due to Rain + Residual Path Loss.**

In conclusion, the residual path losses measured in this experiment shows a consistent residue of about 1dB to 2dB. This extra residual loss (RPL) of 1dB to 2dB happens all through the experiment irrespective of weather conditions. This extra 1dB to 2dB can be attributed to the experimental equipment, as well as mathematical approximations in the calculation for path loss using the ITU path loss models. However, the period with high residual path loss such as 3dB to 9dB cannot be attributed to the mathematical assumptions in the path loss formula. This high residue of between 3dB to 9dB occur during rain events and can be attributed to the complex dimension of rain such as rain drop density, drop shape, width of each rain drop-size, terminal velocity of rain drops, polarization etc. The Drop Size Distribution (DSD), which indicates the number of raindrops with given diameter D contained in 1 m^3 is an important factor in the way rain affects radio waves. During a heavy rainfall, the raindrops fall with a significant canting angle due to the strong winds which occurs together with such events. Therefore, rain attenuation is related to the rain rate and the scattering is related to the absorption mechanism of raindrops at the operating frequency.

There is the need to capture the effect of rain, not just as a function of precipitation intensity *R* but also as Drop Size Distribution, such as shape, diameter, and size of the raindrops, etc., to properly model path loss at 60GHz radio frequency.

Publications

The work detailed in this report has generated or contributed to the following outputs:

Conference Papers and Poster Presentations:

> Linge, N, Odum, R, Hill, S, von Hünerbein, S, Linnebank, P, Sutton, A and Townend, D. (2018). *Atmospheric impact on the performance of a 60GHz point-to-point link for 5G infrastructures*, in: 12th European Conference on Antennas and Propagation (EuCAP 2018), 9-13 April 2018, London, UK.

Linge, N, Odum, R, Hill, S, von Hünerbein, S, Linnebank, P, Sutton, A and Townend, D. (2018).
> *The impact of atmospheric pressure on the performance of 60GHz point to point links within 5G networks*, in Loughborough Antennas & Propagation Conference 2018 (LAPC2018), 12 -13 Nov 2018, Loughborough, UK.

Report Presentation to NEC, BT and EE:

> Linge, N, Odum, R, Hill, S, von Hünerbein, S, Linnebank, (2019). Measurement of atmospheric impacts on v-band (60GHz) point-to-point data link, in: *Report presented to NEC, EE and BT at the University of Salford. Reference number SGCN 0560, Version 1: on 13th March 2019.*

1.7 Thesis Organisation

The remainder of this THESIS is divided into various chapters.

Chapter 2 explains the BACKGROUND OF MILLIMETRE WAVES, citing its advantages and disadvantages, state of the art, the V-band also known as the 60GHz band, the propagation characteristics, as well as other high-data-rate technologies, etc.

Chapter 3 described the THEORY ANALYSIS of the various parameters such as path loss, rain attenuation, and gaseous attenuations with detailed mathematical formulae.

Chapter 4 explains the EXPERIMENTAL REQUIREMENTS such as the setup of the experiment, test procedure and the parameters to be measured.

Chapter 5 details the RESULTS and ANALYSIS. It presents a detailed description and analysis of the results including the system performance data for every single month. The monthly analysis is further broken down into daily analysis in periods of high residual path loss.

Chapter 6 describes the monthly residual path loss and a detailed explanation about the peaks in path loss as it relates to rain and barometric pressure

Chapter 7 concludes this thesis by detailing a summary of this research. It also outlines the CONTRIBUTIONS of this thesis to the field of millimetre wave propagations as well as conclusions and future works. The references and appendices are also added at the end of this thesis.

2   LITERATURE REVIEW

2.1   Background

This chapter explains the general background of the research; it starts with extensive detail review of millimetre wave frequencies and specifically V-Band (60GHz), it covers 5G architecture as well as the history, evolution, advantages, disadvantages, and characteristics of V-Band radio systems. Also covered are other high throughput data systems. This chapter also details the propagation problems of radio signals at extremely high frequencies.

2.2   Millimetre Waves

Millimetre waves (MMW) represent the Radio Frequency Signal spectrum in the range from 30GHz to 300GHz with wavelength (λ) from 1 to 10 mm (Rappaport, et al, 2014) which transmit radio signals (Adhikari, 2008). MMW is mostly grouped into E-Band (71-76GHz and 81-86GHz) and V-band (57-64GHz) that are available to the public for wireless communication (FCC, 1997). James Clerk Maxwell, Heinrich Rudolph Hertz and Guglielmo Marconi, Jagadish Chandra Bose in the 1890s among others started the foundational works of modern radio communications or mobile communications (Harris, 2005).

Due to the demand for high bandwidth and the increase in spectrum occupancy, the need to explore the advantages of millimetre wave band has become imperative (Vihriala, 2015). The availability of large amounts of bandwidth in the millimetre wave has led to the current interest in millimetre wave bands. (Sutton, 2016). Considering current regulatory regimes, V-band typically offers 7GHz bandwidth of contiguous spectrum (57-64GHz), expandable to 9GHz whenever the 64-66 GHz is open for fixed services (Coldrey, 2015). E-band provides twice 5GHz bandwidth, namely 10 GHz aggregate spectrum (71-76GHz and 81 - 86GHz) (Coldrey, 2015). Similarly, at frequency bands above 100GHz, there are blocks of plentiful spectrum that can offer extra bandwidth for future broadband wireless transmission

24

services. Because E-Band and V-Band are significantly different in nature, there are different deployment scenarios for each of them. They can be deployed in macro and small cell backhaul, front-haul applications, Line-of-Sight (LOS) and maybe near Line-of-Sight (nLOS) or Non-Line-of-Sight (NLOS) in the future (Coldrey, 2015).

The millimetre-wave band is the least studied when compared to other wavelengths available for wireless communications in the commercial area (Bowers, 2014). Millimetre wave frequencies are unsuitable for long-haul communications, unlike microwave because of the high level of atmospheric absorption. However, it is the perfect candidate for short-haul because of the large bandwidth available (Hakusui, 2001).

For decades, the military has been using 60GHz MMW spectrum for satellite-to-satellite communications (Bowers, 2014). But due to cost-effective pricing, the quick return on investment (ROI) and the availability of about 13GHz of spectrum in these bands, MMW bands have the potential to become a key player in point-to-point radio solution as we move closer to 5G (Wang et al, 2015).

2.3 Advantages of Millimetre Waves

2.3.1 Ideal Backhaul

The most common types of backhaul in telecommunications are fibre and microwave radio links. Millimetre-wave radio backhaul is becoming more widespread. Millimetre wave, such as 60GHz, is more reliable in terms of interferences and security and can be faster than fibre because of the reduced latency. Specifically, for the small cell system, which is a dominant technology for 5G, millimetre wave backhaul is the ideal candidate. This is because millimetre waves can use smaller base stations like picocells, microcells, and metro cells which will be required for high-density urban areas that will meet 5G requirements. Millimetre waves can

also be used for a wide variety of other applications such as short-range radar, as well as airport body scanners, etc.

2.3.2 Applications

Some of the key applications of millimetre waves are 5G small cell concept because of the high data rate available, also MMW has the potential to replace fibre optics as the dominant technology to connect mobile base stations. In terms of HD video applications, millimetre wave can also transmit UHD video to HDTV without using cables. It can also transmit high definition video sources, high definition game stations, and digital set-top boxes, etc. Millimetre waves also support the IEEE 802.ad WiGig technology. These millimetre waves can also be used as perfect candidates for satellite communications because at high altitudes of orbits MMW can carry large data rate and have very low latency. Another application of MMW is in the automobile industry where autonomous driving is a key realisation of 5G. Other applications are body scanners at airports and security points, high-frequency radar technologies, virtual reality VR applications, medical applications, etc.

2.3.3 Security

One of the major issues concerning wireless communication is security. Because of MMW low beam width, it can transmit signals with a low probability of the signal being detected. Also, because it cannot travel for long distances, this automatically reduces interferences from other radio sources nearby.

2.3.4 Small size

One of the major millimetre-waves advantages is the small size of the equipment. The high frequency associated with millimetre waves makes the possibility of very small ICs for building the small antenna required for small cell movement. This smallness in size makes it easy for

multiple elements phased arrays to be made on a substrate chip self-steering antenna and beamforming that greatly saves energy and power by focusing on the intended target only.

2.4 Disadvantages of Millimetre Waves

One of the key limitations of millimetre waves is the inability to travel long distances because of the short wavelengths. In addition, atmospheric absorptions by gases and rain are dominant in the millimetre wave frequencies. These absorptions and scattering of the signals reduce the transmission distance as well as creating errors on the link especially at 60GHz which is characterised by high oxygen absorption and rain attenuation issues. Another key obstacle with millimetre waves is that it requires line-of-sight because of its inability to penetrate physical objects such as walls, buildings, etc. Other objects like trees, birds, etc., will easily block the signals, resulting in weak signals and reduction in range.

2.5 Millimetre-Wave Propagation

This section explains how various weather phenomena affect radio wave propagation. Weather is one of the major parameters that affect radio signals at millimetre wave frequencies. Different weather parameters such as rain, temperature, humidity, wind, barometric pressure and any sort of water content in the atmosphere combine in several ways to cause attenuation of radio signals (Jones, 1998). These attenuations will prevent the radio signals from reaching their intended target (Alade, 2013). Because of the high complexity of weather and the frequent changes associated with them, there are no specific rules when it comes to predicting weather behaviour for radio signals at millimetre wave frequencies. For the 60GHz frequency range, free-space-path-loss, rain, gaseous absorptions, and barometric pressure changes are the major impairments to signals (Weiler, 2014). Diverse physical mechanisms affect radio wave propagation. The radio frequency determines the extent to which a mechanism affects signal

attenuation. Attenuation is a natural consequence of signal transmission over distance (Bandyopadhyay, 2009).

As attenuation increases, the more distorted and unintelligible the transmission becomes. The factors that typically cause signal attenuation are rain, free space path loss, atmospheric absorption (Oxygen and Water Vapour) etc. the factors and signal losses are shown in table 2.5.1

Table 2.5.1 Weather factors and signal loss

Effects	Signal Loss (dB/km)
Oxygen absorption at sea level	0.22
100% Humidity at 30°C	1.8
Heavy Fog of 50m visibility	3.2
Heavy Rain Shower at 25mm/hr	10.7

2.6   Millimetre-Wave Radio Frequency V-Band (60 GHz)

The V-Band is a term mostly used to describe radio frequencies within 57-66 GHz. The V-band spectrum is useful because it is the only unlicensed spectrum globally that provides about 9GHz of radio bandwidth (Sutton, 2016). This band offers multi-gigabit systems as well as cost-effective deployment and quick return on investment ROI. It also has much wider channel frequency which will be required to enable 5G mobile backhaul (Vihriala, 2015).

Because of the high data rates available at 60GHz frequencies, lots of equipment vendors have built radio systems in this frequency that can match the speed and capacity of the fibre. There is the additional interest outside point-to-point application of using this 60GHz band for radio local area networks RLANs. The 60 GHz band combines the potential for large information bandwidths with highly efficient frequency reuse due to the natural isolation offered by the

oxygen absorption band (Clark et al, 2006). Figure 2.3.4.1 details the benefit of oxygen absorption as it relates to high-frequency reuse, the colour blue represents the traditional working region while green represents the frequency reuse range of 60GHz.
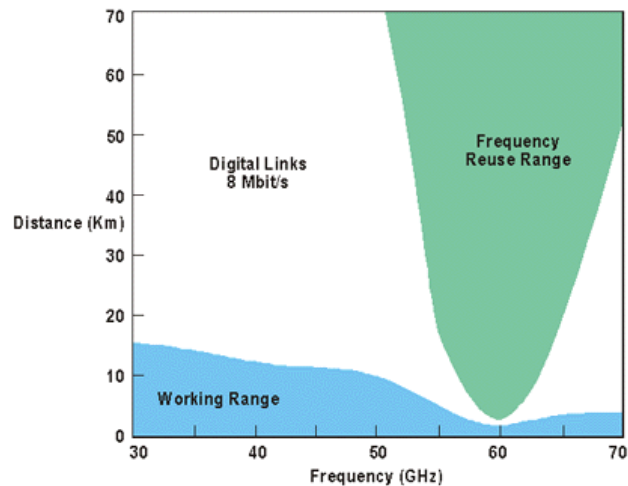
Figure 2.3.4.1 Frequency Reuse (FCC Bulletin 70A, 1997)

Also, because of the narrow beam associated with 60GHz, several similar 60GHz radio terminals can be deployed in an ultra-dense area with little or no interferences. This makes it possible to reuse the same spectrum enabling closely spaced adjacent systems. Applications that have been considered for these bands are short fixed links, high data rate links between buildings, broadband last-mile applications, aircraft links, indoor WLAN, telematics (e.g. vehicle-to-vehicle, advanced vehicle control, co-operative driving, a vehicle to roadside and safety systems), personal broadband applications, etc. An attraction of exploiting these high frequencies is not only the potential availability of high bandwidth systems but also the availability of small-scale technology to reduce size and weight of the equipment deployed.

2.6.1   Regulatory Background of 60GHz

In 2001 the US regulatory authority, the Federal Communications Commission FCC allocated 7 GHz of unlicensed spectrum for operation within 57-64 GHz. This amount of spectrum provides the available bandwidth to make full-duplex (GbE) Ethernet possible. This massive

spectrum allocation for 60GHz is superior to the small spectrum of about 0.5 GHz allocated between 2-6 GHz for Wi-Fi and other unlicensed applications. This allocation of enough spectrum at 60GHz makes multi-gigabit RF links possible for the first time. The (FCC regulation 15.255), has set the maximum EIRP to +40(dBi) dB relative to isotropic (equivalent to 10 Watts) for 60GHz devices.

The regulatory agency in Canada, known as Industry Canada Spectrum Management and Telecommunications (ICSMT), simply adopts the same standards set by the FEC for 60GHz.

In Australia, the Australian Communications and Media Authority (ACMA) has set the EIRP to a maximum of 51.7dBm or 150Watts. The ACMA also makes the frequency from 59 to 63 GHz unlicensed just like the FEC.

European Telecommunication Standards Institute (ETSI) and European Conference of Postal and Telecommunications (CEPT) adopted some general recommendations for the operation of devices in the 57-66 GHz band. The CEPT recommendation (ECC/REC/ (09)01) which was supplemented by (ETSI EN 302 217) harmonized standard, calls for a maximum EIRP power level of +55dBm but typically limits maximum conducted power to +10dBm and the minimum antenna gain to +30dBi. This approach does not allow the trade-off of Executive Summary 1 Regulatory Background antenna gain and power in the way that the more flexible U.S. standard does (ETSI EN 302 217).

Most of the guidelines in Europe are provided by the ETSI, with the goal to harmonize the standards for all members of ETSI. However, each country in the ETSI is free to stipulate regulations for its national aspects. Because each country operates with its rules and regulations in Europe, each country within Europe can have its standards which are usually a subset of the

ETSI standards. All equipment vendors take into considerations the different standards of each country when making equipment.

In the UK, the Office of Communications (OFCOM) approved the 57-64GHz to be unlicensed (OFCOM, 2009). The OFCOM also set the maximum EIRP to be at +55dBm, it set +10dBm as the maximum conducted power and a minimum antenna gain of +30dBi. The antenna gain simply follows the ETSI standards. (OFCOM, 2009).

2.6.2   Licence Exempt Vs Unlicensed

Many countries have assigned the 60GHz spectrum as "Licence Exempt" (Chambers, 2013). In terms of licensed exempt, operators may need to check with regulators if there is a need to pay a nominal registration fee. In these cases, depending on the country regulations, no fees are required for licensed exempt. Unlicensed simply means links can be deployed seamlessly without payments to the regulatory authorities. This makes V-Band very attractive because many other high bandwidth spectrums require hefty license fees to operate (Chambers, 2013).

2.6.3   Key Features of 60GHz V-Band

2.6.3.1   High Capacity and No Shortage of Spectrum

This frequency offers much higher capacity in terms of spectrum availability (Hettak et al, 2009). With the amount of spectrum allocated to 60GHz, GigE/GbE data rates can easily be achieved without using complex modulation schemes that are susceptible to interference and increase latency. (Maruhashi et al, 2000).

2.6.3.2   Interference Resistance and High Security

In the 60GHz band, there are some special propagation characteristics that prevent the signals from travelling to unintended targets thereby increasing security and interferences. These same properties of 60GHz enable the frequency to be reused in ultra-dense deployment scenarios.

The natural oxygen absorption that attenuates the 60 GHz signals makes it impossible to travel long distances. This, in turn, prevents the signals from travelling beyond their intended targets hence making it very secure. This makes 60GHz an excellent choice for communications that require high security such as military covert communications (Koh, 2004).

2.6.3.3 Narrow Beam Directional Antennas

Radios operating at 60 GHz frequency results in a more focused antenna with a narrower beam width for a fixed size antenna. These radios have high power and are very directional as opposed to the 2.4 or 5 GHz radios, which are more Omni-directional. Directivity is a measure of how well an antenna focuses its energy in an intended direction (Koh, 2004) the antenna beam divergence. Higher directivity focuses the beam and reduces wastage of energy and power (Koh, 2004).

2.6.3.4 Ultra-High Gain and Small Size Antennas

An increase in the frequency also increases the antenna gain of the system. Also, smaller more lightweight antennas are easier to handle and install. The antenna gain affects both the transmit power, as well as the received power at the same time. For example, three different antenna sizes with diameters of 15 cm (6 inches), 30 cm (12 inches), and 60 cm (24 inches), and at 60 GHz the antenna gain factors are 36dBi, 42dBi and 49dBi, respectively.

2.7 Alternative High Data Rate Technologies

Network operators and communications officers want more bandwidth for additional capacity, faster speed, security, smaller antenna, cost-efficiency and Return-On-Investment ROI. The V-Band wireless technology can meet these demands. A few technologies can act as alternatives to V-Band and support high data rate connectivity. This section provides a short overview of some of these technologies:

2.7.1 Fibre-Optic Cable

Fibre systems provide the largest bandwidth compared to other technologies currently deployed. Also, fibre optics systems allow for very high data rates to be transmitted over long distances compared to V-Band radio links that is very short. The major problems faced with fibre deployments are in securing rights-of-way (RoW) and digging trenches. Also implementing fibre in a city environment causes many problems in terms of disruption to roads and buildings etc. With all the bottlenecks and bureaucratic delays in securing the rights to lay fibre, V-Band may be more feasible to deploy than fibre in many situations.

2.7.2 Microwave Radio Solutions

The microwave bands are characterised by congestion due to the limited spectrum, and the licensed spectrum has narrow channels when compared to V-Band. Although Microwave radio links can support full-duplex 100Mbps Fast Ethernet or about 500Mbps per carrier in frequency ranges between 4-42GHz and can carry data over long distances compared to V-Band, it does not have the desired capacity and speed required for 5G technologies. In the microwave bands, the frequency channels available for licensing are typically 30 MHz or less but not more than 56 megahertz (MHz). The amount of spectrum available in microwave bands is limited compared to the huge bandwidth available at V-Band.

2.7.3 The E-Band Millimetre-Wave Radio Solutions

The E-band refers to the 70 GHz, 80 GHz and 90 GHz band allocations. Frequency allocations in the E-Band vary according to the regions or countries worldwide. Both E-Band and V-Band technologies have a huge amount of bandwidth, but the major difference is the licensing structure and attenuation issues. The E-Band system requires payment of a license fee for commercial use globally. Of all the high data rate technologies available, E-Band is the closest to V-Band as they are both millimetre waves

2.7.4 Free Space Optics (FSO) or Optical Wireless

Free space optic technology uses infrared laser technology for the transmission of information between locations (Bloom et al, 2003). The technology allows transmitting very high data rates of 1.5Gbps and beyond (Wells, 2009). FSO technology is generally a very secure transmission technology, is not very prone to interference due to the extremely narrow transmission beam characteristics and is also unlicensed worldwide just as V-Band.

FSO is generally affected by weather conditions such as fog and dust. Technically any weather that prevents direct visibility between two locations also affects the performance of FSO technologies. In most cases, it is difficult to predict FSO performance because of the irregularity of dust and fog occurrence.

2.8 **Summary**

The 60 GHz band is an excellent choice for wireless applications requiring gigabit-plus data rates especially considering the large bandwidth and high allowable transmit power. Out of all the currently available wireless technologies, millimetre wave brings the world closer to the promise of gigabit and multi-gigabit wireless speeds required for bandwidth-intensive applications. The cost and ease of bringing this technology to market are minimal since the spectrum is unlicensed and has no regulatory issues that would prevent worldwide approvals. Due to the unique characteristics of the 60GHz millimetre wave region and the raw bandwidth available, wireless communication at 60GHz offers a reliable "last mile" alternative to installing physical fibre. A variety of applications, including metropolitan area networks, campus networks, network backbones, network branch links, temporary emergency restoration and local access can use the 60GHz communications systems.

3 THEORY ANALYSIS

3.1 Theory Analysis

The unlicensed 60GHz band in the millimetre wave frequency offers larger system bandwidth and throughput. The 60 GHz band has the capacity to provide multi-gigabit wireless solutions, and high level of frequency reuse due to the narrow beam; it also has high security and is useful for a wide range of military operations. It is also easy to install and can be used in areas of disaster, etc. However, weather conditions affect the wavelength of 60GHz in different ways. These conditions include Free Space Path Loss FSPL, Precipitation (rain, fog, snow etc.) and absorption by atmospheric gases (oxygen and water vapour). All these conditions attenuate the transmitted signal thereby causing degradation in the signal quality. The following equations describe how each factor affects signal level.

3.2 Attenuation due to Free Space Path Loss (FSPL)

Free space path loss (FSPL) measured in decibels (dB), is the loss in signal strength of an electromagnetic wave that would result from a line of sight path through empty space such as air, with no external obstacles to cause diffraction of the signal or reflection.

This is the effect of a signal spreading out as it propagates from the transmitting antenna. This is typically the greatest portion of path loss, accounting for about 130dB or more of losses. The effects of FSPL are directly proportional to the square of the distance of the link, and the signal frequency, as either increase, so does path loss. Hence a signal at 60GHz undergoes an almost 36dB higher attenuation on the same way to the receiver compared to a signal at 1GHz (IWPC, 2014).

FSPL is the biggest obstacle to generating and receiving signals at the MMW frequencies. The same laws of physics govern millimetre waves and the rest of the radio spectrum and as such, they have limitations related to their wavelength. The shorter the wavelength, the shorter the transmission range for a given power (Frenzel, 2013). Some signal properties remain constant, regardless of factors such as antenna gain for receiver and transmitter, absorption, reflection and diffraction at transmission (Belcher, 1990). FSPL is a key parameter in RF calculations that helps to understand real-life radio propagation situations, especially for short-range radio systems. The signal strength reduces as the radio link distance increases as seen in figure 3.2.1
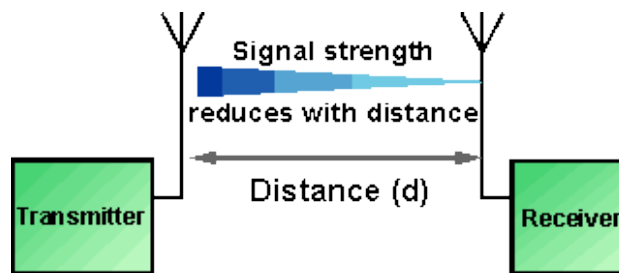
Figure 2.7.4.1 Free Space Path Loss

The general equation for FSPL is as follows:

$$L_{bf} = 20 \, \log\left(\frac{4\pi d}{\lambda}\right) \qquad \text{dB} \quad \text{(Eq. 1)}$$

Where:

L_{bf}:   free-space basic transmission loss (dB)

d: distance

λ: wavelength, and

d and λ are expressed in the same unit.

Equation (1) can also be written using the frequency instead of the wavelength.

$$L_{bf} = 32.4 \; + \; 20 \, \log f \; + \; 20 \, \log d \qquad \text{dB} \quad \text{(Eq. 2)}$$

Where:

f :   frequency (MHz)

d :   distance (km).

3.3   Attenuation due to Absorption by Atmospheric Gases

Attenuation by atmospheric gases at millimetre wave frequencies is mainly due to water vapour and oxygen absorption. Oxygen possesses a permanent magnetic moment and because of the interaction of this moment with the magnetic field of the wave, absorption of wave energy takes place (Barclay, 2003). Energy travelling through the atmosphere suffers from atmospheric attenuation, this absorption becomes critical for high frequencies in the millimetre wave range where the attenuation not only increases, but also becomes more dependent upon peculiar absorbing characteristics of H_2O and O_2. Oxygen absorption relates to the structure and characteristics of molecular oxygen (O_2) as found in the atmosphere.
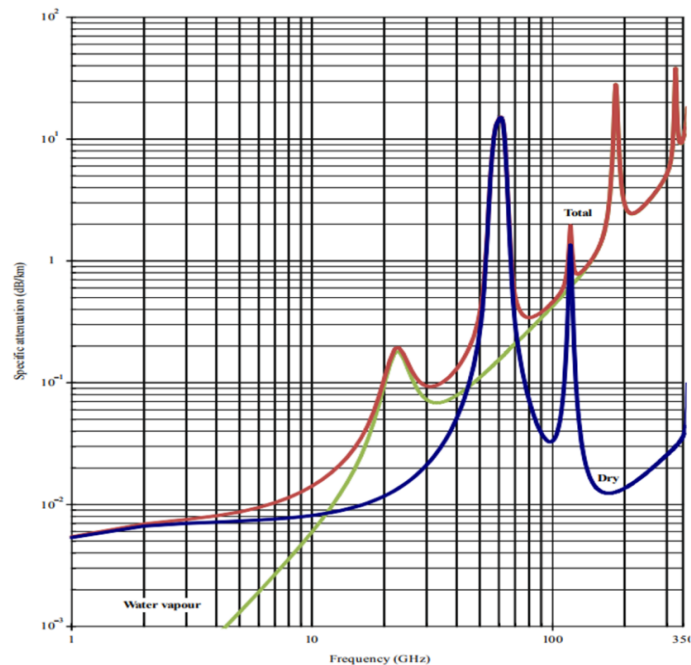
Figure 2.7.4.1 Total dry air and water-vapour zenith attenuation from sea level (pressure = 1013.25hPa; temperature = 15 °C; water vapour density = 8g/m3) Source: ITU-R Recommendation P.676

Normally an oxygen molecule is in a quantum ground state (a low-energy state.) The nature of the electrons around the two atoms (electron "spin") is such that the molecule has a permanent magnetic moment; it acts like a very tiny bar magnet. This magnetic characteristic of the molecule allows it to couple to the magnetic field of an electromagnetic wave (the RF signal.) When the oxygen molecule couples with the electromagnetic field the field energy absorbed by the oxygen molecule result in a reduction in RF signal strength. Oxygen absorption peaks at 60GHz frequency as shown in figure 3.3.1. Oxygen absorption is especially high at 60 GHz; it attenuates the signals, a property that is unique to the 60 GHz spectrum (Hakusui, 2001). While this limits the distances that 60 GHz links can cover, it also offers interference and security advantages when compared to other wireless technologies (Caetano & Li, 2005). Small beam sizes coupled with oxygen absorption makes these links immune to interference from other 60 GHz radios (Caetano & Li, 2005). Another link in the immediate vicinity will not interfere if its path is just slightly different from that of the first link, while oxygen absorption ensures that the signal does not extend far beyond the intended target, even with radio receivers along the exact same trajectory. These same two factors make the signal highly secure.
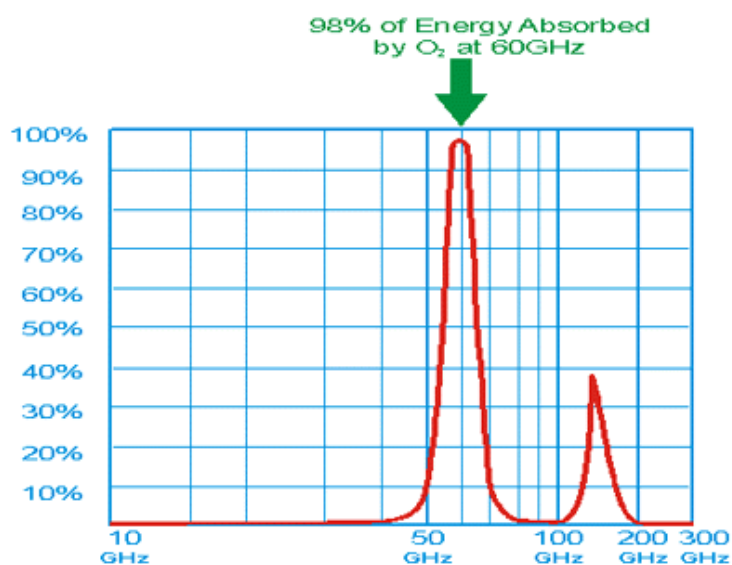
Figure 2.7.4.2 Dry Atmospheric Absorption per Kilometre (FCC Bulletin 70A, 1997)

At the millimetre wave frequency of 60GHz, the absorption is very high, with 98 percent of the transmitted energy absorbed by atmospheric oxygen as shown in Figure 3.3.2

The challenge for systems operating at 60GHz is that attenuation due to oxygen and water vapour peaks at this frequency. Extensive theoretical analysis of the characteristics of radio propagation at this frequency has been carried out. Based on ITU Recommendation P.1411 (ITU, 2017), which is mainly for Propagation data and prediction methods for the planning of short-range outdoor radio communication systems and radio local area networks in the frequency range 300 MHz to 100 GHz. It states that, with directional antennas, the path loss when the boresights of the antennas are aligned is given by equation 3.

$$L_{LoS} = L_0 + 10n \log_{10} \frac{d}{d_0} + L_{gas} + L_{rain} \quad \text{dB}$$

(Eq. 3) Source ITU Recommendation P.1411

Where n is the path loss exponent, d is the distance between Station 1 and Station 2 and L_0 is the path loss at the reference distance d_0. For a reference distance d_0 at 1 m, and assuming free-space propagation $L_0 = 20 \log 10 f - 28$ where f is in MHz L_{gas} are attenuation by atmospheric gases (Oxygen and water vapour) based on ITU Recommendation P.676 (ITU, 2016). Whereas L_{rain} is attenuation by rain which can be calculated from Recommendation ITU-R P.530.

Value of path loss exponent n is listed in Table 3.3.1

Table 3.3.1 Directional path loss coefficients for millimetre-wave propagation. Source ITU Recommendation P.1411.

Frequency (GHz)	Type of environment	Half power beam width (degree)		Path loss exponent
		Tx Ant	Rx Ant	N
28	Urban very high-rise	30	10	2.21
	Urban low-rise	30	10	2.06

60	Urban low rise	15.4	15.4	1.9

Specifically, for this experiment with link length of 210m, and frequency of 60GHz, n=1.9 based on table 1, this approximates to a path loss for the link of:

$$LLos = 111.68 + Lgas + Lrain \, dB \quad (Eq. 4)$$

Other factors that can contribute to link loss are themselves impacted by climatic effects. For example, any movement in the antennas caused by wind will inevitably result in lower received signal power due to the narrow beam width and so, grouping such factors as Lother, results in equation 5.

$$LLos = 111.68 + Lgas + Lrain + Lother \, dB \quad (Eq. 5)$$

Lother: unknown factors that cause signal attenuation

3.3.1 Attenuation due to Oxygen Absorption (Dry Air)

For dry air, the attenuation γ_o (dB/km) is given by:

$$\gamma_o = \frac{(f-60)(f-63)}{18}\gamma_o(57) - 1.66 r_p^2 r_t^{8.5}(f-57)(f-63) + \frac{(f-57)(f-60)}{18}\gamma_o \quad (Eq. 6)$$

Source: ITU-R Recommendation P.676

For 57 GHz $\leq$ f $\leq$ 63 GHz.

Where:

f: frequency (GHz)

r_p: = $p / 1013$

r_t: = $288 / (273 + t)$

p: pressure (hPa)

t: temperature (°C).

3.3.2 *Specific Attenuation Due to Water Vapour*

For water vapour, the attenuation γ_w (dB/km) is given by:

$$\gamma_w = \left[3.27 \times 10^{-2} \; r_t + 1.67 \times 10^{-3} \; \frac{\rho \; r_t^7}{r_p} + 7.7 \times 10^{-4} \; f^{0.5} + \frac{3.79}{\left(f - 22.235\right)^2 + 9.81 \; r_p^2 \; r_t} + \frac{11.73 \; r_t}{\left(f - 183.31\right)^2 + 11.85 \; r_p^2 \; r_t} + \frac{4.01 \; r_t}{\left(f - 325.153\right)^2 + 10.44 \; r_p^2 \; r_t} \right] f^2 \; \rho \; r_p \; r_t \times 10^{-4}$$

(Eq. 7) Source: ITU-R Recommendation P.676

For f ≤ 350 GHz

Where ρ is the water-vapour density (g/m^3).

The water-vapour partial pressure, *e*, at an altitude can be obtained from the water-vapour density, ρ, and the temperature, *T*, at that altitude using the expression:

$$e = \frac{\rho \; T}{216.7}$$ (Eq. 8)

Source: ITU-R Recommendation P.676

In most countries, water vapour density is not available for propagation interest due to lack of metrological data; hence, it can be calculated from concurrent measurements of temperature and relative humidity using:

Water vapour density ρ= (H5.752) × (T6×10(10-9.834× (T)))   (Eq. 9) (Feldhake, 1997)

Where H is the relative humidity in percent. T is the inverse temperature constant, given by:

T = 300 /T$_o$

T$_o$ is the temperature at the surface in Kelvin (Feldhake, 1997)

3.4   Attenuation due to Rain

The presence of raindrops can severely degrade the reliability and performance of communication links; radio waves above 10 GHz are subject to attenuation by rain (ITU-R P.837-5). Attenuation due to rain is a function of various parameters including elevation angle, carrier frequency, the height of earth station, latitude of earth station and rainfall rate. The primary parameters, however, are drop-size distribution and the number of drops that are present in the volume shared by the wave with the rain. It is important to note that, attenuation is determined not by how much rain has fallen but the rate at which it is falling (Green, 2004). Rain attenuation is generally proportional to the frequency and wavelength of the radio wave (Kishore, 2009).

Raindrops is more significant in attenuation than any other form of precipitation (Kestwal, et al, 2014). Attenuation caused by absorption, in which the raindrop, acting as a poor dielectric, absorbs power from the radio wave and dissipates the power by heat loss or by scattering (Jones, 1998). Raindrops cause greater attenuation by scattering than by absorption at frequencies above 100 megahertz. At frequencies above 6 gigahertz, attenuation by raindrop scatter is even greater (Simmons & Ace, 1995). The Crane and ITU are the two models generally used for rain modelling. Radio link planners generally prefer the ITU model. The ITU has developed a scheme to classify rain into regions. The ITU use alphabetical order to classify the expected rain statistics. The areas classified as "Region A," represents those that experience the least rainfall, while the highest rainfall rates are in "Region Q." Figure 3.4.1 shows a global ITU rain zone map and a listing of the rainfall rates in specific regions of the world.
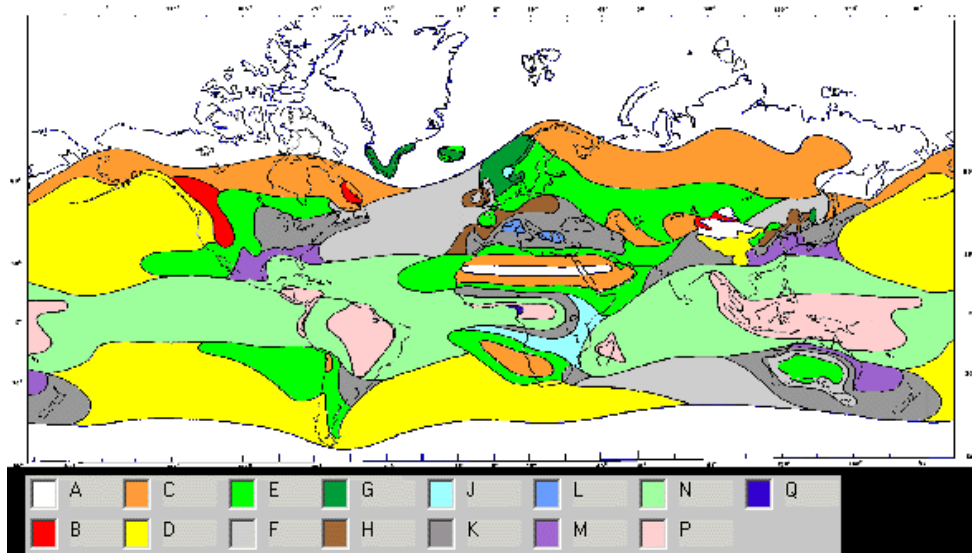
Figure 3.3.2.1 ITU rain zone classification of different regions around the world (top) and actual statistical rainfall rates as a function of the rain event duration

There are extensive studies of rainfall statistics to support MMW link deployments. The ITU has taken statistics of rain for several years and come up with a regional map of rainfall detailing the intensities of rain for each zone. It is recommended that the maximum link length is designed based on the rainfall zone of the specific location. Figure 3.4.2 shows a useful rain Fade map with the 0.01% annual rainfall exceedance rate:
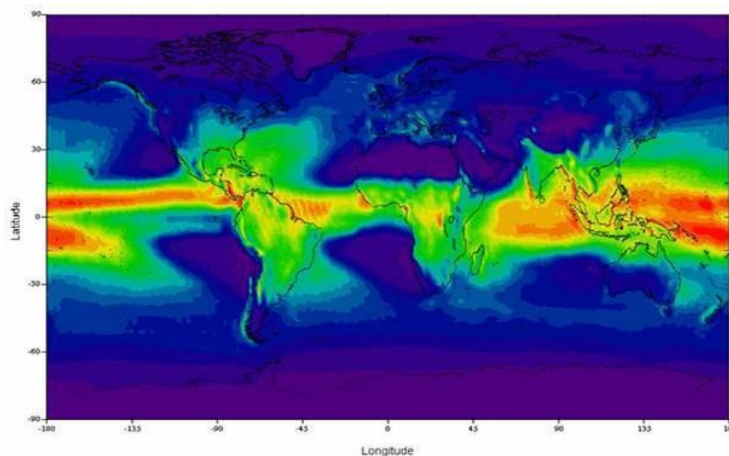
Figure 3.3.2.2 ITU-R Rain Fade Map – Global for 0.01% annual rainfall exceedance
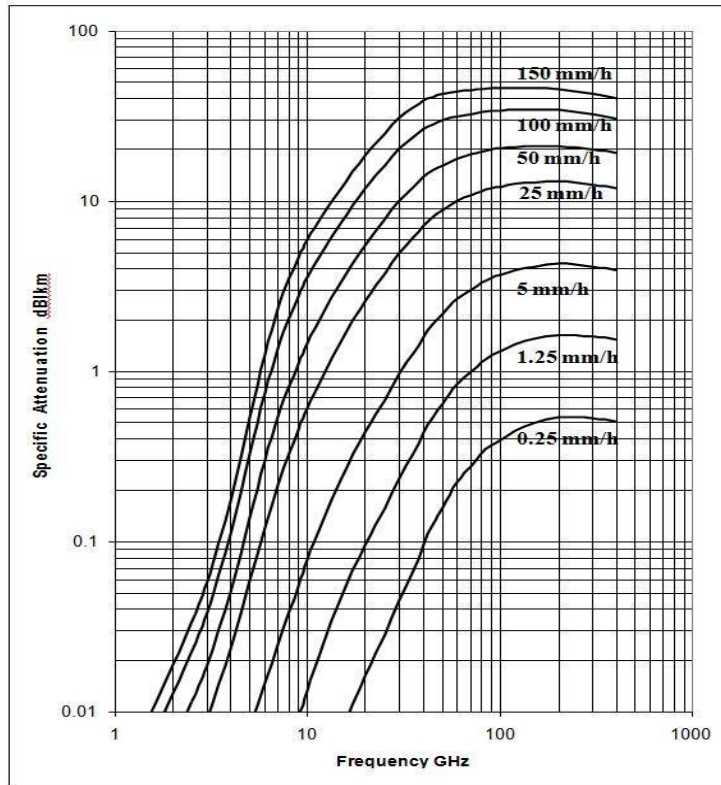
Figure 3.3.2.3 attenuation per unit length versus frequency and rain rate (Miya K, 1982)

Rainfall is a big impairment to a radio signal and causes major losses to signal transmission. The higher the rain intensity the higher the reduction in signal quality. Figure 3.4.3 shows how the intensity of precipitation can affect atmospheric attenuation. Millimetre-wave performance at 60GHz strongly dependents on rainfall. Even though rainfall affects the availability at 60GHz, links can still be successfully deployed in areas of high rainfall.

The specific attenuation γ_R (dB/km), express the loss in propagation loss due to rain attenuation. Based on (ITU-R P 838. 3), specific attenuation model, it is found that specific attenuation due to rain γ depends only on rainfall rate, measured in millimetres per hour.

Table 3.4.1 shows how the intensity of precipitation can affect atmospheric attenuation.

Rainfall Type	Rain Rate (mm/hr)	Signal Loss (dB/km)
Light shower	1	0.9
Normal Rain	4	2.6

Heavy Burst	25	10.7
Intense Storm	50	18.4

Based on ITU-R P.838-3 Specific attenuation model for rain used in prediction methods. The specific attenuation γ_R (dB/km) is obtained from the rain rate R (mm/h) using the power-law relationship:

$$\gamma_R = kR^\alpha \quad \text{(Eq. 10)} \quad \text{Source: ITU-R Recommendation P.838}$$

where the parameters k and α are functions of the signal wavelength and polarization. ITU-R Rec. P-838 gives a table with the k and α value, for Vertical and Horizontal polarizations, in the frequency range 1 to 400 GHz. Formulas are given for the case of any linear or circular polarization. The coefficients for α_V for vertical polarization and α_H for Horizontal are shown in table 3.4.2

Values for the coefficients k and α are determined as functions of frequency, f (GHz), in the range from 1 to 1 000 GHz, from the following equations, which have been developed from curve-fitting to power-law coefficients derived from scattering calculations:

$$\log_{10} k = \sum_{j=1}^{4} \left(a_j \exp\left[-\left(\frac{\log_{10} f - b_j}{c_j} \right)^2 \right] \right) + m_k \log_{10} f + c_k$$

$$\alpha = \sum_{j=1}^{5} \left(a_j \exp\left[-\left(\frac{\log_{10} f - b_j}{c_j} \right)^2 \right] \right) + m_\alpha \log_{10} f + c_\alpha$$

where:

f: frequency (GHz)

k: either k_H or k_V

α: either α_H or α_V.

Table 3.4.2 Constants for the coefficient α$_V$ for vertical polarization and α$_H$ for Horizontal. Source: ITU-R Recommendation P.838

Frequency (GHz)	k_H	α_H	k_V	α_V
57	0.8032	0.7771	0.7931	0.7587
58	0.8226	0.7731	0.8129	0.7552
59	0.8418	0.7693	0.8324	0.7518
60	0.8606	0.7656	0.8515	0.7486
61	0.8791	0.7621	0.8704	0.7454
62	0.8974	0.7586	0.8889	0.7424
63	0.9153	0.7552	0.9071	0.7395
64	0.9328	0.7520	0.9250	0.7366

Converting Rainfall into Rain Rate. In the prediction of atmospheric attenuation or rain attenuation, rainfall rate plays a significant role. Since most of the data from weather station collection centre is available in millimetre (mm.) and rain attenuation is related to rain rate in mm/hr rather than rainfall intensity in (mm), it is necessary to first convert the available rainfall data into rainfall rate. Converting rainfall data into exceeded rain rate expression required is as follows.

Divide the given data by observation time (10 min, 20 min… etc.) where R_D is the rain rate in mm/hr and L is the maximum rainfall in mm for time interval min

$R_D = L * (60/T)$

Where R_D is the rain rate in mm/hr and L is the maximum rainfall in mm for time interval Tmin

3.5 Influence of barometric pressure at 60GHz

Pressure distribution becomes more complicated near ground level, as it does not depend solely on airflow and wind velocity, but also surrounding buildings plants and geographic surface. The near ground pressure is changing randomly and does not follows a steady pattern. For this experiment, we decided to concentrate on the rate of change of pressure instead of the absolute pressure value.

The correlation of episodes of data loss with pressure changes to low-pressure situations, in which those losses cannot currently be accounted for, leads to possible speculation of other pressure-based effects that may be adding a contribution.

One of these is pressure broadening. It is well established that the familiar Oxygen absorption peak centred around 60GHz is in fact not a single entity but the combination of a series of pressure broadened lines that merge into the apparent continuum of the Oxygen absorption feature. Pressure broadening arises due to random collisions between atoms, which disturb internal interactions and shorten the lifetime of the absorbing state. For an isolated molecule, the typical natural lifetime of a state is about 1×10^{-8} s resulting in a 5×10^{-4} cm line width. However, as the pressure increases, the distance between molecules becomes shorter and they can no longer be considered in isolation. As the molecules get closer, their potential fields overlap and change the 'natural line width'; effectively collisions between molecules can shorten the lifetime, and hence the line width becomes larger.

Millimetre-wave radiation interaction with diatomic oxygen in the atmosphere is through magnetic dipole transitions between fine structure spin rotational levels of oxygen's electronic-vibrational ground state. These transitions give rise to a single spectral line at 118.75 GHz and a complex of lines between 50 GHz and 70 GHz. These complex lines are pressure broadened to form the familiar Oxygen absorption feature. Theoretical and experimental studies of the 60 GHz band have a long history, beginning in the first half of the twentieth century (Van Vleck,

1934 & 1945). General theoretical expressions for the shape of the bands formed by overlapping lines were developed (Baranger, 1958 & Fano, 1963). For the 60 GHz molecular-oxygen band, a model considering the mixing effect to first order in pressure was suggested in (Rosenkranz, 1975), and, later, a more thorough description with extension to second order was given in (Smith, 1981). A Millimetre-wave Propagation Model (MPM) by Liebe, et al (1992) is widely used to provide a computationally efficient; line-by-line model of atmospheric absorption is shown in Figure 3.5.1
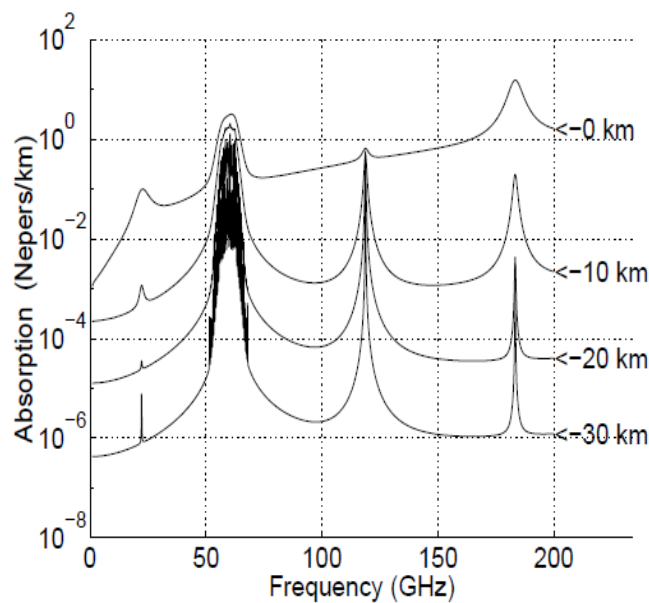
Figure 3.3.2.1 Modelled atmospheric absorption due to O2; H2O; and N2 at four altitudes in a standard tropical (M15) atmosphere. Absorption expressions are from the MPM model. (Liebe et al, 1992)

Although it is assumed that the effect of line separation should be minimal in normal barometric pressure variations at low altitudes, it may be worth revisiting this effect as a possible contribution to low-pressure path loss increases seen in the data.

3.6   Summary

Weather conditions have an adverse effect on all RF transmissions, especially in the millimetre wave region. As the distance of radio transmission increases, the fade margin needed to compensate for weather effects increases proportionately. Since radio links operating at 60GHz

transmit only over short distances, the compensation for weather effects is not as great as for systems transmitting one kilometre and beyond. At 60GHz, the extremely high atmospheric absorption level is due primarily to the molecular composition of the atmosphere. The atmosphere absorbs millimetre waves, restricting their range. Oxygen (O2) absorption is especially high at 60GHz, but it is not the only limiting factor of link range in the 60 GHz frequency. Rain and the presence of any form of water in the atmosphere causes signal attenuation, thereby reducing transmission distance. The presence of water and water vapour in the atmosphere makes it difficult to calculate the exact effect of weather on any radio wave propagation. Considering the factors: Total path attenuation = Attenuation Free Space Path Loss + Attenuation caused by Oxygen + Attenuation due to Water vapour + Attenuation due to Rain.

4   EXPERIMENTAL REQUIREMENTS

4.1   Experimental Requirements

This Chapter describes the experimental set up across the campus. It includes explanations of the various devices used in the setup as well as data acquisition and analysis. Based on the theories of atmospheric effects on radio link at 60GHz described in chapter three, the experimental setup is used to get tractable data. Figure 4.1.1 shows the block diagram of the link configuration and experimental setup.
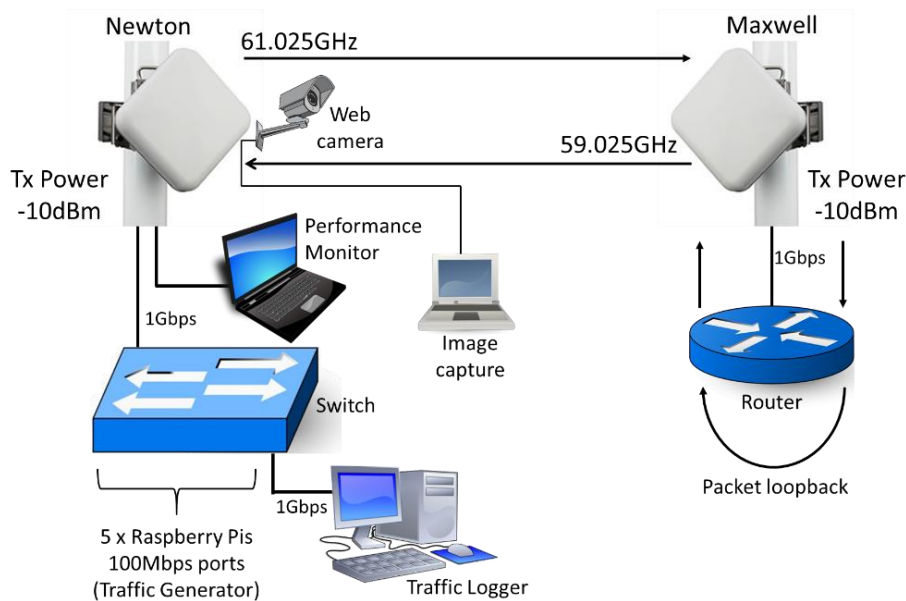
Figure 3.3.2.1 University of Salford 60GHz test-bed network system configuration

This link was successfully installed in August 2016 between Newton building with coordinates 53° 29' 7.6308" N 2° 16' 25.4388"W and Maxwell building rooftop with coordinates 53° 29' 7.2384" N2° 16' 15.4524"W with 210m as the link length. The height is 15meters near the ground. Initial data collection started in December 2017. During the first few months of data collection, the NEC performance monitoring PC recorded changes in QAM levels and power levels. It recorded these sets of data and stored them for a period of two days then they were replaced by the third day. This meant that if data was not retrieved after two days, we would

lose a day worth of data. The other problem was during the weekend because we had to download the data on Friday and Monday there was always missing data due to the equipment being able to store the data for only two days. The other problems faced initially was the issue of time. We had to manually delete redundant chunks of data which affected the time. These problems meant the data for the initial months from December 2016 to July 2017 were not used for this research. In July 2017 a new script was installed which automatically stored data daily in excel format. The new script automatically retrieved data such as transmit and receive power levels, bit error rate, temperature, sent and receive packets etc. Because of these changes to the method of retrieving the data, the month of August 2017 is therefore considered as the starting month for data processing. Therefore, the starting month for this research was August 2017.

Performance monitoring is accomplished through the extraction of management data on each radio. A traffic logger monitoring the volume of loop-backed data received at the Newton end of the link and a web camera maintains a regular visual image capture of the link to identify weather events such as fog, which is not as readily identifiable from the weather station data. This latter feature was included to identify weather events such as fog. From August 2017 automatic transmit power control (ATCP) was disabled and the modulation was fixed at 256QAM on both radio transceivers to enable us to monitor BER. The transmit power at both ends is reduced to a level on the edge of the opposite site receiver 10^{-10} BER value. The Newton end of the link is configured to transmit at 61.025GHz, whereas the Maxwell end transmits at 59.025GHz. The transmit power at both ends is set to -10dBm and the gain of each antenna is rated at 37dBi with a beam width of 1.7degrees. The traffic used for this experiment comprises of randomised IP/Ethernet packets generated from a cluster of five Raspberry Pi computers using Ostinato packet generator to deliver a continuous load of about 320Mbps at the Newton end of the link. The raspberry pi and ostinato traffic generator are configured such that there will be no packets drop at the switch port. Packets received at the Maxwell end are

then loop-backed to Newton via a Router as shown in Figure 4.1.1. The main function of the ostinato traffic generator is to saturate the link.

*Note: Because of the loopback at Maxwell building, data loss is recorded times two (X2). This means that if we lose two packets going into Maxwell end of the link, we will ultimately lose two packets going back to Newton which makes it 4 packets. This can be observed in the BER to received power.

4.2 Experimental test setup

In this section, the background of testing will include the explanations of devices used in this experiment and the setup procedures as well as an overview of data collected.

4.2.1 Background of testing

The devices used in this experiment are as follows:

➢ **Transmitter and Receiver***:* they are two identical units all in one antenna (iPASOLINK SX 60 GHz Packet Radio System) built by NEC. The iPASOLINK SX is a narrow band point-to-point system operating at radio frequency RF band 59-63GHz. It provides a LAN interface module and offers very high data rates up to 400Mbps (50 MHz bandwidth). The system is a single outdoor unit that provides simultaneous connection to native Ethernet. The system has a high modulation scheme from (QPSK to 256QAM) with an adaptive operation. It supports up to 2 ports of GbE, and up to 99.999% carrier-grade reliability, low power consumption, DC input apply PoE+ and synchronous Ethernet. The system has an antenna gain of 37dBi.

Figure 4.2.1.1 Newton End ODU (all outdoor) (59-63GHz) Radio

➤ **Weather Monitor***: this is a weather monitoring station located very close to the link. It provides sophisticated monitoring and logging of essential weather conditions such as WS-Air Temp °C, WS-Barometric Pressure mbar, WS-Rainfall mm, WS-Relative Humidity %, WS-Wind Direction Degrees, WS-Wind Speed m/s. it records these parameters with a 1-minute granularity.

➤ **Switch***: The Cisco switch with GbE port. It connects the raspberry pi computers and the traffic logger PC to the 60 GHz radio link.

➤ **Router***: The Cisco router with a GbE port is in the Maxwell end of the experiment. It acts as a loopback that routes traffic back from through the Maxwell antenna to the traffic logger.

➤ **Traffic Generator***: Raspberry Pi computers are used to generate nonstop IP packets traffic of up to 400 Mbps. The cluster of raspberry pi computers is connected to the Cisco switch. The OSTINATO traffic generator is used to generate the IP packets traffic.

➤ **Throughput logger PC***: this is a PC connected to the GbE port of the switch, all traffic sent from the raspberry pi is routed back from the router to the throughput logger. The throughput logger records both transmit and received packets.

> *Web Camera:* this is a QVIS MB-4MP-FW web camera. It is used to take pictures at an interval of 1 minute and send the pictures to a PC using FTP. It is strategically located pointing in the direction of the link facing Maxwell.

> *Performance Monitor PC:* this is another PC located in Newton building. It runs a Linux script that captures and records daily performance metrics of key parameters such as timestamp, Tx modulation, Rx modulation, Tx power, Rx power, BER, Temperature, Rx traffic [bps], Tx traffic [bps], Drop ratio [%]. The performance monitor is also used to access the equipment and download or monitor other crucial parameters such as event log, alarms etc. The performance monitor records daily data and saves it in Microsoft Excel .xlsx format.

4.3   The Test Procedure across the Campus

The University of Salford's main campus is set in 160 acres of parkland on the banks of the River Irwell, adjoining Peel Park, 1.5 miles west of Manchester City Centre. A test-bed network was created on this campus to provide a 60GHz point-to-point link operating over 210m and connecting the Newton and Maxwell buildings as shown in Figure 4.3. A weather station is conveniently located on the nearby Cockcroft building which records local climatic data at a one-minute interval and saves it in Microsoft Excel .xlsx format.

The experiment is performed using NEC IPASOLINK 60GHz packet radio system with an integrated flat antenna of 37dBi gain, 50MHz channel spacing and modulation from QPSK up to 256QAM. It is a line of sight connection between two building rooftops at the University of Salford, U.K, over a surface of roads, and grasses with a river and trees near the link as well as other buildings as illustrated in Figure 4.3.1 All data is collated in the transmitter site (Newton end) of the experiment using the performance monitoring PC.
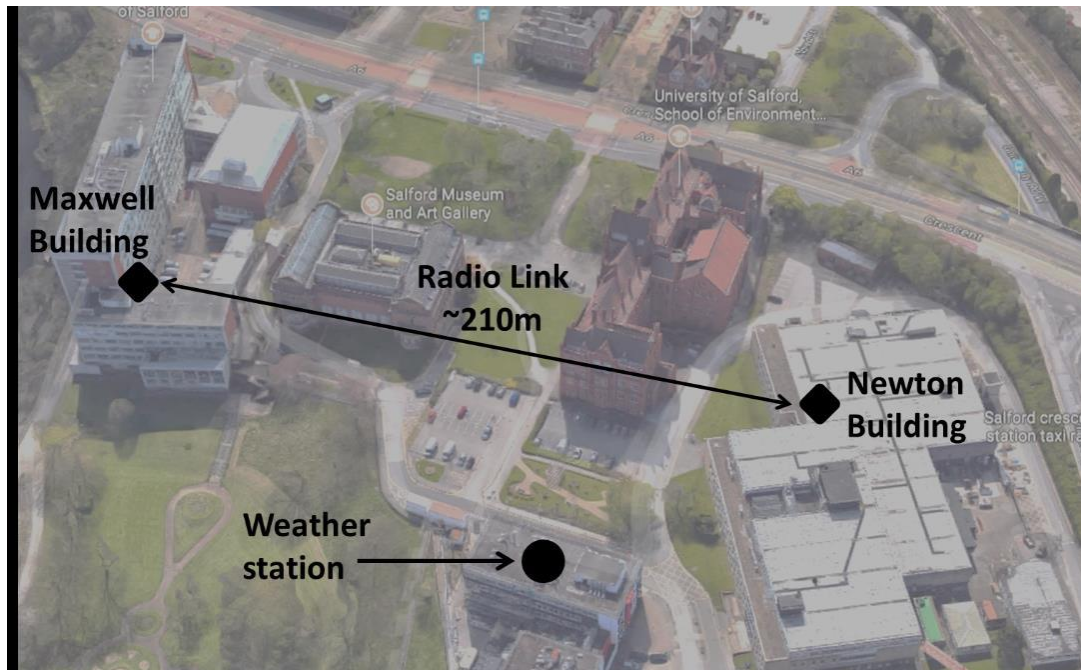
Figure 4.2.1.1 Aerial view of University of Salford 60GHz test-bed network location

The configuration of the radio units is summarised in Table 4.3.1.

Table 4.3.1 Configuration of the radio units

Link end	Frequency	Antenna gain	Beam Width	Polarisation
Newton	61.025GHz	37 dBi	1.7 degrees	Vertical
Maxwell	59.025GHz	37 dBi	1.7 degrees	Vertical

4.4 Data Collection

There are two groups of data collected, one is the data coming from the NEC equipment located in Newton building and the other is the weather data coming from the weather station. The data from the NEC IPASOLINK equipment includes a timestamp, Tx modulation, Rx modulation, Tx power, Rx power, BER, Temperature, Rx traffic [bps], Tx traffic [bps], Drop ratio [%]. The other group of data collected from the weather station at Crowcroft building includes WS-Air Temp °C, WS-Barometric Pressure mbar, WS-Rainfall mm, WS-Relative Humidity %, WS-Solar Output (kWm2), WS-Wind Direction Degrees, WS-Wind Speed m/s.

4.4.1   The Parameters Measured from the NEC IPASOLINK SX

Linux OS based script was created to capture data on a 24hour basis at intervals of 10 seconds. These parameters include:

- ➢ *NE Timestamp***:** time spent since 1970-01-01 in seconds.

- ➢ *NE name:* This represents the name of the location of the link. The two locations are Newton and Maxwell.

- ➢ *IP address:* This is the IP address of the two ends of the link. 172.17.253.252 is the IP address for Maxwell while 172.17.253.253 is the IP address for Newton.

- ➢ *Slot/Port:* This is the name and number of the slot and port used by the equipment. It is represented by (S1/P1) which means slot 1 and port 1.

- ➢ *TX Modulation:* this is the modulation of the transmitter. Adaptive coding and modulation automatically step down the signal to compensate for bad weather as opposed to link outage but with reduced throughput until the weather impairment disappears then the link automatically move back to higher throughput. This is extremely useful for industry as operators are looking at the availability and number of link outages. *Note the lower the modulation the more output power. The QAM modulation changes when certain events trigger the link. Weather events often trigger the link to change modulation from 256QAM to 4QAM or QSPK and vice versa. It is worth to note that specifically for this experiment and equipment the modulation changes are triggered by Forward Error Correction algorithm and Carrier to Noise Ratio. The Newton end of the link drops its modulation level based on feedback received from Maxwell end. Whenever modulation changes the gain also changes.

➢ **RX Modulation:** This is the Receiver modulation changes. This is like Tx modulation. The Rx of Maxwell depends on the Tx of Newton and vice versa. Adaptive Coding and Modulation (ACM), is the matching of the modulation, coding and other signal and protocol parameters to the conditions on the radio link such as path loss, interference, the sensitivity of the receiver, transmitter power margin, etc. (Hole & Oien, 2001). ACM operates in a dynamic mode where the link changes automatically adapt to current conditions of the link. Generally, a system using ACM and operating at a maximum capacity of 256QAM under clear sky conditions can automatically step down to 16QAM or less when it encounters rainfall or high interferences, by stepping down to lower modulations it keeps the link alive and reduces the capacity without losing connection thus increasing availability. The link automatically steps up back to 256QAM when the temporary interference or rain ceases to regain full capacity. Prior to the development of ACM, millimetre engineers had to plan a link based on a worst-case scenario. The benefits of using ACM include longer link lengths, smaller antennas sizes, and Higher Availability (link reliability). Figure 4.4.1 shows the ACM range for QAM modulation scheme.
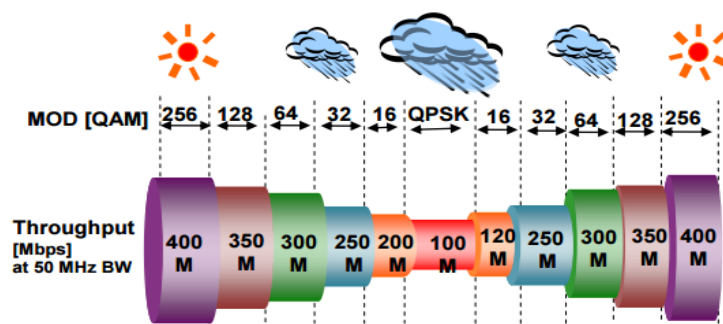
Figure 4.4.1.1 ACM range for channel spacing and modulation scheme of IPASOLINK SX.

➢ **TX Power:** Transmit Power. This can either be Automatic Transmit Power Control (ATPC), Multiple Transmit Power Control (MTPC) or Fixed Transmit Power (FTP).

Using MTPC Newton end can be set to transmit at -12 decibels while Maxwell transmits at -10 decibels. When this happens, it affects the modulation changes. For this experiment, all three scenarios of transmitting power were observed, but from August 2017, which is the starting date for data processing, the ATCP was disabled. The minimum Tx Power is -17dBm

➤ **RX Power:** Received Power or received signal. This is a very important parameter in radio frequency. The received power is measured in negatives of decibels. The RX power, TX power and the antenna gain were used to calculate the link path loss.

➤ **BER:** Bit Error Rate. When the QAM is not fixed but changing, the BER will be zero because of FEC. BER can only be when the QAM is fixed and the ATCP is disabled.

➤ **Temperature:** This is the operational temperature of the equipment. It ranges from -33°C to +50°C.

➤ **Traffic timestamp:** The traffic was collected asynchronously, so the time was following the main timestamp but there was a few seconds' difference always. For precise analysis, this timestamp can be used for correction if necessary.

➤ **RX Traffic [bps]:** This is the traffic received in bits per second, also known as throughput.

➤ **TX Traffic [bps]:** This is the original traffic transmitted from the Ostinato traffic generator. It transmits at roughly 320 megabits per second. *Note all the traffic is generated at Newton end of the link, the Maxwell end has a router that acts as a loopback.

➤ **Drop ratio [%]:** This is simply the percentage of packets dropped.

4.4.2 *The Parameters Measured from the Local Weather Station*

The local weather report is represented by the parameters measured using the University of Salford Weather station. To understand the effects of these weather parameters on the transmission quality of a 60GHz radio link it is important to understand the meaning of these parameters.

> **Temperature**: the temperature is represented by (WS-Air Temp °C) measured in degree Celsius. This is the measure of the average kinetic energy of the particles in an object. Alternatively, it is the measure of how hot or cold an object is. The SI unit Centigrade (or Celsius). Specifically, for this experiment, the atmosphere is near the ground, so temperature is variable with altitudes, winds and the surrounding environment. Hence temperature variation is directly associated with the surrounding environmental changes.

> **Relative Humidity**: represented by WS-Relative Humidity percentage. This is the ratio of the actual amount of water vapour present in the air to the amount of water vapour the air can hold at a given temperature. Relative humidity is measured in percentage. The amount of invisible water vapour present in the air is called humidity.

> Relative humidity depends strongly on the water vapour content of the air and the capacity to hold water vapour. The following ways can change relative humidity:

>> Relative humidity increases when moisture is added to the atmosphere by the process of evaporation.

>> Relative humidity will also increase when the temperature drops.

> Relative humidity is an important factor in the climate because it determines the rate and amount of evaporation.

➤ **Rainfall:** represented by (WS-Rainfall mm). Rainfall is precipitation in the form of drops of water or the amount of rain that falls in a place during a period. Depending on the method used to measure rainfall, stated in terms of the depth of water that has fallen into a rain gauge. Rainfall rate, measured in mm/hour, is a big factor in the signal loss, the harder it rains, the signal strength drops accordingly. Signal Propagation loss is also directly proportional to distance if the distance between transmitter and receiver is doubled, the loss in decibels is also doubled. Millimetre wave performance strongly dependents on rainfall and affects the Availability. However, successful links can even be set up in areas of occasional heavy downpours.

➤ **WS-Barometric Pressure mbar:** Barometric pressure also known as atmospheric pressure is the force per unit area exerted against a surface by the weight of the air above that surface. It is the weight of air pressing down on the land, ocean and earth surface. Barometric pressure measurements are affected by air density, which changes based on altitude and temperature. Specifically, for this experiment, the barometric pressure is in millibars (mbar). Normal pressure at sea level is 1013.3 millibars. The pressure at a given point increases as the weight of air above it also increases and vice versa. When low-pressure weather systems move in over a certain area, not only is pressure in the atmosphere shifted, it causes the barometric pressure reading to drop. A low-pressure system indicates that low-pressure air rises and begins to cool. Once the low-pressure air has risen into the atmosphere, it creates condensation and causes it to rain, snow or create ice. Specifically, for this experiment, the weather station measures Total Barometric Pressure, which is a combination of dry air pressure and water vapour pressure. The water vapour partial pressure is obtained from water vapour density.

➤ **Wind Speed:** represented by WS-Wind Speed m/s is when there is a difference between pressures, the airflow will move from high pressure to lower pressure. Wind speed is

simply the speed of airflow moving or the movement of air through Earth's atmosphere caused by the uneven heating by the sun.

➢ **WS-Wind Direction Degrees:** This simply means the direction the wind originated from, measured in degrees. The values represented are 0°/360° means north, 90° means east, 180° means south, and 270° means west. For example, if the wind direction is 45 degrees, the winds are coming out of the northeast and blowing towards the southwest. This would be called a north-easterly wind. For this experiment, wind direction has so far been measured from 0 to 354 degrees.

➢ **WS-Solar Output (kW/m2):** This is the amount of useful energy absorbed or used from the sun radiant power. It is measured in kW per meter square **kW/m2**

4.5 Key Measurement Parameters

This section describes key performance parameters to be considered in the transmission of a signal through a wireless medium, such performance parameters includes Tx power, Rx power, BER, Modulation, FEC, Throughput, Temperature, Drop ratio [%], etc.

Every data communications system consists of a transmitter, receiver, and other forms of communications channels. The transmitter produces the data stream and the clock controls the timing of each bit generated. Data communications systems use a more efficient method to divide data into a fixed length, blocks or frames (Simon et al, 1995). The throughput is the number of information bits on a frame divided by the total time taken to transmit and receive the frame (Duck et al, 1996). The major factors that cause received throughput, bits, packets etc. to be less than transmitted rate is as follows:

➢ **Frame Overhead**: Content of a frame that contains the information bits, header and trailer. The header also contains the control bits while the trailer contains the error-

checking bits. This automatically reduces the bits in any frame due to the addition of additional information bits.

➢ **Propagation delays**: this is the time taken for any frame to propagate from one end of the link to the other. This is a major factor in wireless radio links.

➢ **Processing time**: this is the time spent by the receiving station to process the data received

➢ **Acknowledgements**: using ARQ in the transmission, the time spent for the acknowledgement to reach the sender of the information causes reduction in throughput because the information frames are longer than the acknowledgements.

➢ **Retransmission**: retransmission of some frames due to error automatically reduces the throughput.

4.6   Summary

This experiment on millimetre wave propagation took place at the University of Salford, in Manchester, UK. The objective of this testbed in Salford was to test the resilience of 60GHz radio in a line of sight against varying weather conditions for a period of more than one year. This experiment gathered propagation data in the 60GHz band and after proper analysis proposes modifications to the ITU propagation model used for millimetre wave frequencies. The set-up of this experiment is described in detail in section 4.1 and section 4.2. The test site provides a unique opportunity with the proximity of the weather monitoring station adjacent to the link, this proximity gives the captures the exact influence and weather condition as it directly affects the link. The process of data collection is described in section 4.4.

In conclusion, an evaluation of the Atmospheric impact on the performance of a 60GHz point-to-point link for 5G infrastructures was carried out. We needed a long period of weather measurement to describe the seasonal variation and effects of different weather parameters

because of the non-uniform nature of these parameters. For successful prediction, the weather data must be taken for a period of one year or more. For this research, the raw weather data is retrieved from the University of Salford weather station. The data were collected from August 2017 until July 2018. The data has been processed using statistical means to find the correlation between various weather conditions and signal attenuation. The results of these measurements were used to compare with the results from existing ITU-P path loss models. Then after proper analysis, a correction factor has suggested a modification to the existing ITU path loss models. The key performance criterions have been discussed in the previous section. These parameters include BER, Transmit Power, Received Power, QAM Modulation Changes, and Throughput. Analysing the performance parameters applied in this experiment, BER, Signal Losses are key attributes to describe the quality of transmission in the system. Specifically, for this research, BER, Transmit Power, Received Power also known as signal losses were measured along with weather data such as rainfall rate, temperature, relative humidity, pressure etc. to determine the effects of these weather parameters on the transmission quality of the 60GHz radio link.

5 SYSTEM PERFORMANCE DATA AND RESULTS

5.1 Results and Analysis

This section presents and analyses the results from the experiment. The results presented here are from August 2017 until July 2018. The results are analysed monthly, each month is separately analysed to determine the behaviour of the link in terms of performance. The key parameters in this analysis are link path loss, rainfall and barometric pressure. All processing is done in Microsoft Excel. Both weather data coming from the weather station and propagation data from the radio equipment combined to form a single spreadsheet with synchronised time.

5.2 System Performance data

The results are collected through the experiments operated in the campus. This chapter mainly deals with the weather data and transmission data analysis. The weather parameters are investigated using cluster methods. Rain rate and barometric pressure are found to be the crucial parameters that cause attenuation and affects data transmission quality. Rain rate and changes in barometric pressure will be the main procedure to investigate how residual path loss can be modelled. The data is analysed on a monthly interval starting from August 2017. Each month, the graphs for barometric pressure, rain rate and link path loss will be compared. After comparing these three key components, we will then analyse the daily data in cases where residual path loss is more than 3dB to ascertain the exact cause of the high residual path loss. For each day of very high residual path loss, we will check the effects of rain and changes in barometric pressure. The colour configurations are such that blue represents barometric pressure, green represents rain rate while red represents link path loss.

The Total attenuation at 60GHz which is given by

Total path attenuation = Attenuation Free Space Path Loss + Attenuation by Oxygen Absorption + Attenuation due to Water Vapour Absorptions + Attenuation due to Rain.

The individual formula for each segment of the total attenuation is calculated separately based on the following equations.

For Rain Rate, the specific attenuation γ_R (dB/km) is obtained from the rain rate R (mm/h) using the power-law relationship:

$$\gamma_R = kR^\alpha \qquad \text{(ITU-R P.838-3)}$$

A detailed explanation of how the formula was used is given in section 3.4 of Chapter 3.

For Attenuation due to FSPL the following equation is used: =H3+37+37-I2

Total Path Loss was also added for each entry based on:

$$\text{PathLoss}_{\text{Newton}} = \text{TxPower}_{\text{Maxwell}} + 37 + 37 - \text{RxPower}_{\text{Newton}}$$

and similarly, for PathLoss$_{\text{Maxwell}}$, where 37 is the stated gain of the NEC radio unit.

For attenuation due to Oxygen absorptions, the formula used was based on ANNEX 2 of the ITU-R P.676-3

For dry air, the attenuation γ_o (dB/km) is given by:

$$\gamma_o = \frac{(f-60)(f-63)}{18}\gamma_o(57) - 1.66 r_p^2 r_t^{8.5}(f-57)(f-63) + \frac{(f-57)(f-60)}{18}\gamma_o \qquad \text{(Eq. 6)}$$

For 57 GHz $\leq$ f $\leq$ 63 GHz.

Details of how this formula was used can be found in section 3.3.1 of Chapter 3.

For attenuation due to Water Vapour absorptions, the formula used was based on ANNEX 2 of the ITU-R P.676-3. The attenuation γ_w (dB/km) is given by:

$$\gamma_w = \left[3.27 \times 10^{-2} \; r_t + 1.67 \times 10^{-3} \frac{\rho \, r_t^7}{r_p} + 7.7 \times 10^{-4} \; f^{0.5} + \frac{3.79}{(f - 22.235)^2 + 9.81 \, r_p^2 \; r_t} + \frac{11.73 \, r_t}{(f - 183.31)^2 + 11.85 \, r_p^2 \; r_t} + \frac{4.01 \, r_t}{(f - 325.153)^2 + 10.44 \, r_p^2 \; r_t} \right] f^2 \, \rho \, r_p \, r_t \times 10^{-4}$$

(Eq. 7)

For $f \leq 350$ GHz

The Residual Path Loss: These are losses that are unaccounted for by the ITU path-loss model after all the losses have been removed.

To get the residual path loss, the major components of losses such as attenuations due to oxygen absorptions, attenuations due to water vapour absorptions and attenuations due to rain rate are subtracted from the path loss.

Residual Path Loss = Path Loss – Oxygen – Water Vapour– Rain

*Note. All the data processing of the results is based on these formulae and calculations.

Table 5.2.1 summarises the averages, maximum and minimum for pathloss and received power

Table 5.2.1 Summary of monthly Path Loss data with respect to the Newton radio

Month	Rx Power (Min) dBm	Rx Power (Avg) dBm	Rx Power (Max) dBm	Path Loss (Min) dBm	Path Loss (Avg) dBm	Path Loss (Max) dBm
Aug 2017	-57.7	-52.5	-51.7	115.5	116.2	121.8
Sep 2017	-58.8	-52.4	-51.8	115.5	116.3	122.9
Oct 2017	-59.7	-52.4	-51.9	115.6	116.3	123.5
Nov 2017	-58.4	-52.5	-52.0	115.7	116.4	122.5
Dec 2017	-58.9	-52.5	-52.1	115.8	116.5	123.0
Jan 2018	-59.0	-52.5	-51.9	115.7	116.5	123.1
Feb 2018	-58.7	-52.5	-52.0	115.7	116.5	122.9
Mar 2018	-57.1	-52.5	-52.0	115.7	116.5	121.1
Apr 2018	-57.8	-52.4	-51.7	115.5	116.4	121.8
May 2018	-57.0	-52.3	-51.7	115.4	116.2	121.0
Jun 2018	-58.7	-52.2	-51.7	115.4	116.2	122.7
Jul 2018	-56.6	-52.2	-51.7	115.5	116.2	120.7
Aug 2018	-58.0	-52.2	-51.7	115.4	116.2	122.1

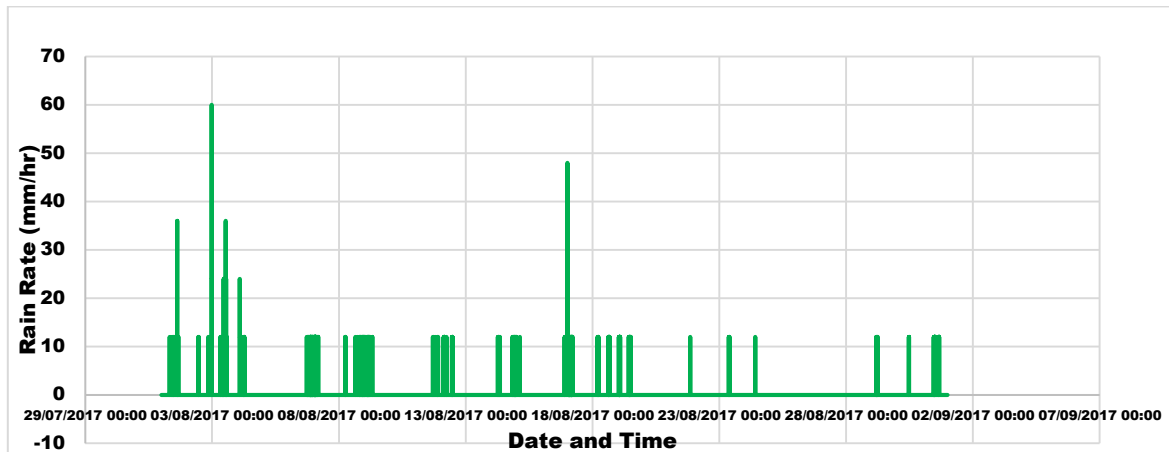### 5.2.1 August 2017 Results and Analysis

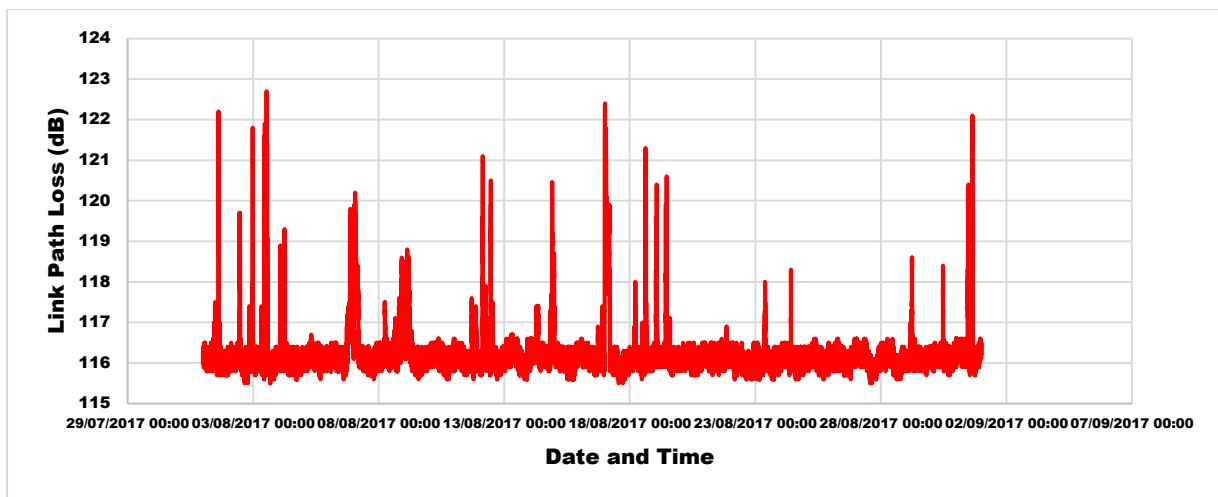*Figure 5.2.1.1 Link rain rate in mm/hr for August 2017*

Figure 5.2.1.2 Link path loss for August 2017

Rain rate for august 2017 is shown in figure 5.2.1 while, figure 5.2.2 represents path loss for august 2017. Figure 5.2.2 shows that having considered impacts due to atmospheric gases and rain as per the ITU recommendations, there is a general residue of between 1dB and 2dB path loss throughout the month, interspersed by definite larger peaks ranging from 3dB to 9dB. When plotted against rain rate (mm/hr) there seems to be a strong correlation between the residual path loss and rain periods of sustained rain. To get a more detailed understanding of the high residual path loss above 3 dB, we take each day of such peak losses and analyse them separately.
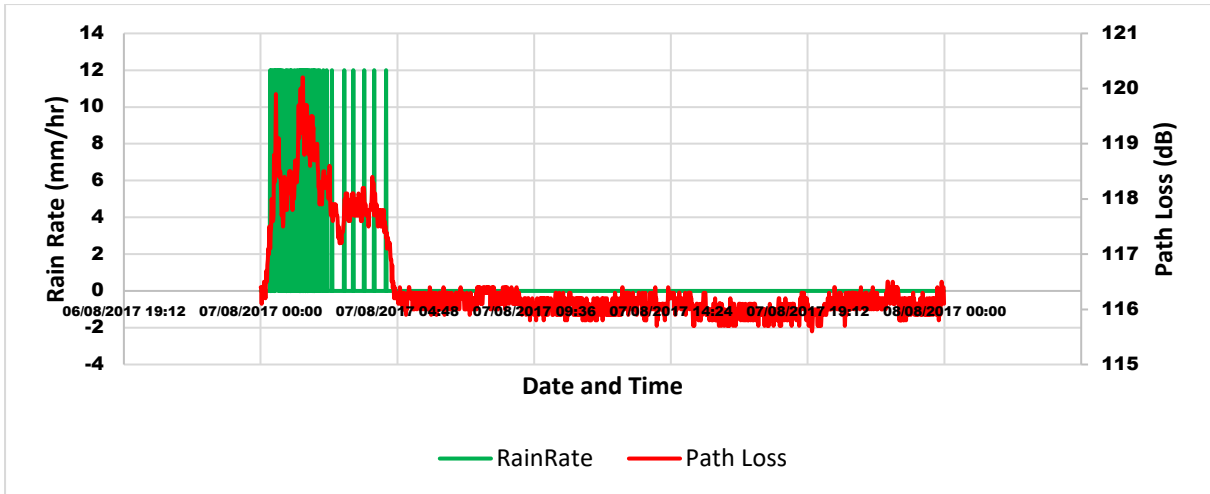
Figure 5.2.1.3 Residual link path loss plotted against rain rate for 7th August 2017

We plot rain rate against path loss as shown in figure 5.2.3 to examine the period of peak residual path-loss. By plotting rain rate against path loss there is a strong correlation between the duration of rainfall from 00:27 am until 02:30 am and this period of steady rainfall correlates to the period of high link residual path loss of about 6dB. This show that rain duration plays a crucial role in the link path loss
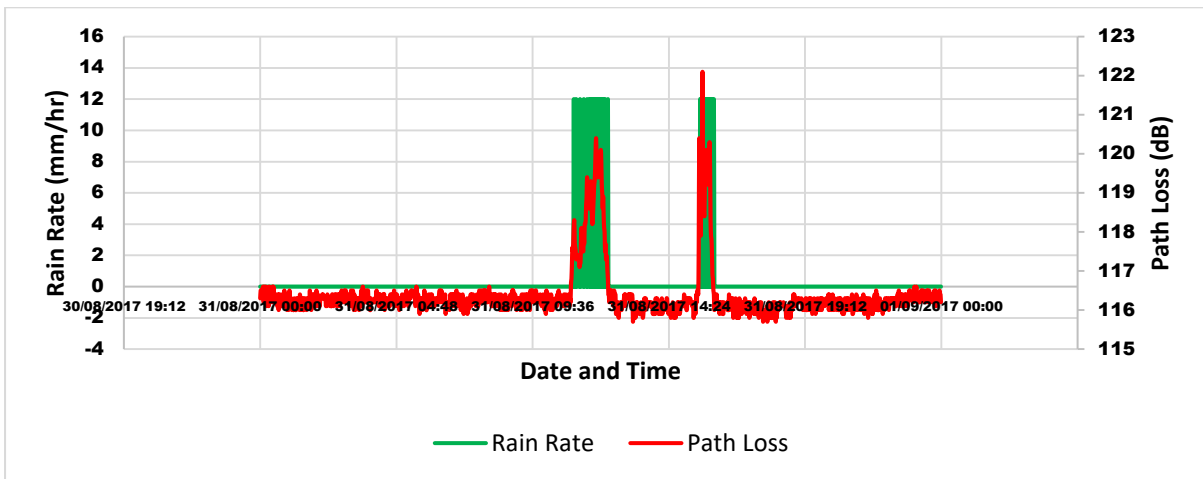

Figure 5.2.1.4 Link path loss plotted against rain rate for 31st August 2017

Figure 5.2.4 shows link path loss plotted against rain rate for 31st August 2017. It shows a strong correlation between rain rate and link residual path loss. The periods of high rain intensity and duration corresponds to the period of high link residual path loss. This is consistent for the entire day.

5.2.2   September 2017 Result and Analysis
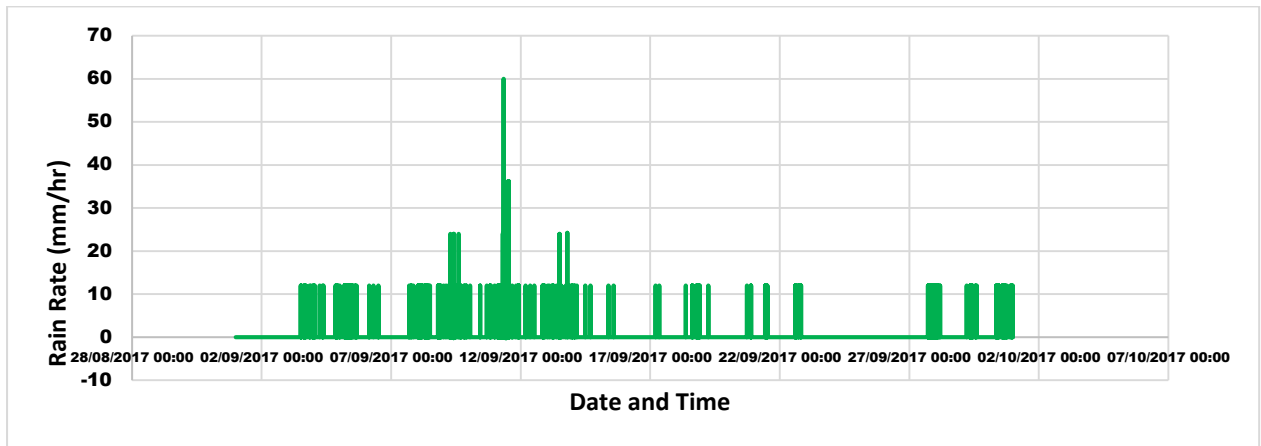
Figure 5.2.2.1 rain rate (mm/hr) for September 2017
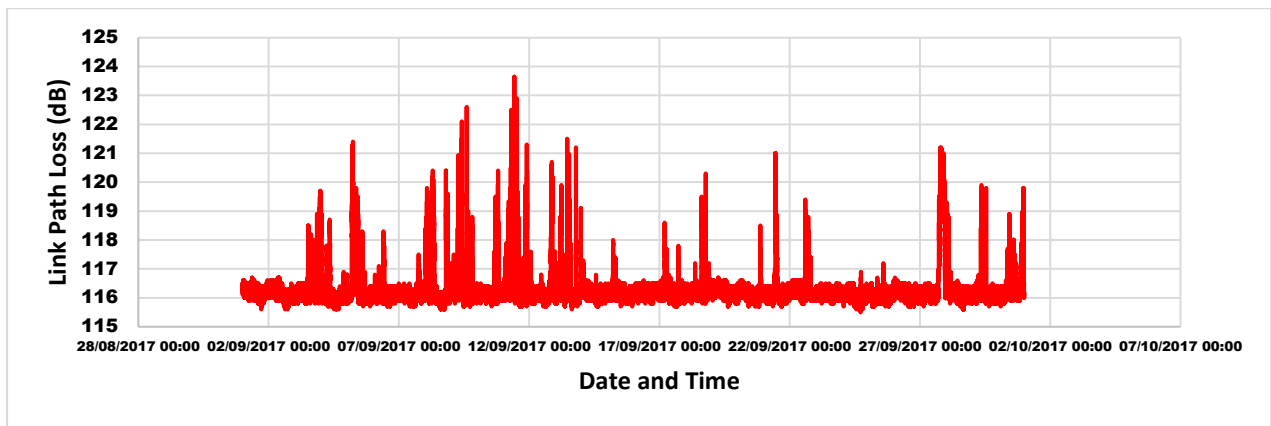
Figure 5.2.2.2 Link path loss for September 2017

September 2017 was a wet month with lots of rain spread across the month. This led to lots of residual path loss across various times in the month., having considered impacts due to atmospheric gases and rain as per the ITU recommendations, there is a general residue of between 1dB and 2dB path loss throughout the month, interspersed by definite larger peaks ranging from 3dB to 9dB. Figure 5.2.5 shows rain rate (mm/hr) for the month of September 201, while, figure 5.2.6 represents the plot for Path-loss. Detail analysis of peak residual path loss is detailed below.
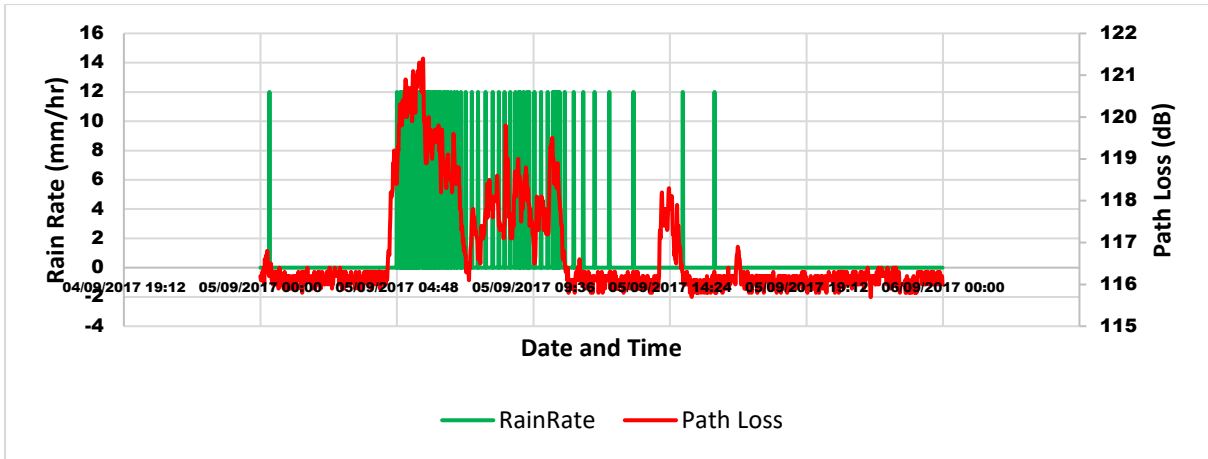
Figure 5.2.2.3 Residual link path loss plotted against rain rate for 5th September 2017

On the 5th of September 2017, plotting link path loss against rain rate (mm/hr) as seen in figure 5.2.7 shows a strong correlation between the periods of high path loss and rain duration. From 04:48 am until 11:01 am saw, a period of steady rain and this, in turn, recorded the highest link path loss of about 7dB. This graph shows the critical role played by rain duration in calculating path loss at 60GHz.

Figure 5.2.2.4 Link path loss plotted against rain rate for 8th September 2017

Similarly, the Figure 5.2.8 above illustrates the situation that occurred on the 8th of September 2017 when plotting the residual link path loss against rain rate (mm/hr). This shows a strong correlation between the periods of rain and residual path loss. Again, the periods of the high residual path loss of about 6dB correlates to the period of steady rainfall from 07:09 am until 08:35 am. This highlights the effect of rain duration on path loss

70
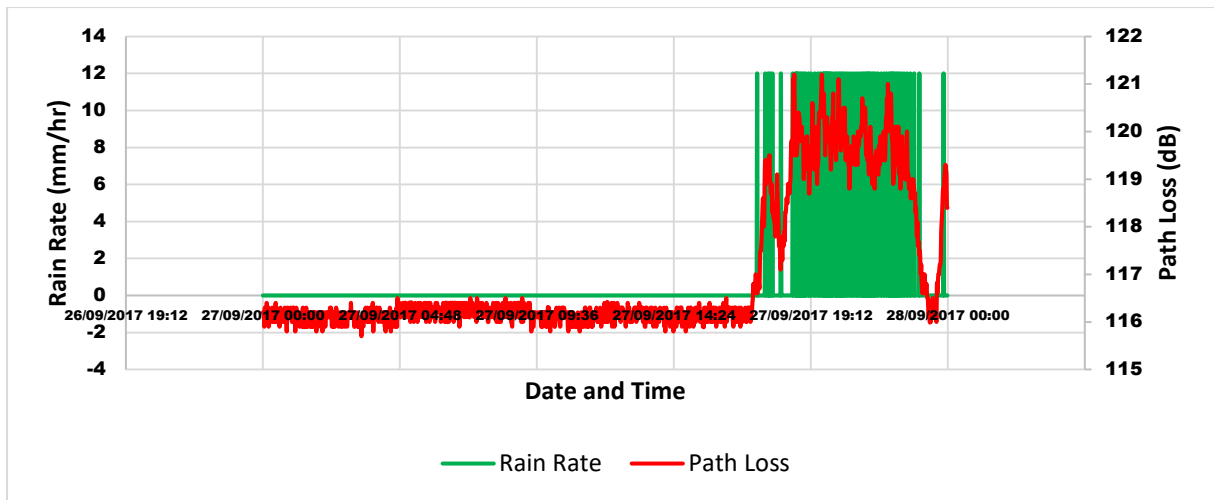
Figure 5.2.2.5 Link path loss plotted against rain rate for 27th September 2017

Further examples of the impact of rain can be seen in figure 5.2.9. Link path loss plotted against rain rate for 27th September 2017. The period of sustained rainfall corresponds to the peak residual path loss. This is evidence that the high link residual path loss occurred at the period of rain duration.

5.2.3 October 2017 Result and Analysis
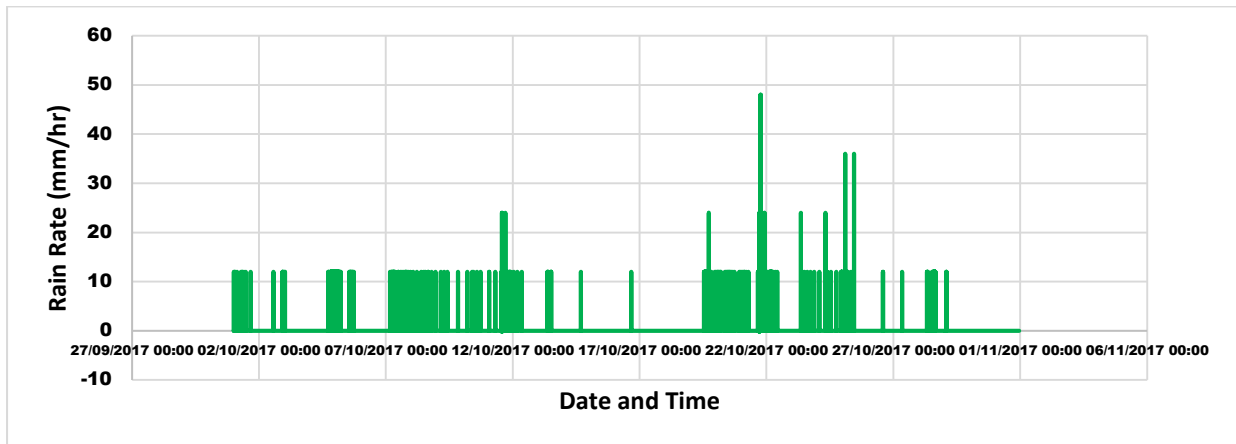
Figure 5.2.3.1 Rain rate (mm/hr) for October 2017
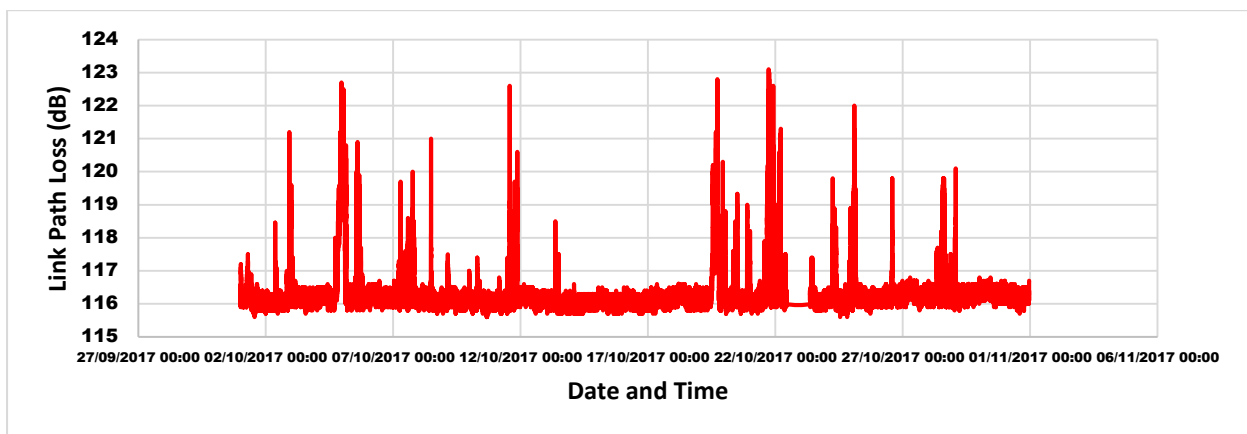
Figure 5.2.3.2 Link path loss for October 2017

October 2017 was a wet month with lots of rain spread across the month. This led to lots of residual path loss across various times in the month. Having considered impacts due to atmospheric gases and rain as per the ITU recommendations, there is a general residue of between 1dB and 2dB path loss throughout the month, interspersed by definite larger peaks ranging from 3dB to 9dB. Figure 5.2.10 represents rain rate (mm/hr) while figure 5.2.11 in red is plotted for link path-loss. Detail analysis of this month shows strong correlation between periods of rainfall and peaks in link path-loss
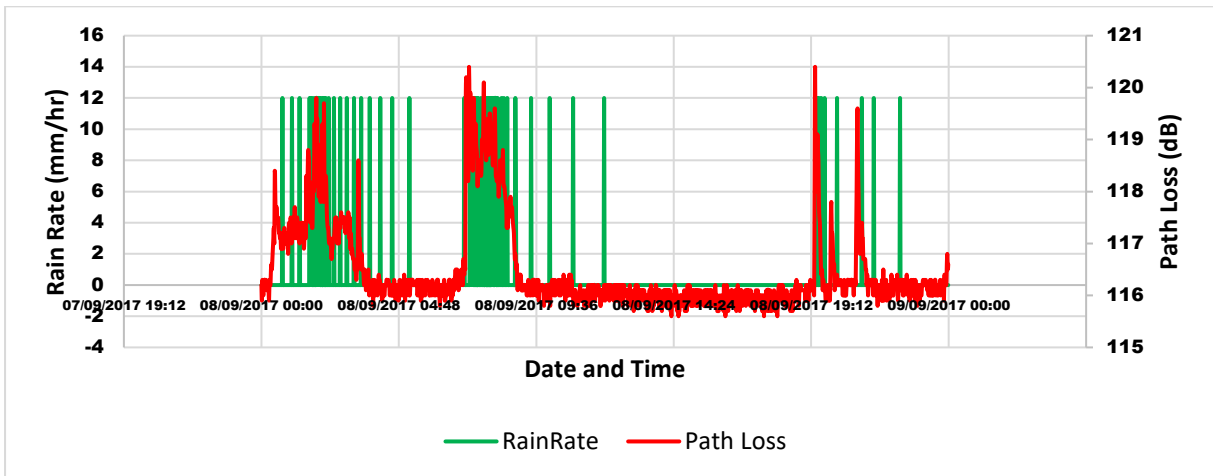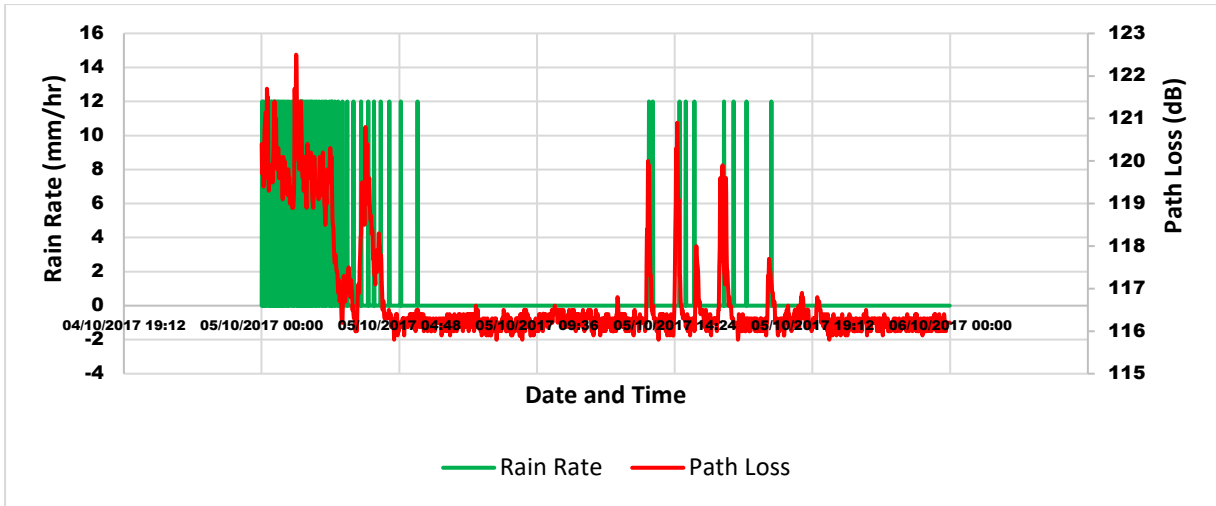
Figure 5.2.3.3 Link path loss plotted against rain rate for 5th October 2017

Interestingly, figure 5.2.12 illustrates the situation that occurred on the 5th of October 2017 and plots the residual link path loss against rain rate (mm/hr). Here the largest peaks in residual link path loss at about 7dB correlate to the period of rain duration from 00:12 am until 04:09 am.

Figure 5.2.3.4 Link path loss plotted against rain rate for 19th October 2017

Figure 5.2.13 shows link path loss plotted against rain rate for 19th October 2017. There are periods of isolated rainfall that have zero effect on the link residual path loss. However, the period of sustained rainfall corresponds to the peak residual path loss. This is evidence that the high link residual path loss occurred at the period of rain duration.

Figure 5.2.3.5 Link path loss plotted against rain rate for 25th October 2017

Link path loss plotted against rain rate for 25th October 2017. In figure 5.2.14, there are periods of isolated rainfall that have little effect on the link residual path loss. Significantly, there was an isolated rain rate of 36 mm/hr that occurred at 10:49 am yet had zero effect on the link path loss. This shows that only sustained rain rate affects the link. The period of sustained rainfall corresponds to the peak residual path loss. This is evidence that the high link residual path loss occurred at the period of rain duration.

5.2.4   November 2017 Result and Analysis
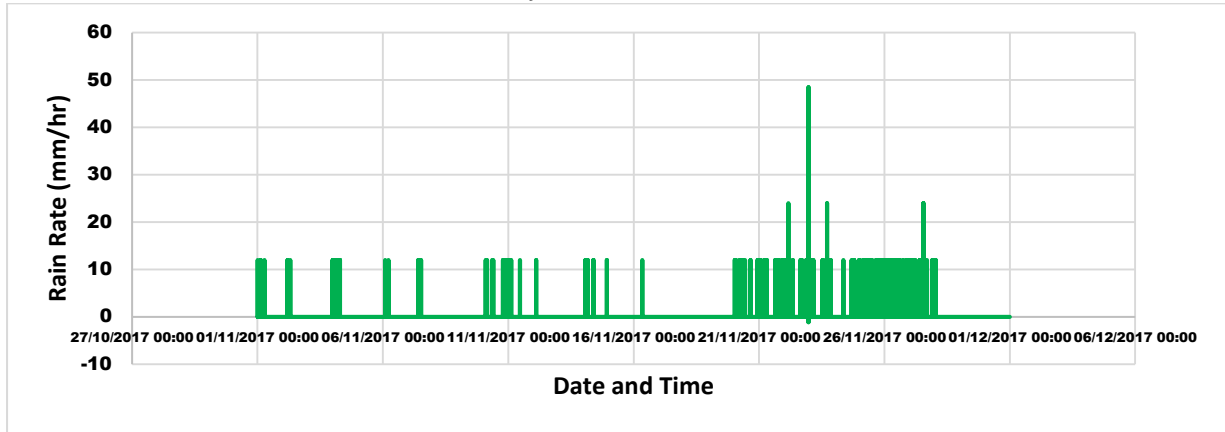

Figure 5.2.4.1 Rain rate (mm/hr) for November 2017
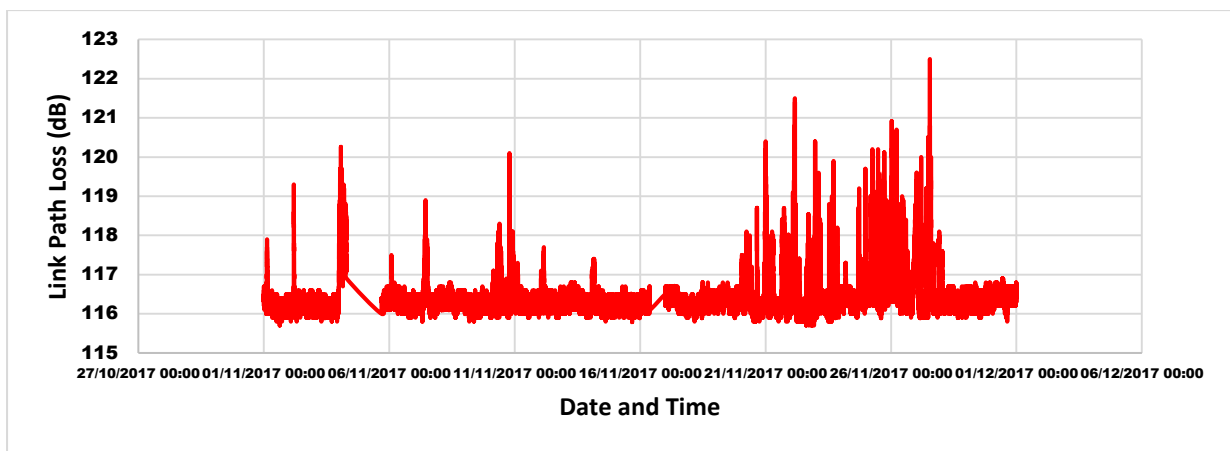
Figure 5.2.4.2 Link path loss for November 2017

Figure 5.2.15 represents rain rate (mm/hr) while, figure 5.2.16 shows link path loss (dB) for November 2017.

Note* It is worthy to note that the period from 07:14 am on the fourth of November 2017 until 21:25 pm on the fifth of November had no activity in the link as the data for that period was skipped due to electrical power shut down. Similarly, the period from 08:12 am on the 16th November until 03:32 am on the 17th November also had electrical power restart hence there were no records for these days.
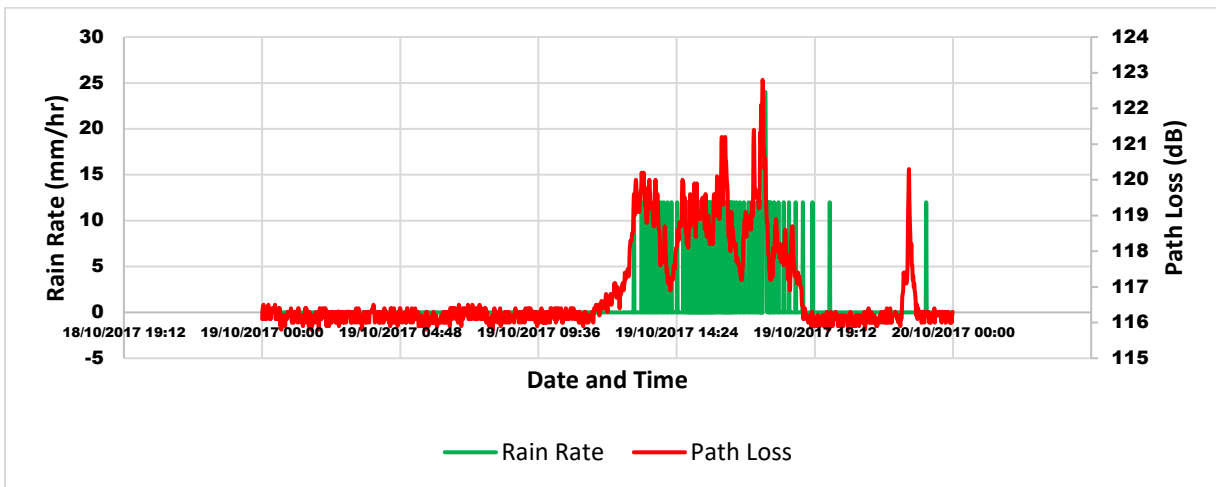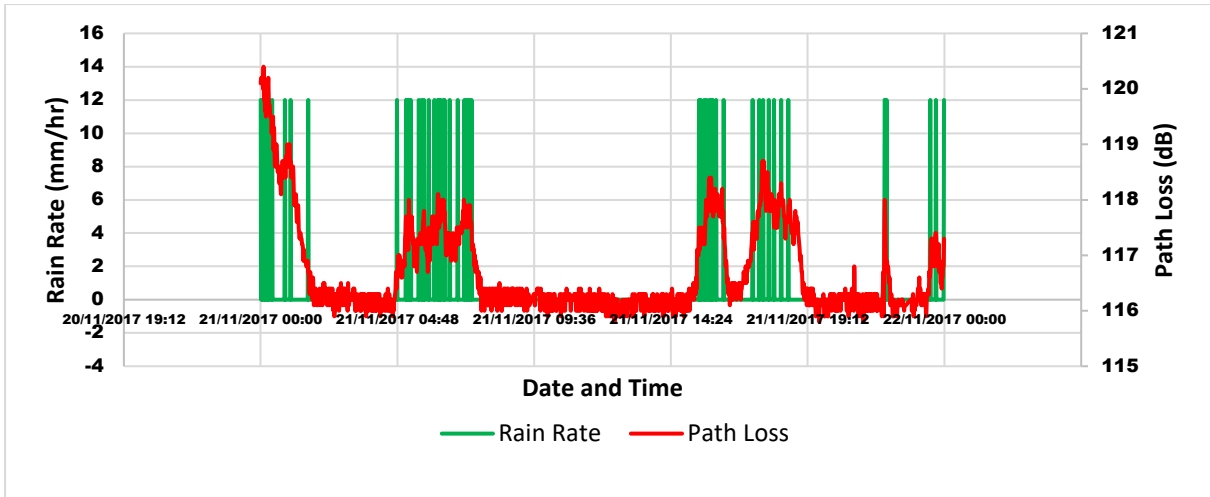
Figure 5.2.4.3 Link path loss plotted against rain rate for 21st November 2017

Link path loss plotted against rain rate for 21st November 2017 is shown in figure 5.2.17. The period of sustained rainfall shows a direct correlation to the peak residual path loss. This is evidence that the high link residual path loss occurred at the period of rain duration.

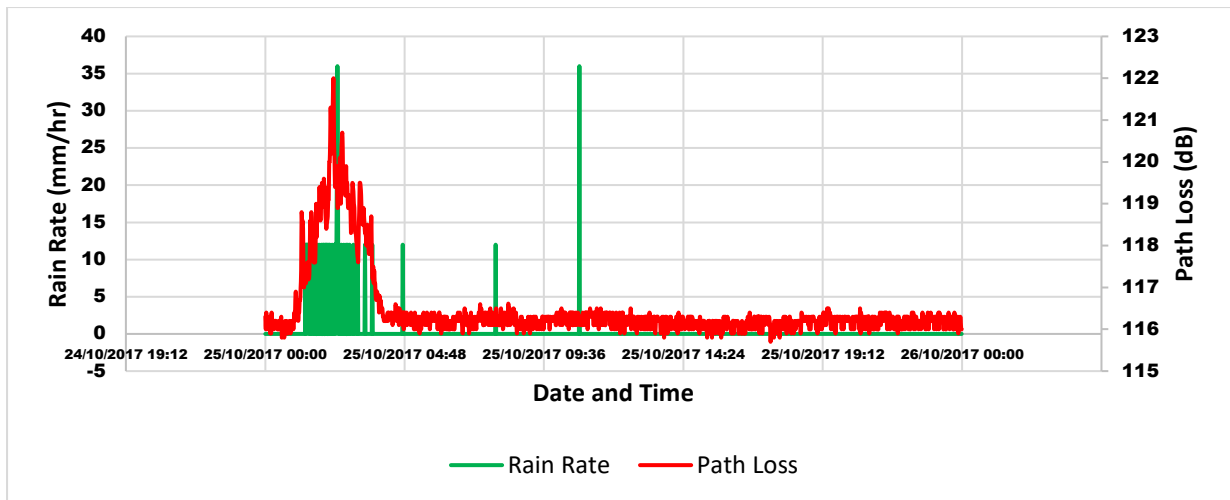*Figure 5.2.4.4 Link path loss plotted against rain rate for 26th November 2017*

Again, on the 26th of November 2017, when plotting link path loss versus rain rate (mm/hr). The periods of sustained rainfall correlate with link residual path loss. There is a direct correlation between rain and residual path loss at 60GHz. This can be seen in figure 5.2.18

5.2.5 December 2017 Result and Analysis
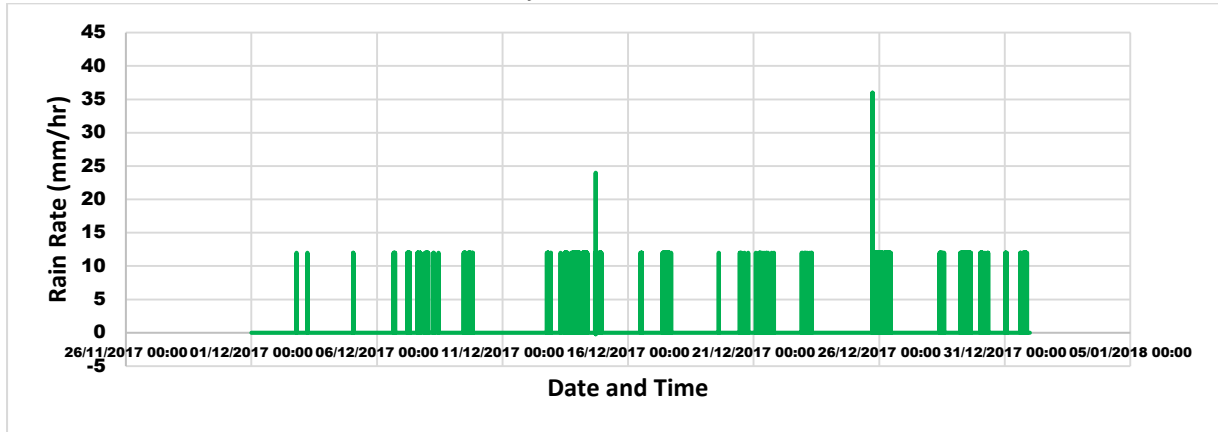
Figure 5.2.5.1 Rain rate (mm/hr) for December 2017
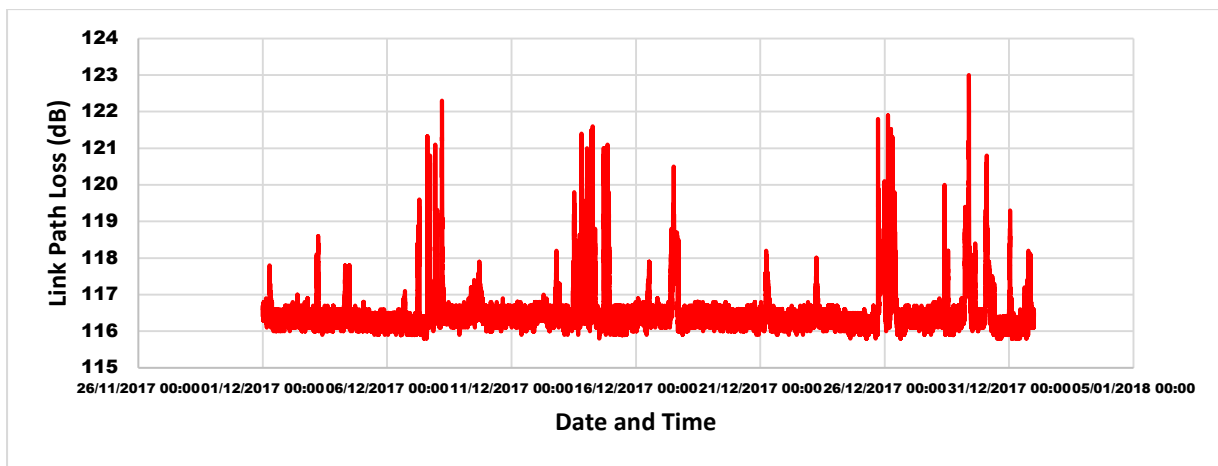
Figure 5.2.5.2 Link Path loss (dB) for December 2017

Figure 5.2.20 shows link path loss while, figure 5.2.19 shows rain rate for December 2017. December 2017 and shows that having considered impacts due to atmospheric gases and rain as per the ITU recommendations, there is a general residue of between 1dB and 2dB path loss throughout the month, interspersed by definite larger peaks ranging from 3dB to 9dB. Each of these peaks in residual path-loss is further analysed daily.
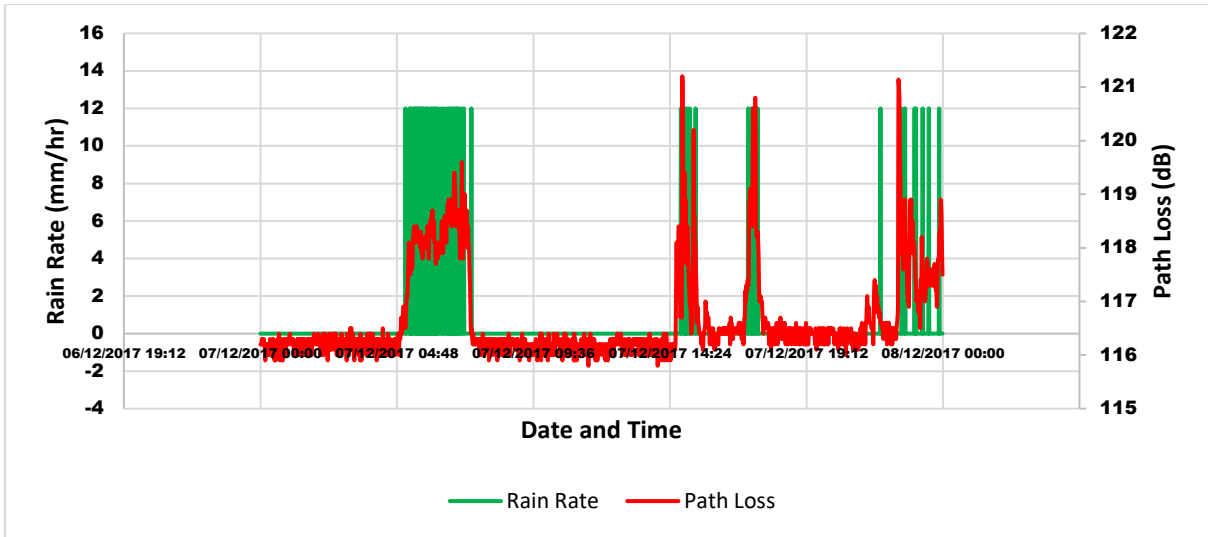
Figure 5.2.5.3 Link path loss plotted against rain rate for 7th December 2017

The 7th of December 2017 was a day with high path loss. We plotted this link path loss against the rain rate for that day as shown in figure 5.2.21. there is a strong correlation between these peaks in the residual path loss and rain events. The periods of sustained rainfall such as 05:06 am until 07:25 am corresponds to the period of high residual path loss. Also, from 14:50 pm until 15:18 also shows a direct correlation between rainfall and high link residual path loss. This is consistent for the other events of peak residual path loss that occurred on the 7th of December 2017.
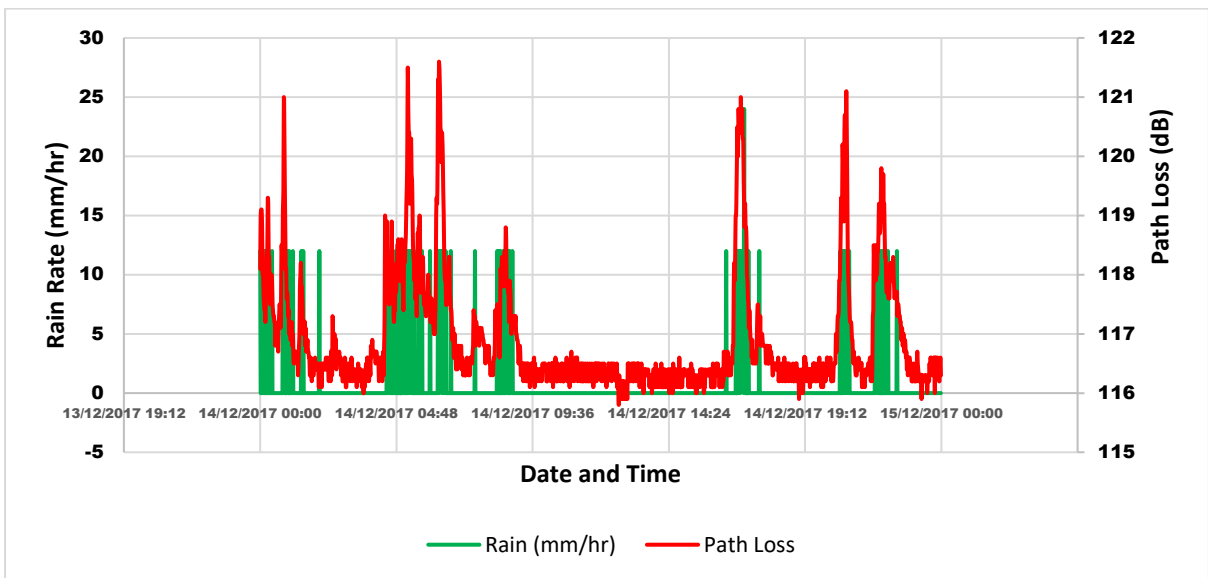
Figure 5.2.5.4 Link path loss plotted against rain rate for 14th December 2017

Figure 5.2.22 plots link path loss against rain rate for the 14th of December 2017. This shows a strong correlation between these peaks in the residual path loss and rain rate. This is consistent for the other events of peak residual path loss that occurred on the 14th of December 2017.

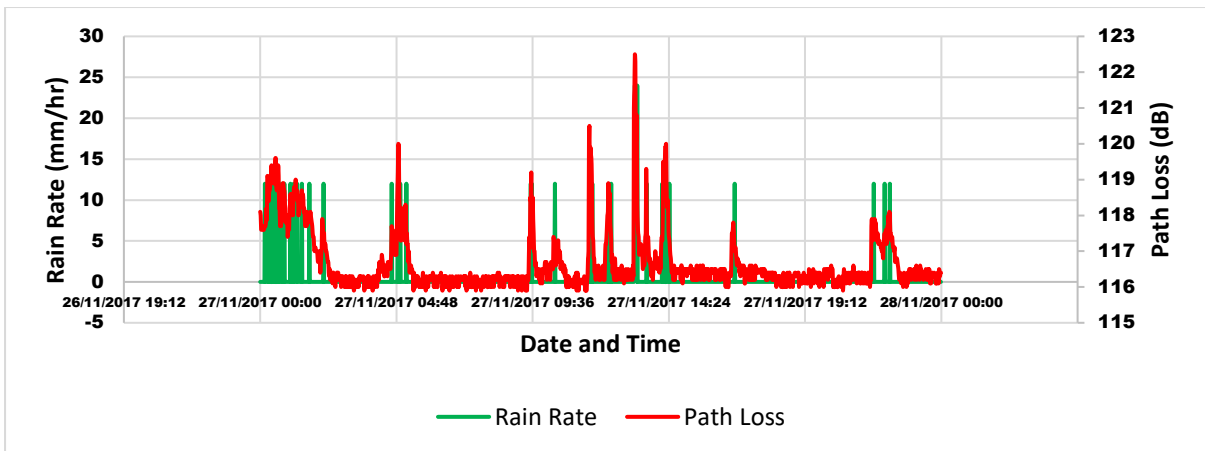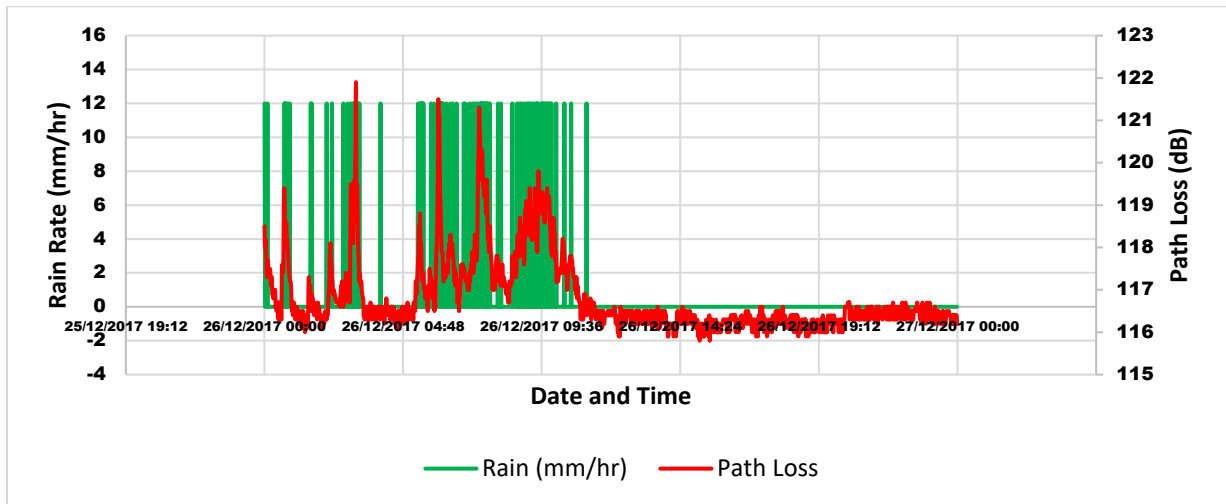*Figure 5.2.5.5 Link path loss plotted against rain rate for 26th December 2017*

Also, on the 26th of December 2017. We plotted this link path loss against the rain rate as shown in figure 5.2.23. This shows a strong correlation between these peaks in the residual path loss and rain rate. This is consistent for the other events of peak residual path loss that occurred on the 26th of December 2017. It can be seen that path loss remained flat and consistent when there was no rain event.

5.2.6   January 2018 Result and Analysis
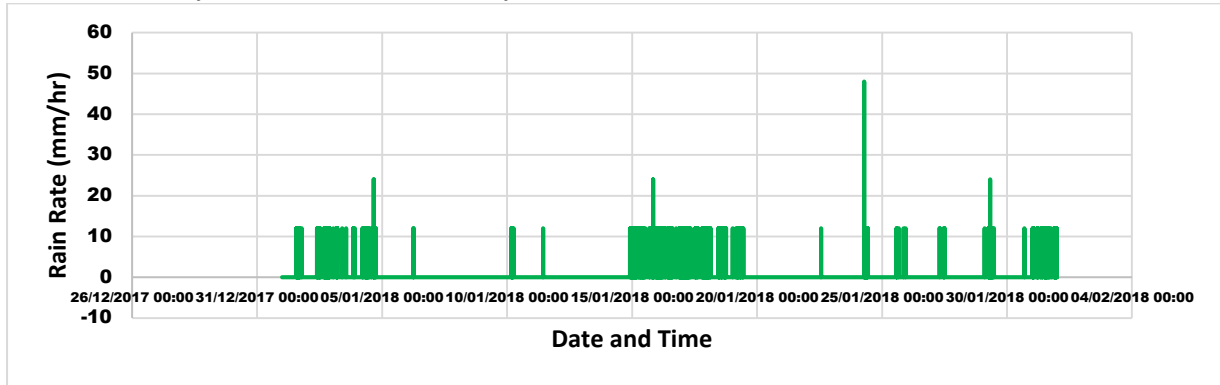
Figure 5.2.6.1 Rain rate (mm/hr) for January 2018

Figure 5.2.6.2 Link path loss for 2018

January 2018 was a wet month with lots of rain spread across the month as shown in figure 5.2.24. This led to lots of residual path loss across various times in the month. Having considered impacts due to atmospheric gases and rain as per the ITU recommendations, there is a general residue of between 1dB and 2dB path loss throughout the month, interspersed by definite larger peaks ranging from 3dB to 9dB. Figure 5.2.25 plots link path loss for January 2018 to highlight the periods of peak link path loss. Further analysis shows the relationship between these peaks in path loss and rain.
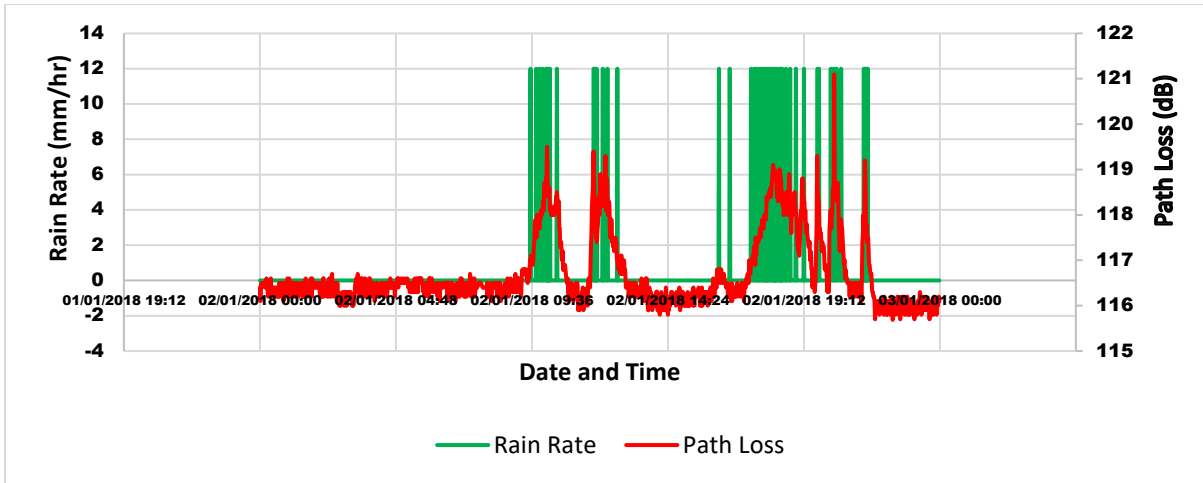
Figure 5.2.6.3 Link path loss plotted against rain rate for 2nd January 2018

We plotted this link path loss against the rain rate for the 2nd January 2018 as shown in figure 5.2.26. There appears to be a strong correlation between these peaks in the residual path loss and duration of rain rate. This is consistent for the other events of peak residual path loss that occurred on the 2nd January 2018.
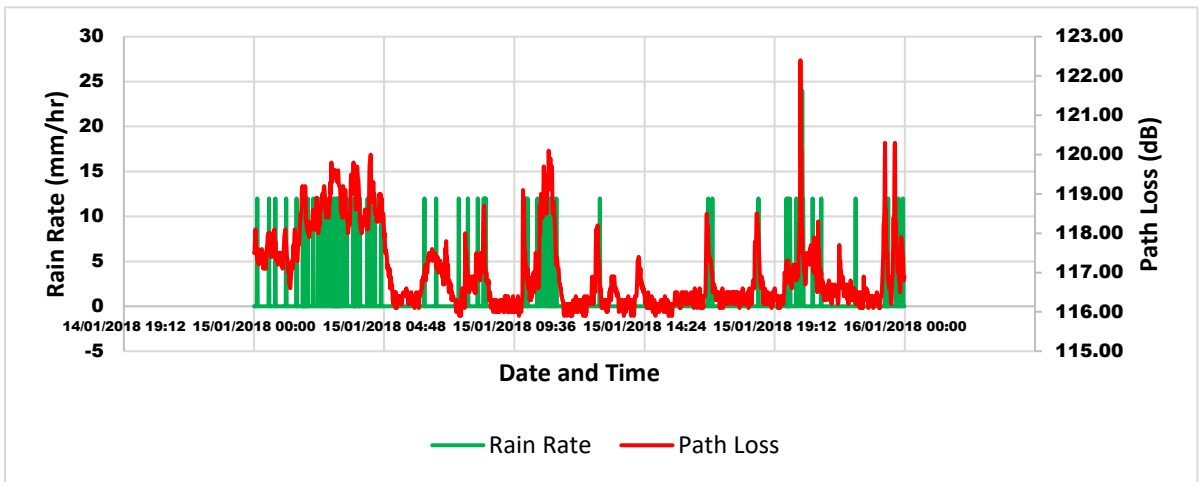
Figure 5.2.6.4 Link path loss plotted against rain rate for 15th January 2018

Again, on the 15th January 2018, when plotting link path loss versus rain rate (mm/hr), it is observed that the rain is evenly spread from 00:07 am until 23:55 pm as shown in figure 5.2.27. the peaks in path loss only occur during rain events.

81
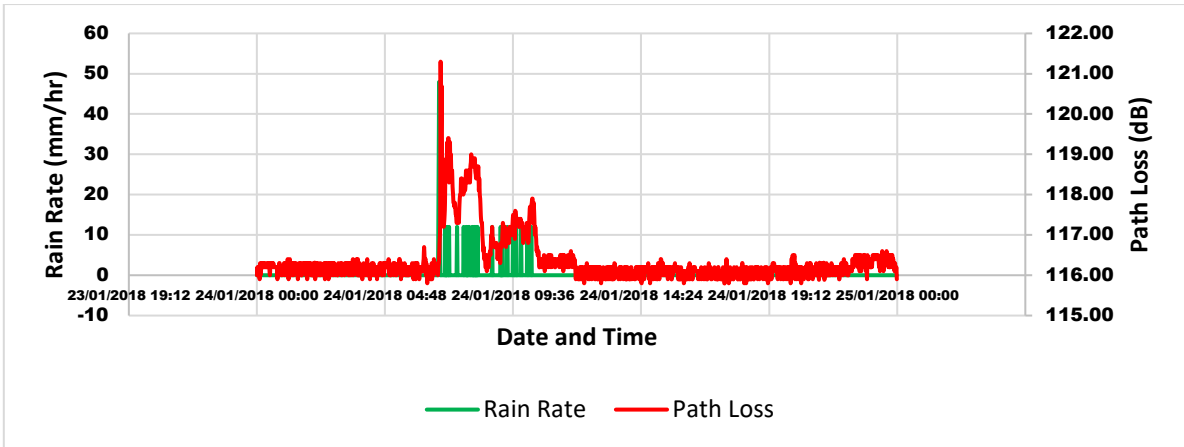
Figure 5.2.6.5 Link path loss plotted against rain rate for 24th January 2018

Again, on the 24th January 2018, when plotting link path loss versus rain rate (mm/hr), the high peaks in residual path loss occurred at the period of sustained rainfall. From figure 5.2.28 rainfall is a critical component that affects link performance at 60GHz frequency.

5.2.7   February 2018 Result and Analysis
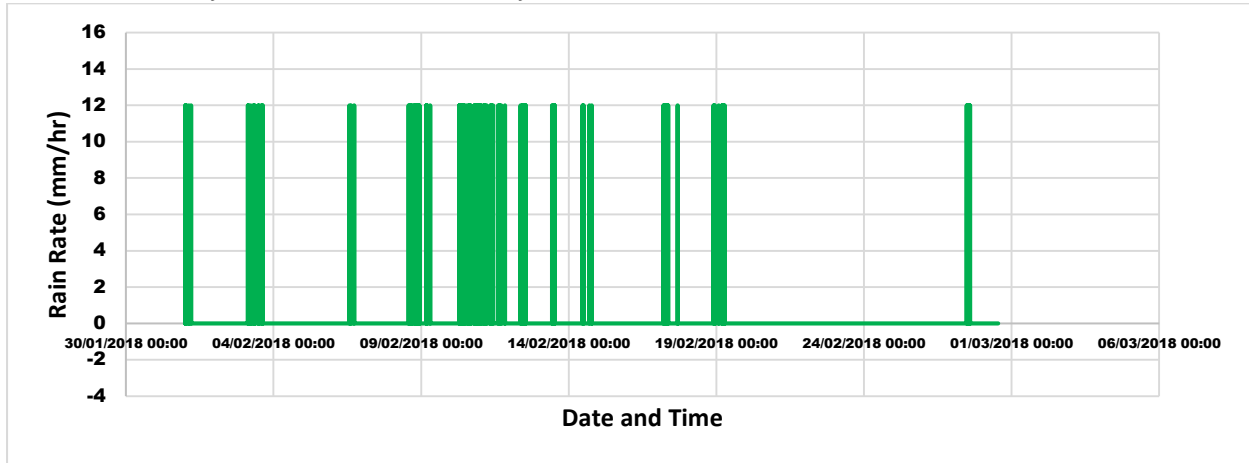
Figure 5.2.7.1 Rain rate (mm/hr) for February 2018
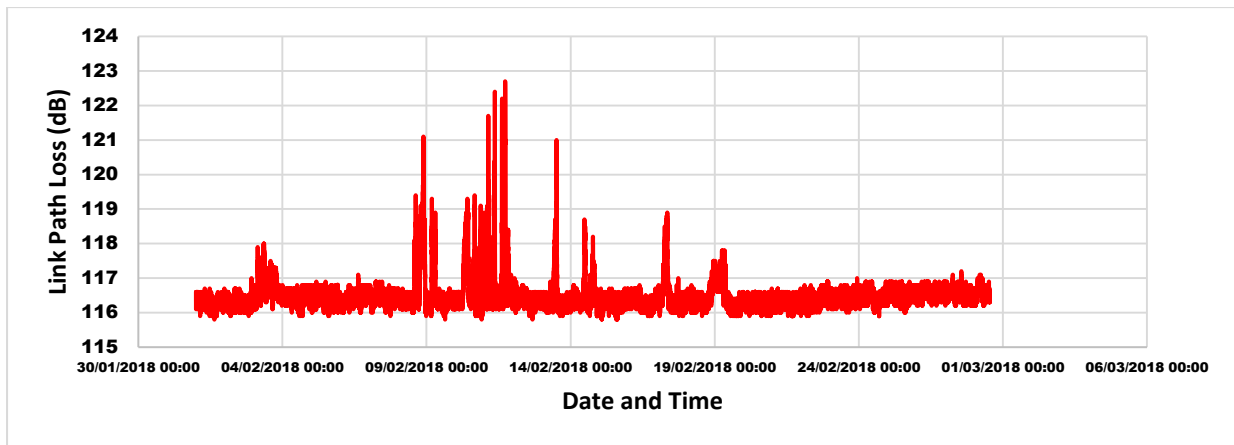
Figure 5.2.7.2 Link path loss for February 2018

February 2018 was another wet month with lots of rain spread across the month as shown in figure 5.2.29. This led to lots of residual path loss across various times in the month. , having taken into account impacts due to atmospheric gases and rain as per the ITU recommendations, there is a general residue of between 1dB and 2dB path loss throughout the month, interspersed by definite larger peaks ranging from 3dB to 9dB. Figure 5.2.30 shows the peaks in path loss for February 2018. Further analysis of these peaks is detailed below.

Figure 5.2.7.3 Link path loss plotted against rain rate for 8th February 2018

Link path loss plotted against rain rate for 8th February 2018 as shown figure 5.2.31. The period of sustained rainfall corresponds to the peak residual path loss. This is evidence that the high link residual path loss occurred at the period of rain duration.

Figure 5.2.7.4 Link path loss plotted against rain rate for 9th February 2018

Link path loss plotted against rain rate for 9th February 2018 as shown in figure 5.2.32. There are periods of isolated rainfall that have no effect on the link residual path loss. However, the period of sustained rainfall corresponds to the peak residual path loss. This is evidence that the high link residual path loss occurred at the period of rain duration.

84

5.2.8 April 2018 Result and Analysis
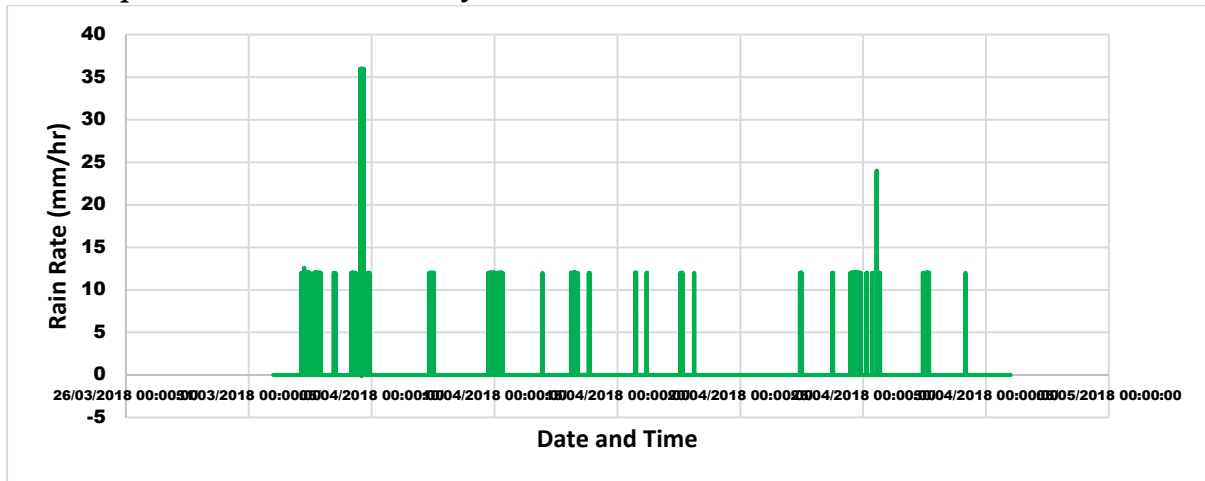
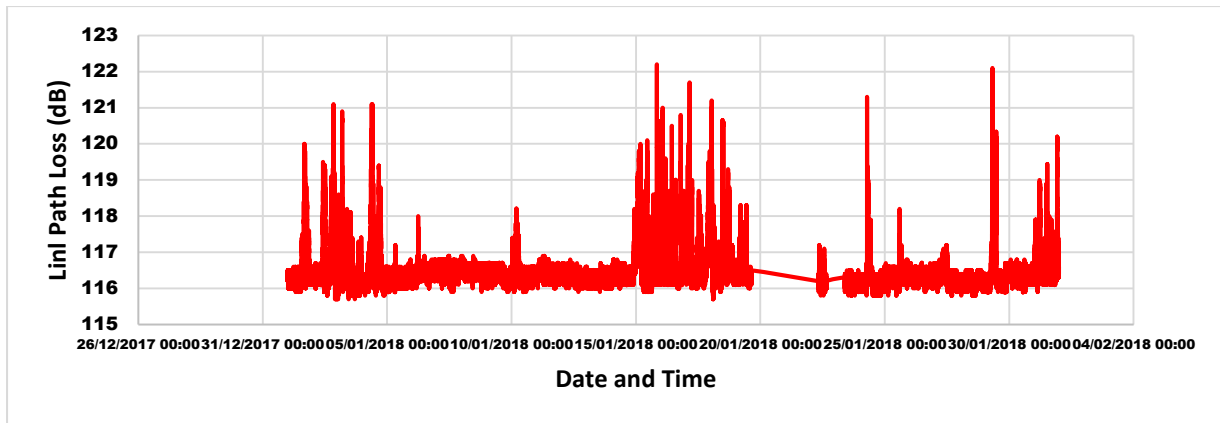*Figure 5.2.8.1 Rain rate (mm/hr) for 2018*
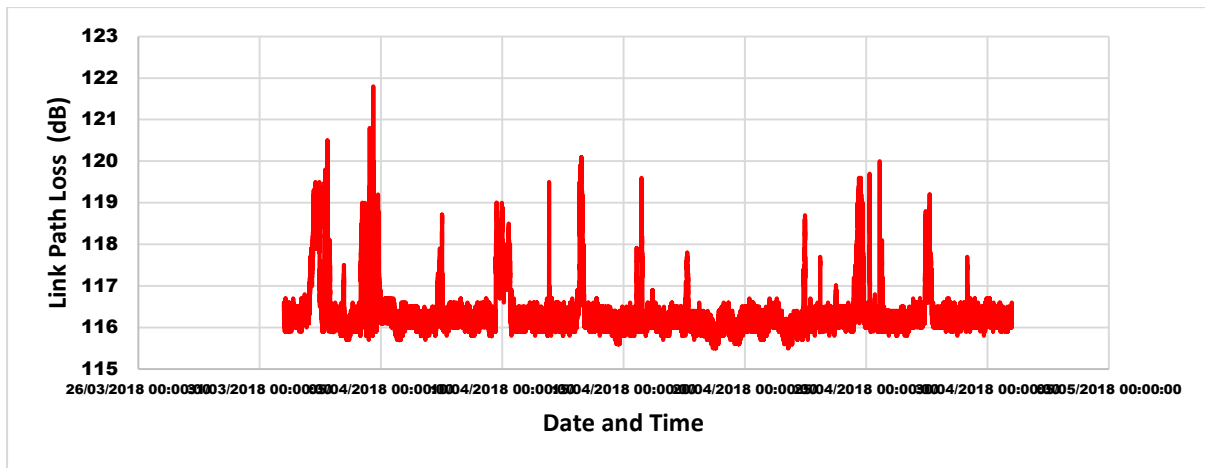
Figure 5.2.8.2 Link path loss for April 2018

April 2018 was a wet month with lots of rain spread across the month as shown in figure 5.2.33.

This led to lots of peak residual path loss across various times in the month as shown in figure

5.2.34. , having taken into account impacts due to atmospheric gases and rain as per the ITU

recommendations, there is a general residue of between 1dB and 2dB path loss throughout the

month, interspersed by definite larger peaks ranging from 3dB to 9dB. Detailed analysis of the

peaks in path loss are described below
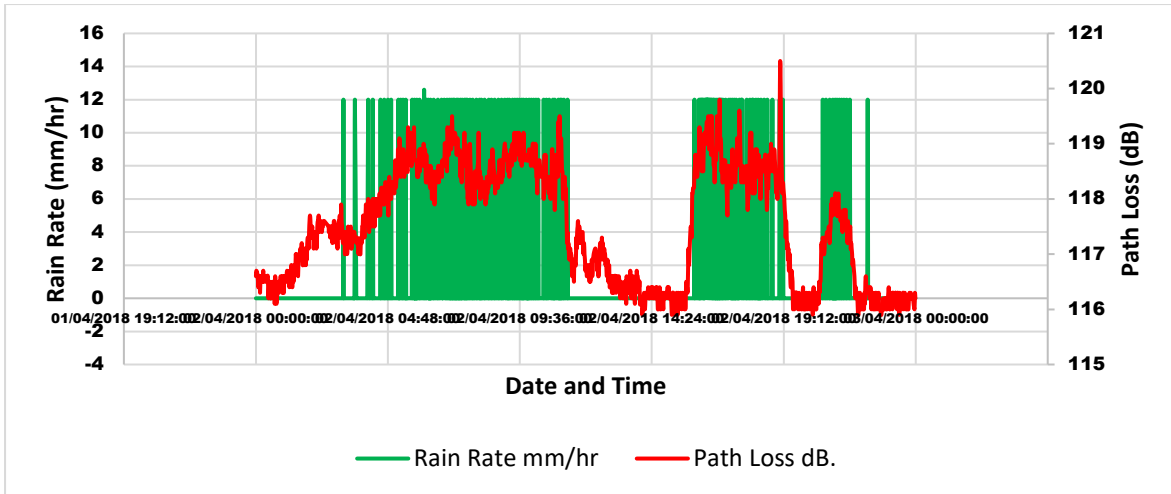
Figure 5.2.8.3 Link path loss plotted against rain rate for 4th April 2018

The 4th of April 2018 was a day of high rain durations. By plotting rain rate against link path loss for the 4th April 2018 shows a direct correlation between high residual path loss and rain duration. The figure 5.2.35 shows that the high residual path loss occurred only at periods of sustained rain events. This shows that the longer it rains the bigger the effect it has on the path loss.
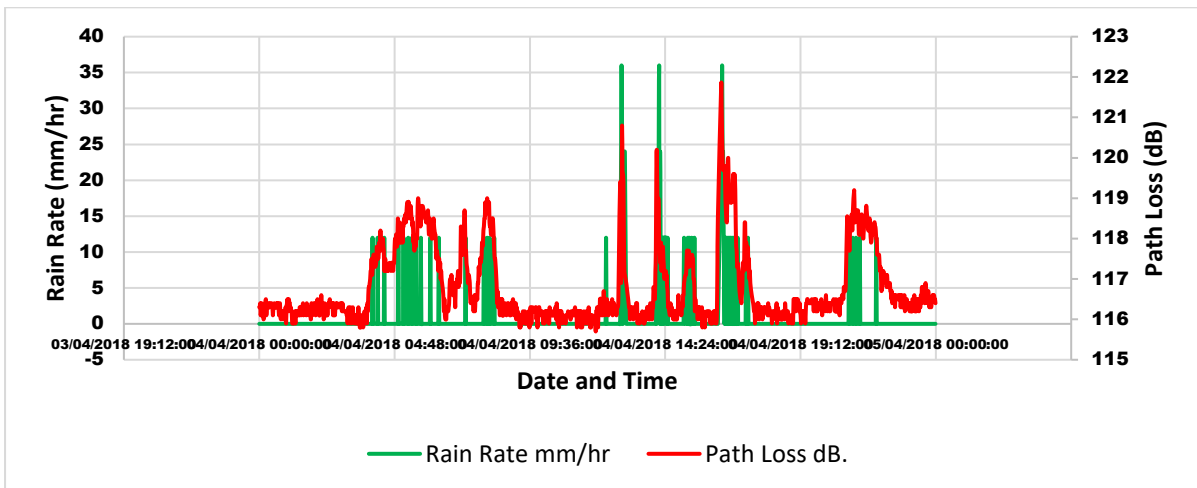
Figure 5.2.8.4 Link path loss plotted against rain rate for 4th April 2018

Link path loss plotted against rain rate for 4th April 2018 shows a direct correlation between high residual path loss and rain activities. Figure 5.2.36 shows that high residual path loss corresponds to periods of rain events. This shows that rain is crucial to path loss at 60GHz.
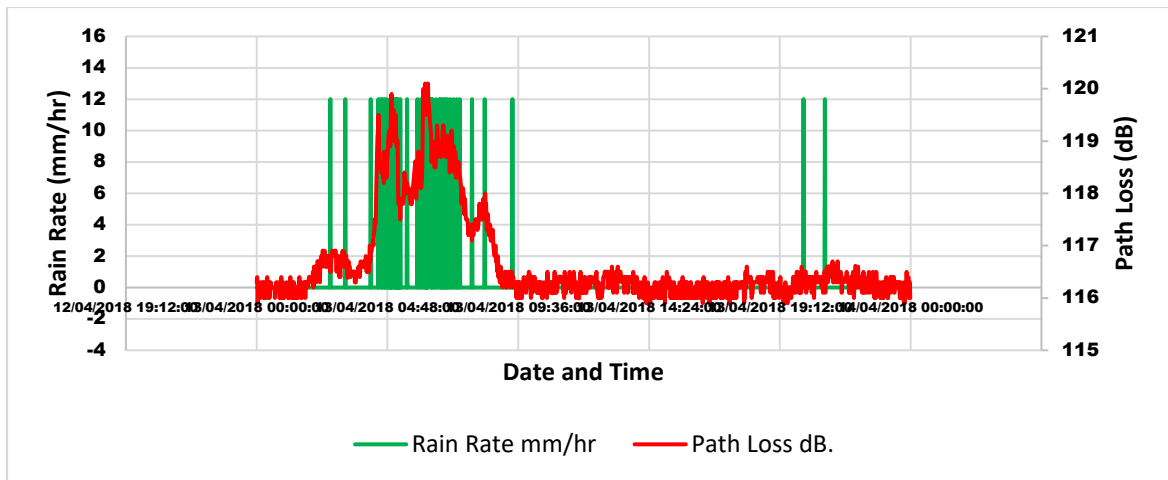
Figure 5.2.8.5 Link path loss plotted against rain rate for 13th April 2018

Figure 5.2.37 plots link path loss against rain rate for 13th April 2018. The peaks in residual path loss correlate to periods of rain duration. There are isolated events of rainfall, but this does not cause any spikes in residual path loss. This proves that the sustained period of rainfall has a crucial effect on the link path loss.

5.2.9 May 2018 Result and Analysis
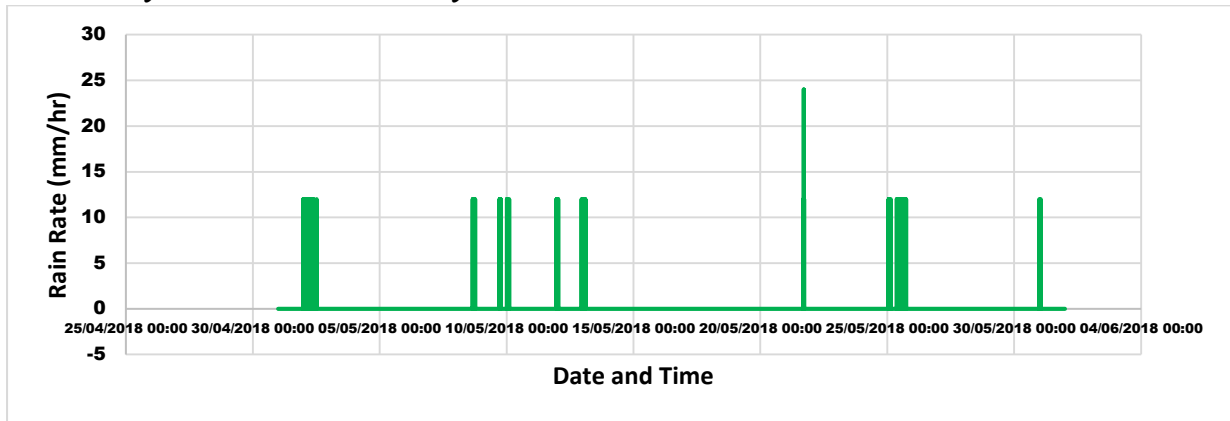
Figure 5.2.9.1 Rain rate (mm/hr) for May 2018
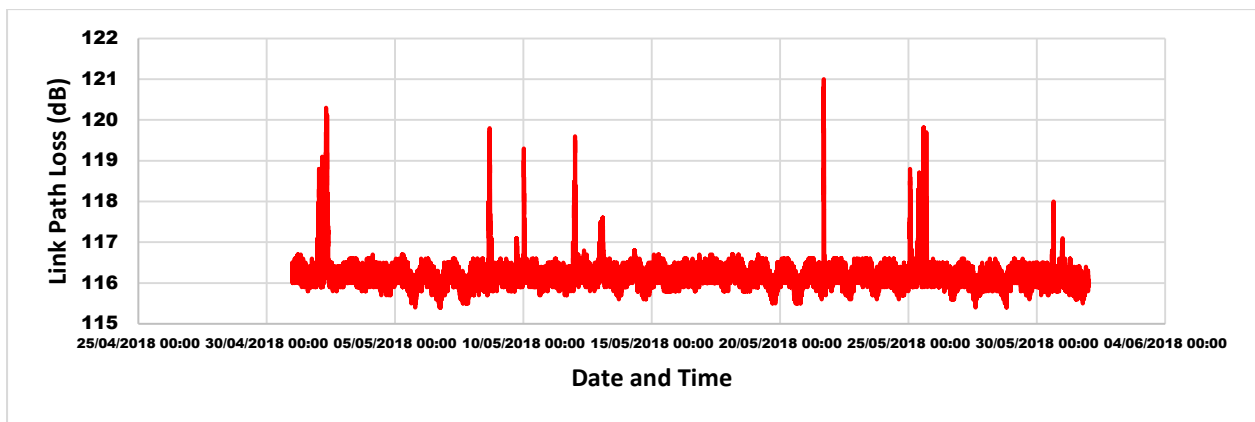
Figure 5.2.9.2 Link path loss for May 2018

Figure 5.2.38 shows rain rate, while figure 5.2.39 shows link path loss for May 2018. Having considered impacts due to atmospheric gases and rain as per the ITU recommendations, there is a general residue of between 1dB and 2dB path loss throughout the month, interspersed by definite larger peaks ranging from 3dB to 9dB. When plotted against rain rate (mm/hr) there seems to be a direct correlation between the residual path loss and rain duration.
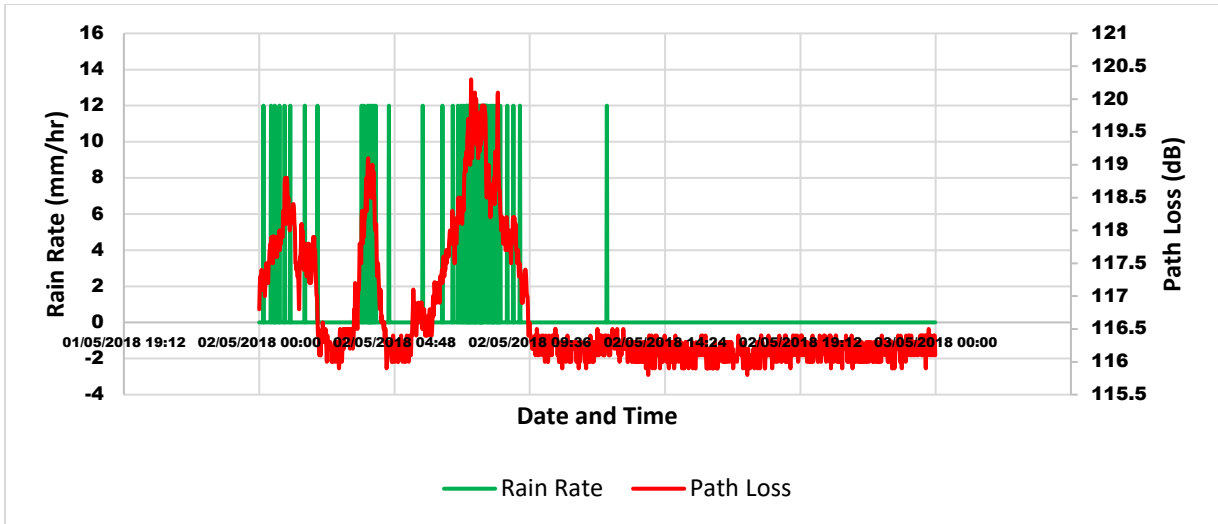
Figure 5.2.9.3 Link path loss plotted against rain rate for 2nd May 2018

Figure 5.2.40 shows link path loss plotted against rain rate for 2nd May 2018. The high peaks in residual path loss correspond to period of sustained rainfall. The isolated rain event at 12:20 pm had no effect on residual path loss.
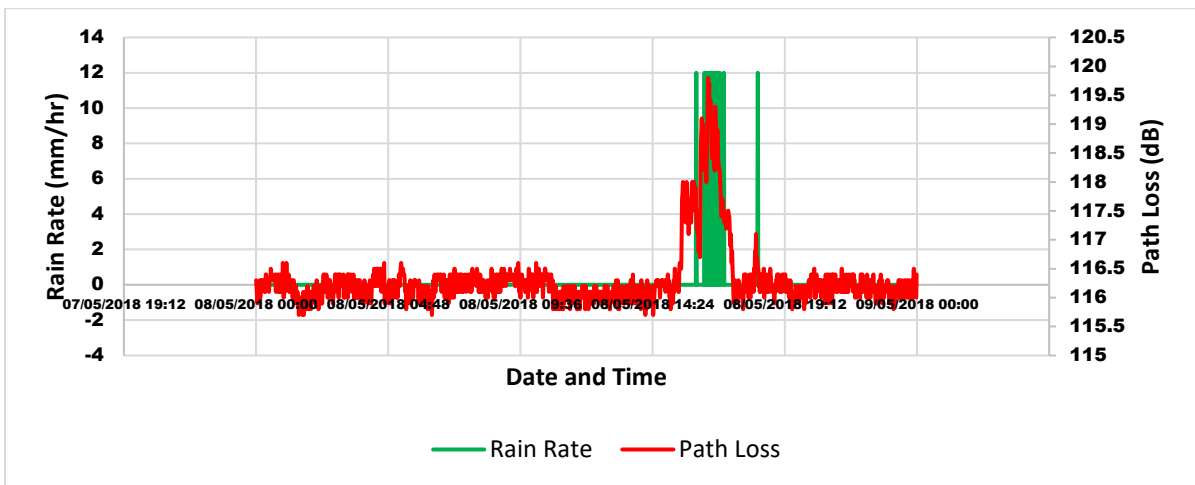
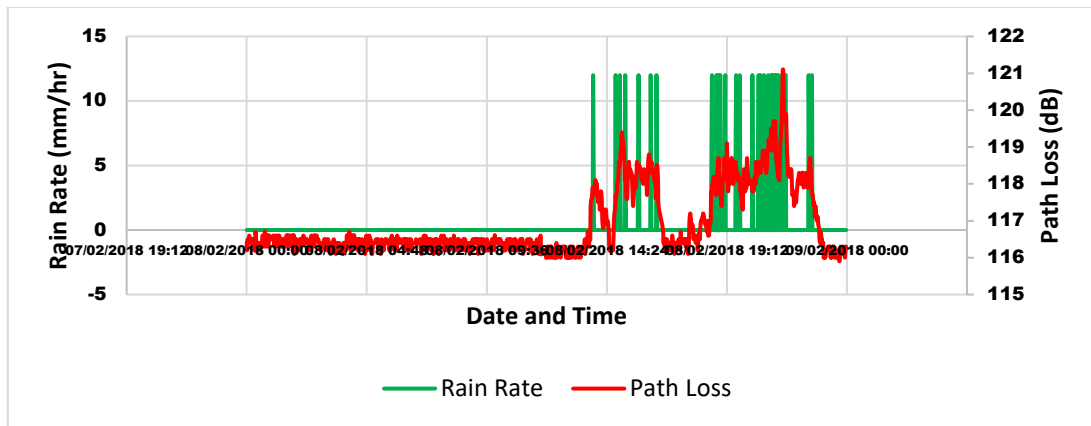*Figure 5.2.9.4 Link path loss plotted against rain rate for 8th May 2018*

Link path loss plotted against rain rate for 8th May 2018. The high peaks in residual path loss correspond to period of sustained rainfall as shown in figure 5.2.41

5.2.10 June 2018 Results and Analysis
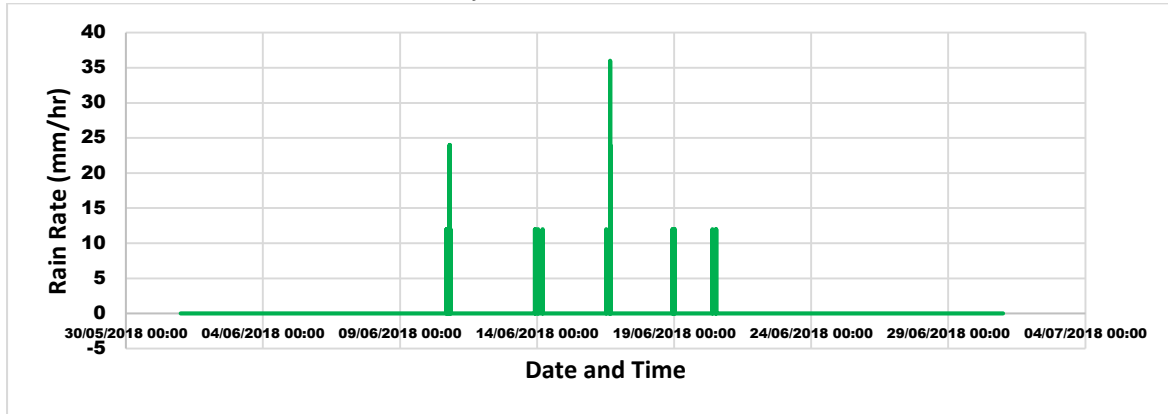
Figure 5.2.10.1 Rain rate (mm/hr) for June 2018
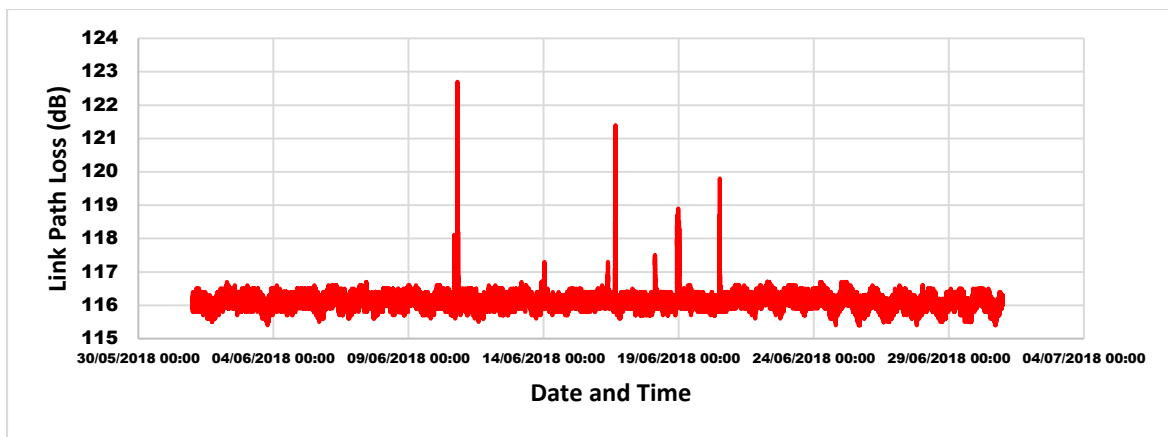
Figure 5.2.10.2 Link path loss for June 2018

Whilst there is a general residue of between 1dB and 2dB throughout the month of May 2018, there are also definite larger peaks of discrepancy ranging from 3dB to 9dB that are unaccounted. Looking for other factors, which could account for these, Figure 5.2.43 shows the residual link path loss for June 2018 while, figure 5.2.42 plotted rain rate (mm/hr). Interestingly, there appears to be a correlation between the peaks in the residual path loss and fluctuations in pressure.
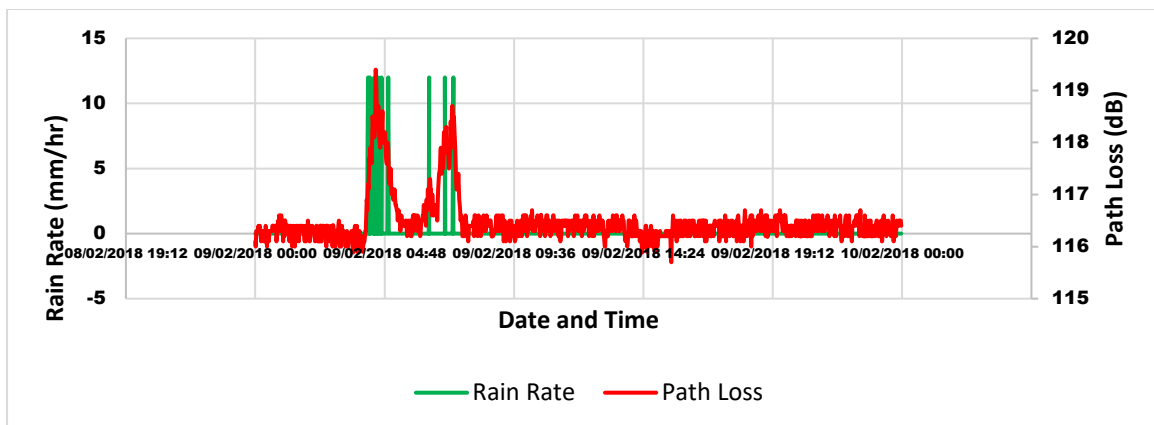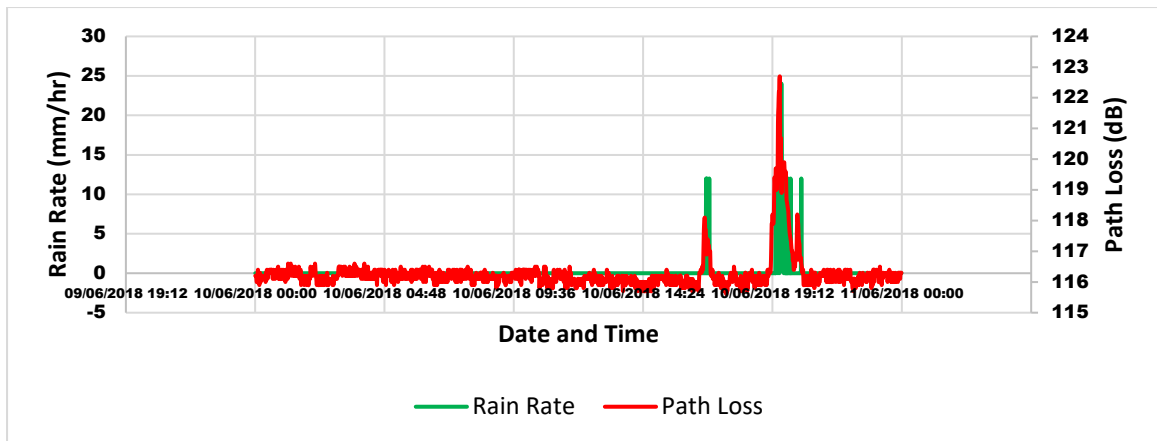
Figure 5.2.10.3 Link path loss plotted against rain rate for 10th June 2018

Link path loss plotted against rain rate for 10th June 2018. This figure shows a direct correlation between rain events and the peak residual path loss. The period of sustained rainfall correlates to the high peaks in residual path loss.

5.2.11 July 2018 Result and Analysis
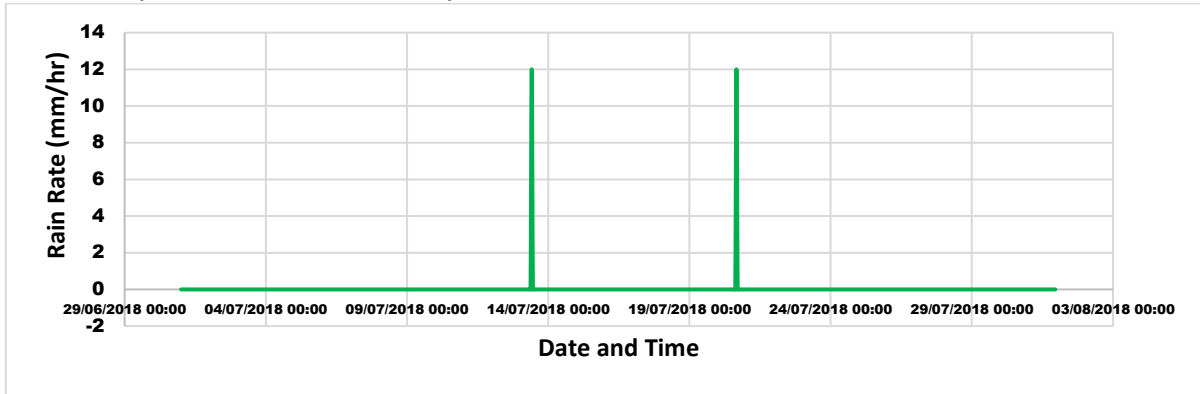
Figure 5.2.11.1 Rain rate (mm/hr) for July 2018
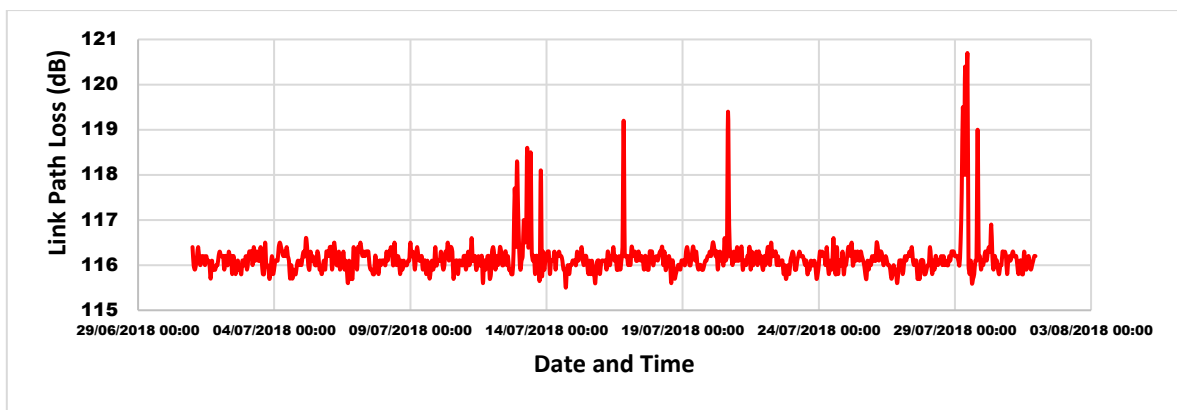
Figure 5.2.11.2 Link path loss for July 2018

The results for July 2018 are not analysed because of changes in the granularity of the weather data from per minute interval to an hourly interval. This change in the mode of collecting weather data has a detrimental effect to the entire month of July in terms of synchronising with the 10sec intervals of the radio data.

6   RESIDUAL PATH-LOSS ANALYSIS

6.1   Residual Path Loss Analysis

The calculations of the residual path loss have been described in section 5.2 System Performance data. A more detailed description can be found in section 3.1 of the Theory Analysis.

The Residual Path Loss

To get the residual path loss, the major components of losses such as attenuations due to oxygen absorptions, attenuations due to water vapour absorptions and attenuations due to rain rate are subtracted from the path loss.

Residual Path Loss = Path Loss – attenuation due to Oxygen absorptions – attenuations due to Water Vapour – attenuations due to Rain.

It can be seen from the figures in section 6.1 that all residual path loss has a direct correlation with periods of rain fall. There was no event of high residual path loss without a period of rain. However, this high residual path loss can be attributed to the complex nature of rain. Rain fall can take up different shapes and dimensions, when the raindrop sizes takes up the same shape and size as the radio wave it can lead to attenuations.

The experimental data and results presented confirms that during rain events, there are huge residual path loss that is not captures by the ITU path loss models. However, it cannot make exact conclusions because of the complex nature of rain. The results below show the residual path loss (red) as it compares to rain (green) and barometric pressure (blue).

6.1.1 August 2017 Residual Path Loss

Figure 6.1.1.1 Residual Path Loss for August 2017
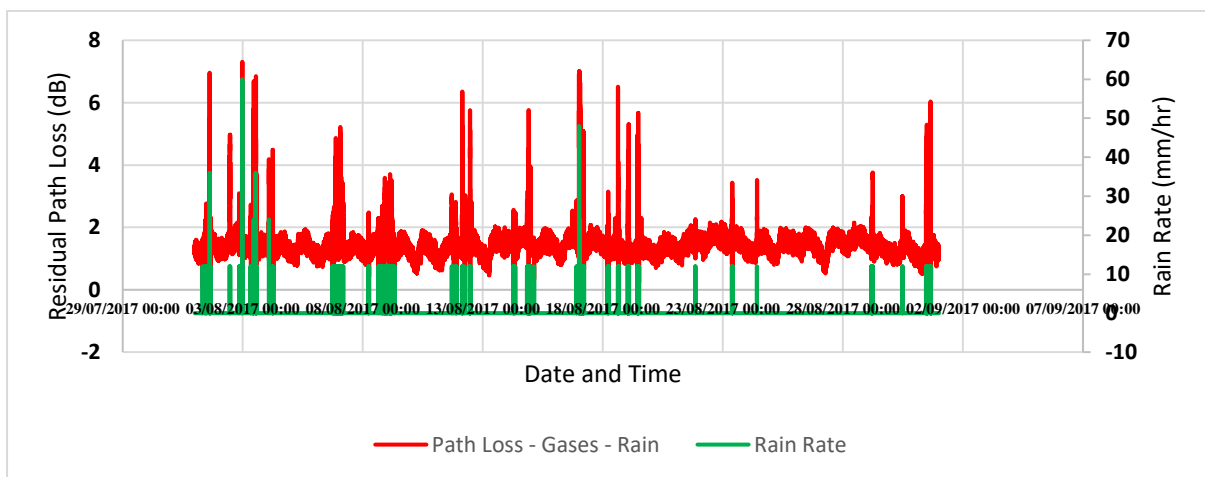
Figure 6.1.1.2 Residual Path Loss (dB) plotted against Rain rate (mm/hr) for August 2017

Figure 6.1.1 shows Residual Path Loss (RPL) for August 2017. Having considered impacts due to atmospheric gases and rain as per the ITU recommendations, there is a general residue that is unaccounted by the ITU. This extra residue shows a strong correlation with rain as shown in figure 6.1.2. the RPL observed for august 2017 is almost 8dB of losses

94

6.1.2 September 2017 Residual Path Loss
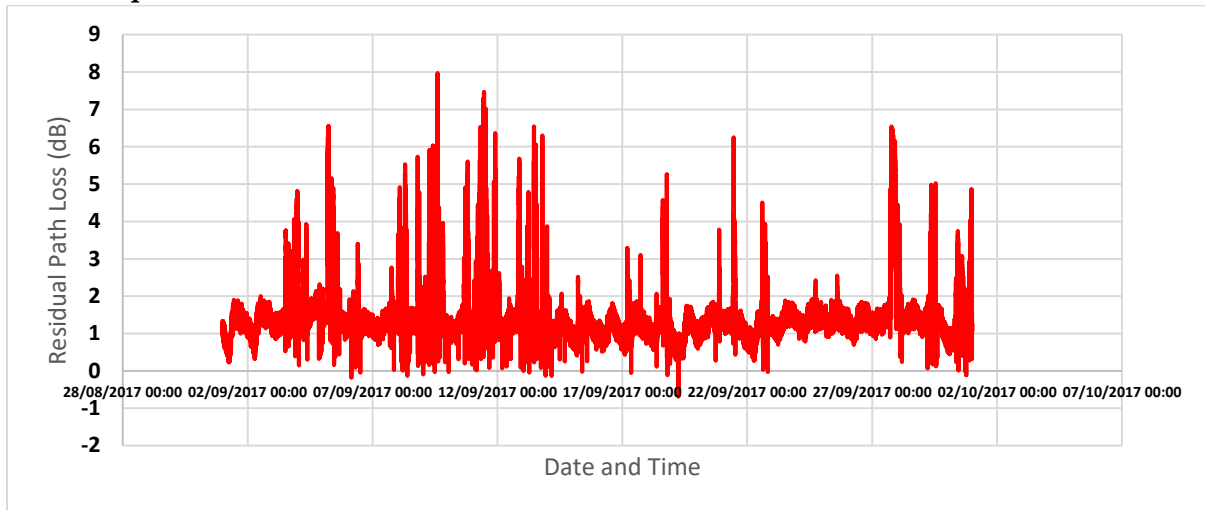
Figure 6.1.2.1 Residual Path Loss for September 2017
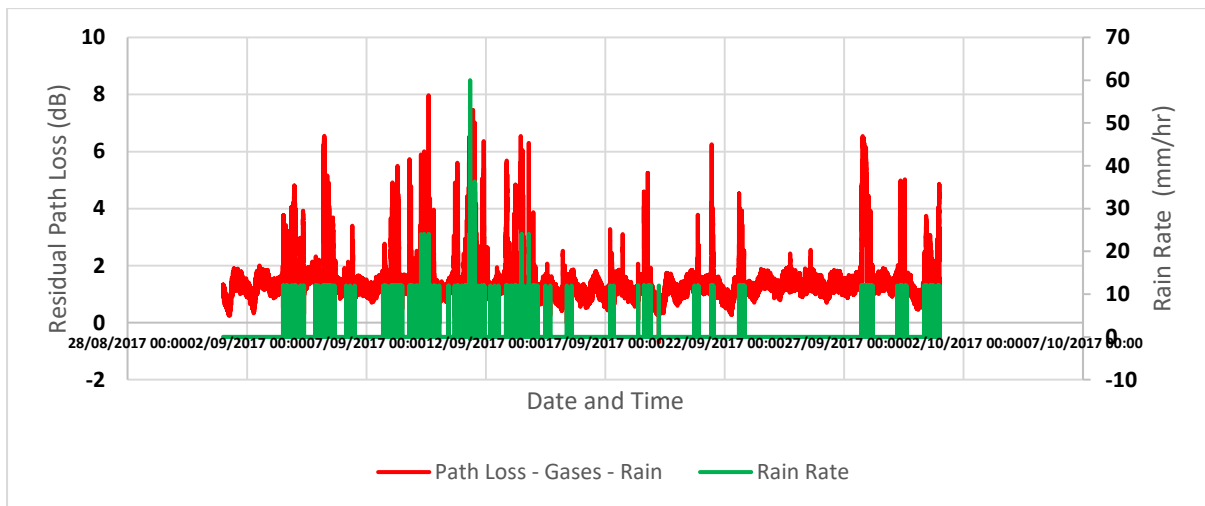
Figure 6.1.2.2 Residual Path Loss (dB) plotted against Rain rate (mm/hr) for September 2017

Figure 6.1.3 shows Residual Path Loss (RPL) for September 2017. Having considered impacts due to atmospheric gases and rain as per the ITU recommendations, there is a general residue that is unaccounted by the ITU. This extra residue shows a strong correlation with rain as shown in figure 6.1.4. The RPL observed for September 2017 is almost 8dB of losses.

6.1.3 October 2017 Residual Path Loss
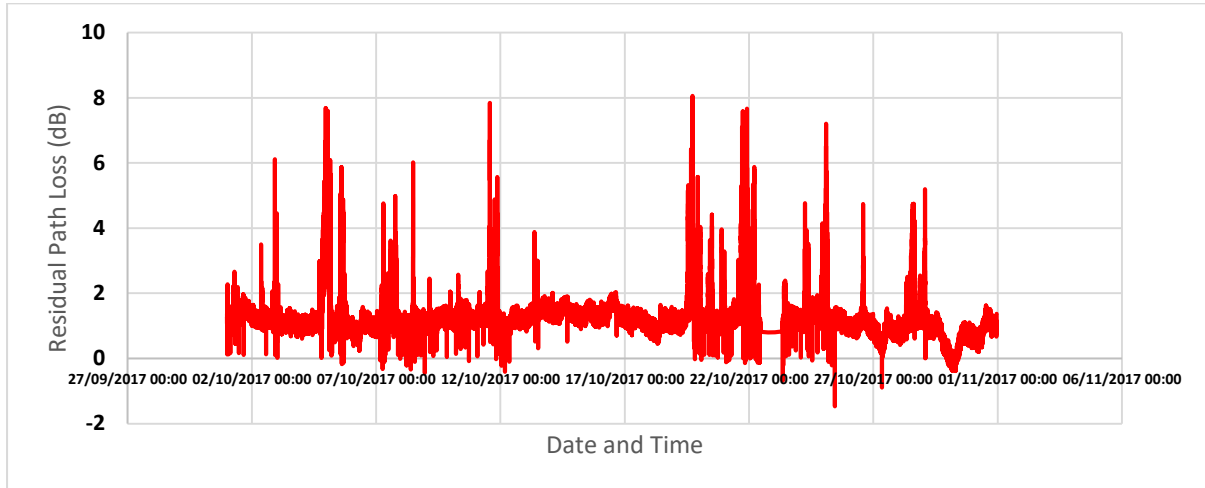
Figure 6.1.3.1 Residual Path Loss for October 2017
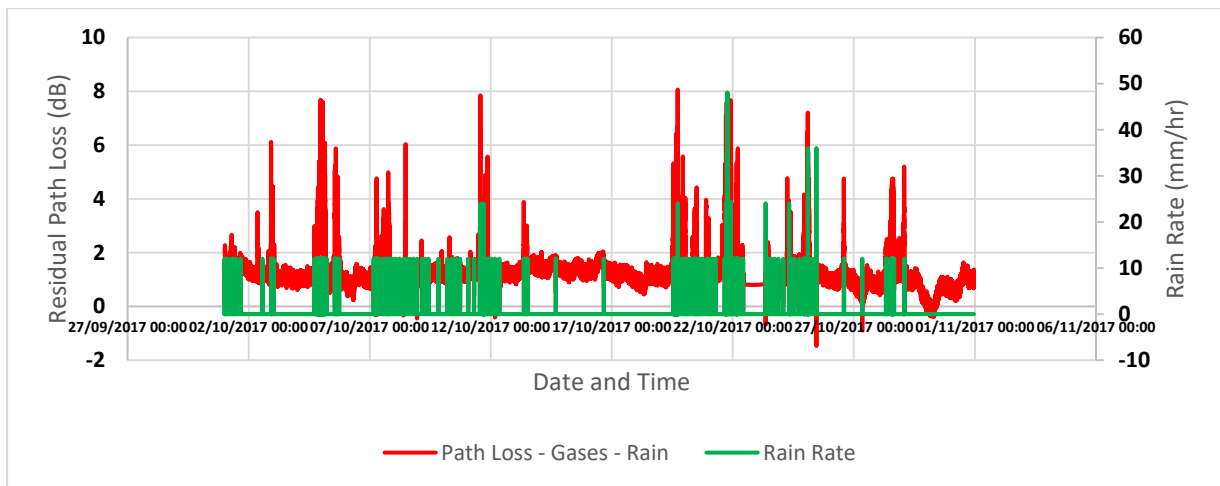
Figure 6.1.3.2 Residual Path Loss (dB) plotted against Rain rate (mm/hr) for October 2017

Figure 6.1.5 shows Residual Path Loss (RPL) for October 2017. Having considered impacts due to atmospheric gases and rain as per the ITU recommendations, there is a general residue that is unaccounted by the ITU. This extra residue shows a strong correlation with rain as shown in figure 6.1.6. The RPL observed for October 2017 is almost 8dB of losses.

6.1.4   November 2017 Residual Path Loss
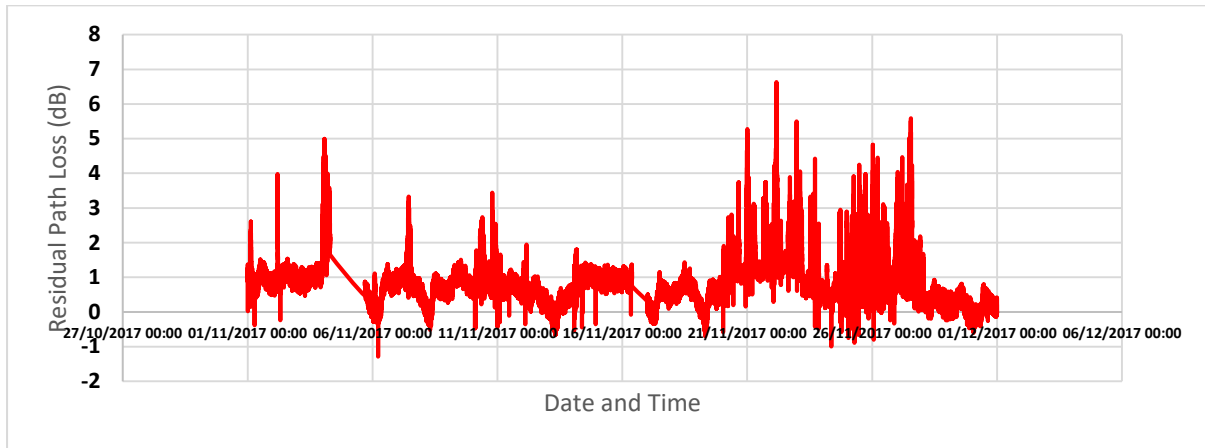
Figure 6.1.4.1 Residual Path Loss for November 2017
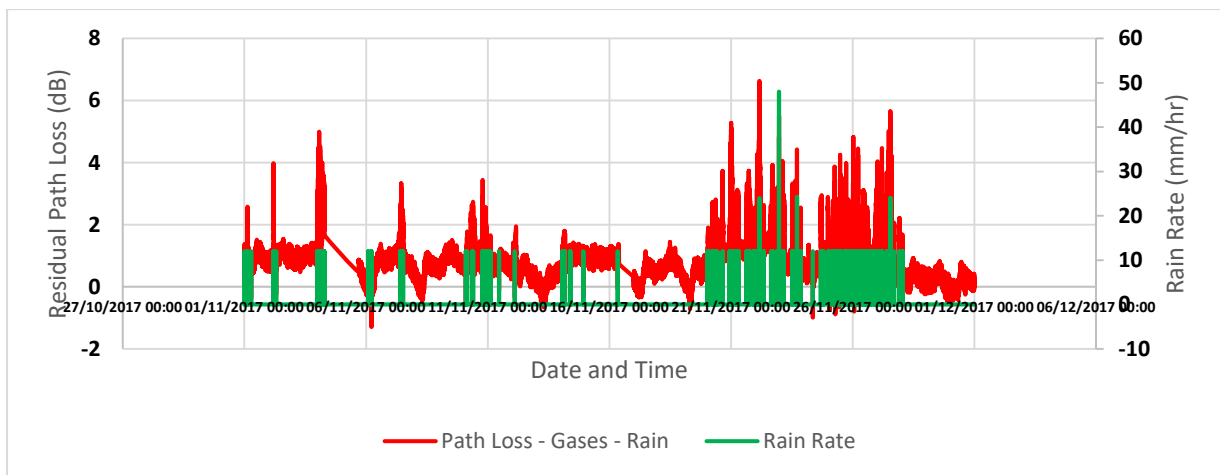
Figure 6.1.4.2 Residual Path Loss (dB) plotted against Rain rate (mm/hr) for November 2017

Figure 6.1.7 shows Residual Path Loss (RPL) for November 2017. Having considered impacts due to atmospheric gases and rain as per the ITU recommendations, there is a general residue that is unaccounted by the ITU. This extra residue shows a strong correlation with rain as shown in figure 6.1.8. The RPL observed for November 2017 is almost 7dB of losses.

6.1.5   December 2017 Residual Path Loss
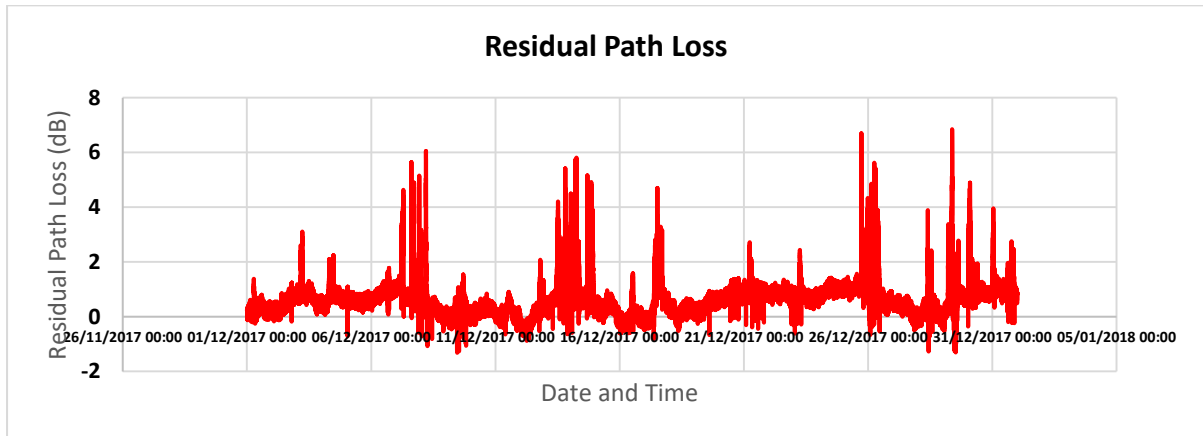
Figure 6.1.5.1 Residual Path Loss for December 2017
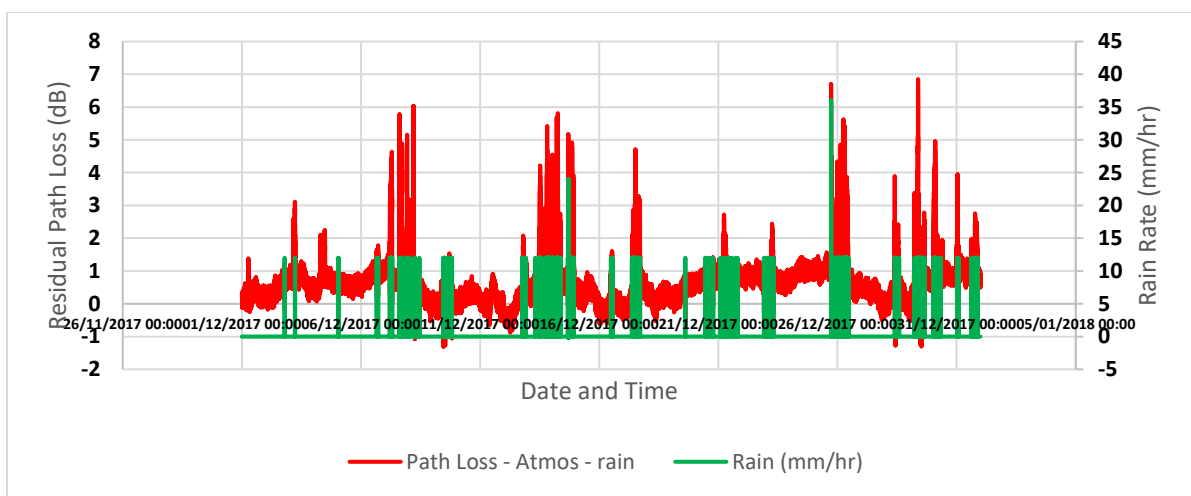
Figure 6.1.5.2 Residual Path Loss (dB) plotted against Rain rate (mm/hr) for December 2017

Figure 6.1.9 shows Residual Path Loss (RPL) for December 2017. Having considered impacts due to atmospheric gases and rain as per the ITU recommendations, there is a general residue that is unaccounted by the ITU. This extra residue shows a strong correlation with rain as shown in figure 6.1.10. The RPL observed for December 2017 is almost 7dB of losses.

6.1.6 January 2018 Residual Path Loss
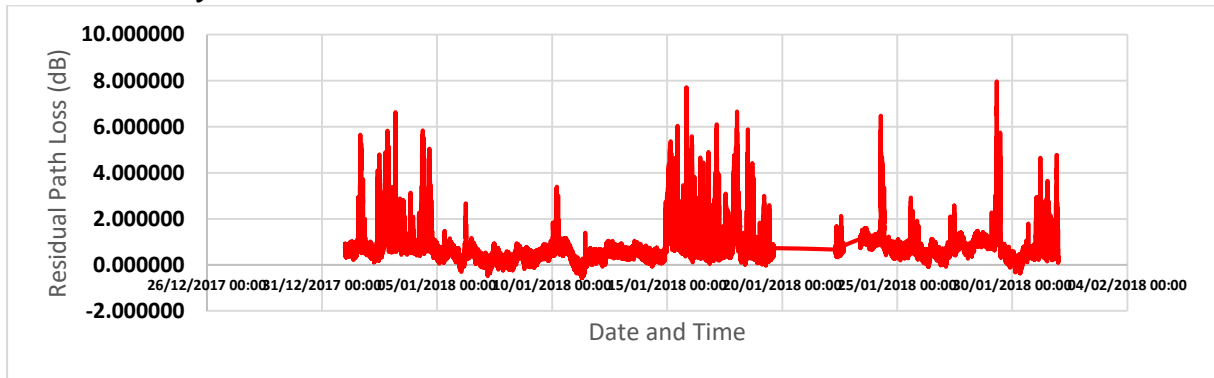
Figure 6.1.6.1 Residual Path Loss for January 2018
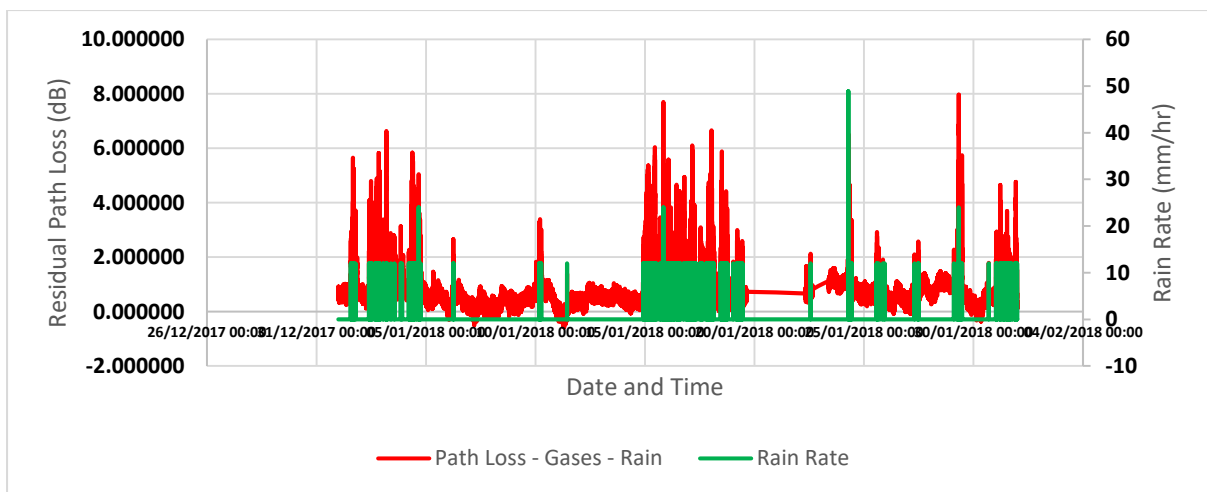
Figure 6.1.6.2 Residual Path Loss (dB) plotted against Rain rate (mm/hr) for January 2018

Figure 6.1.11 shows Residual Path Loss (RPL) for January 2018. Having considered impacts due to atmospheric gases and rain as per the ITU recommendations, there is a general residue that is unaccounted by the ITU. This extra residue shows a strong correlation with rain as shown in figure 6.1.12. The RPL observed for January 2018 is almost 8dB of losses.

6.1.7 February 2018 Residual Path Loss
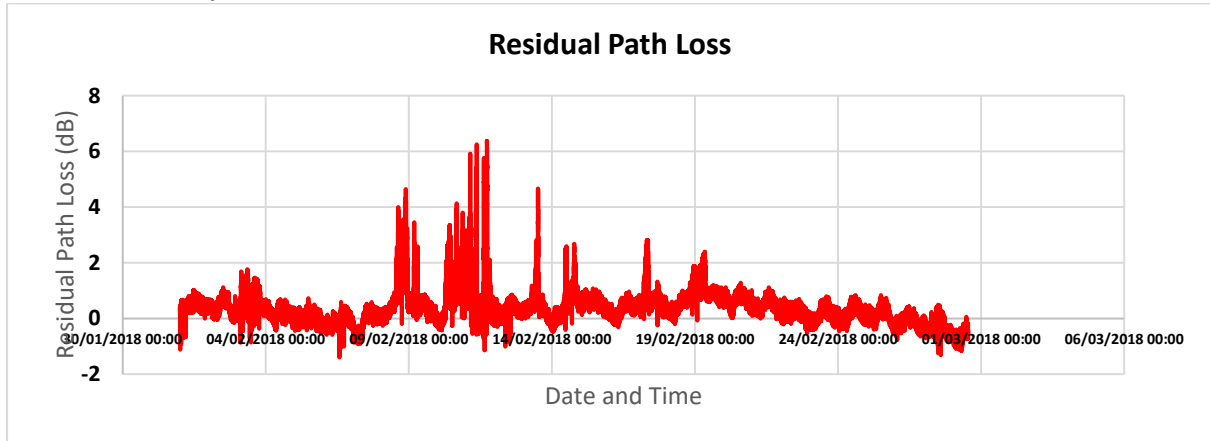
Figure 6.1.7.1 Residual Path Loss for February 2018
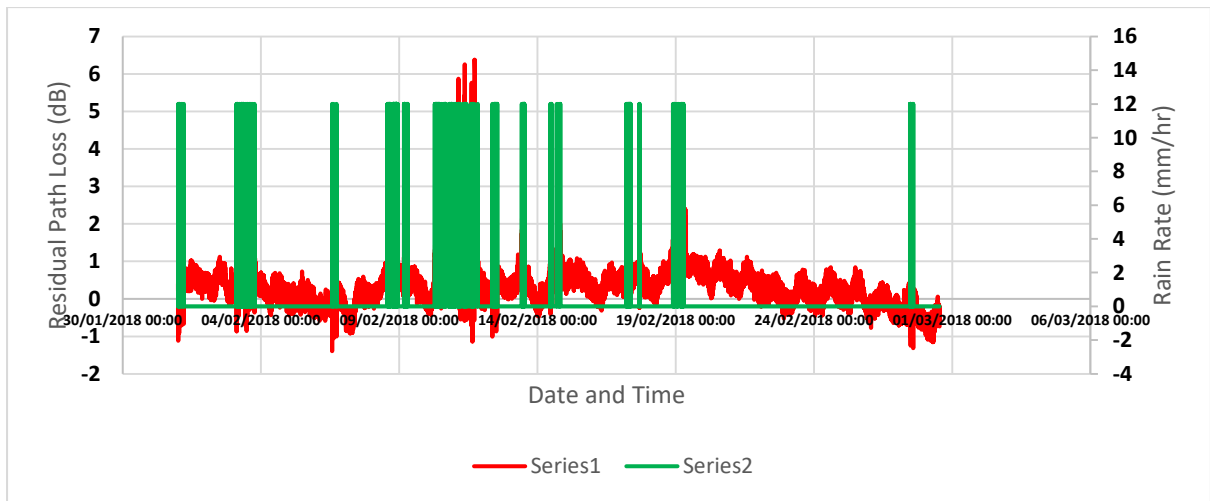
Figure 6.1.7.2 Residual Path Loss (dB) plotted against Rain rate (mm/hr) for February 2018

Figure 6.1.13 shows Residual Path Loss (RPL) for February 2018. Having considered impacts due to atmospheric gases and rain as per the ITU recommendations, there is a general residue that is unaccounted by the ITU. This extra residue shows a strong correlation with rain as shown in figure 6.1.14. The RPL observed for February 2018 is almost 7dB of losses.

6.1.8 April 2018 Residual Path Loss
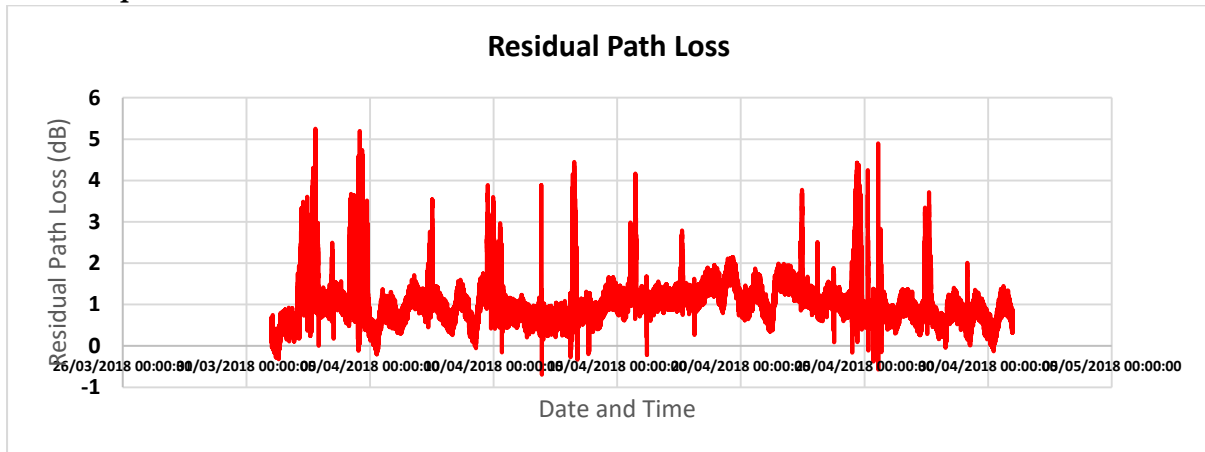
Figure 6.1.8.1 Residual Path Loss for April 2018
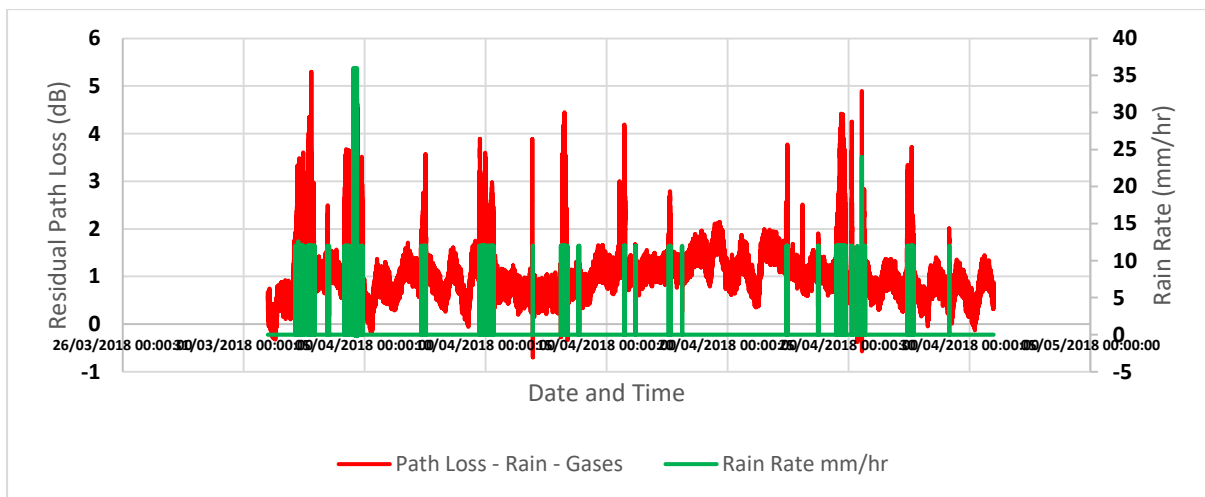
Figure 6.1.8.2 Residual Path Loss (dB) plotted against Rain rate (mm/hr) for April 2018

Figure 6.1.15 shows Residual Path Loss (RPL) for April 2018. Having considered impacts due to atmospheric gases and rain as per the ITU recommendations, there is a general residue that is unaccounted by the ITU. This extra residue shows a strong correlation with rain as shown in figure 6.1.16. The RPL observed for April 2018 is almost 6dB of losses.

6.1.9 May 2018 Residual Path Loss
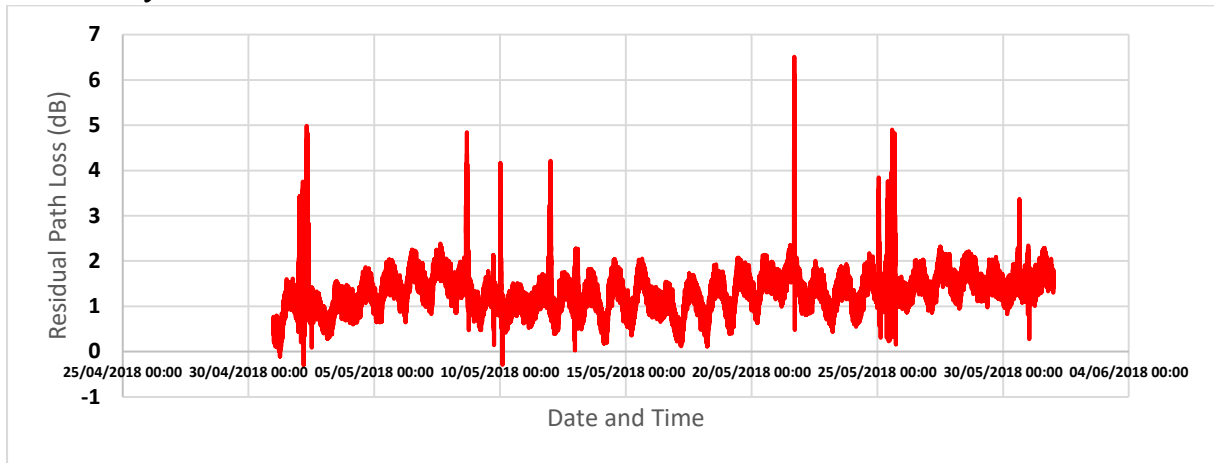
Figure 6.1.9.1 Residual Path Loss for May 2018
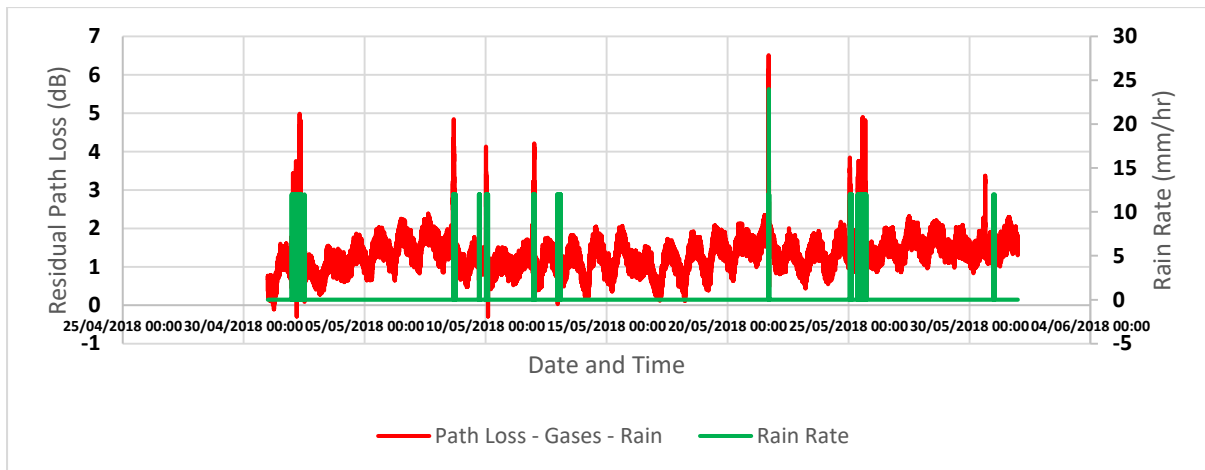
Figure 6.1.9.2 Residual Path Loss (dB) plotted against Rain rate (mm/hr) for May 2018

Figure 6.1.17 shows Residual Path Loss (RPL) for May 2018. Having considered impacts due to atmospheric gases and rain as per the ITU recommendations, there is a general residue that is unaccounted by the ITU. This extra residue shows a strong correlation with rain as shown in figure 6.1.18. The RPL observed for May 2018 is upto 6dB of losses.
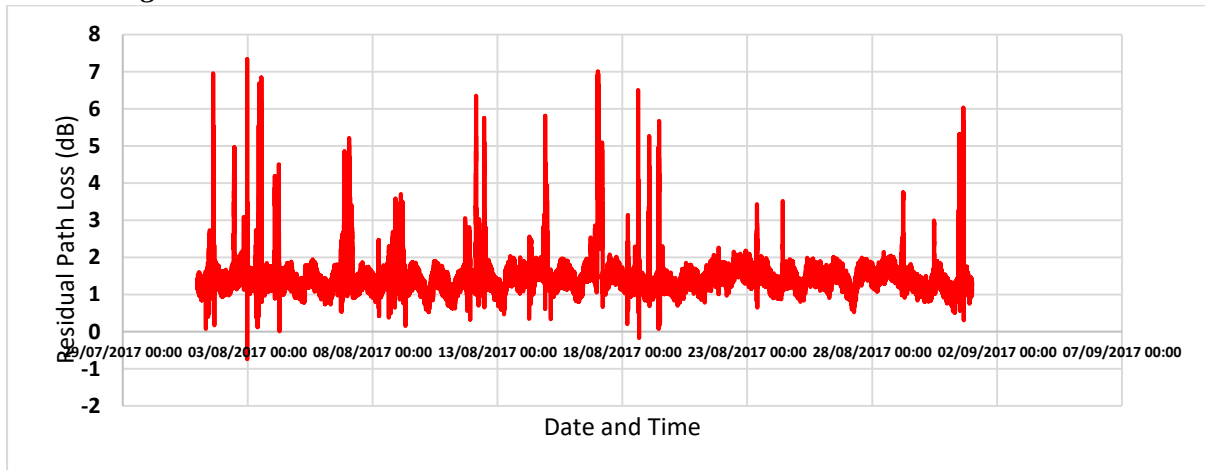
6.1.10 June 2018 Residual Path Loss
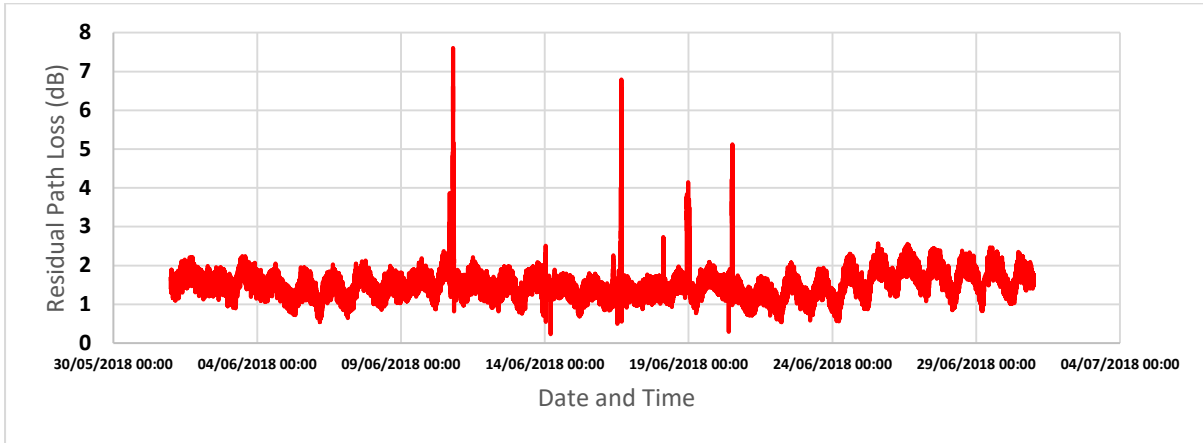
Figure 6.1.10.1 Residual Path Loss for June 2018
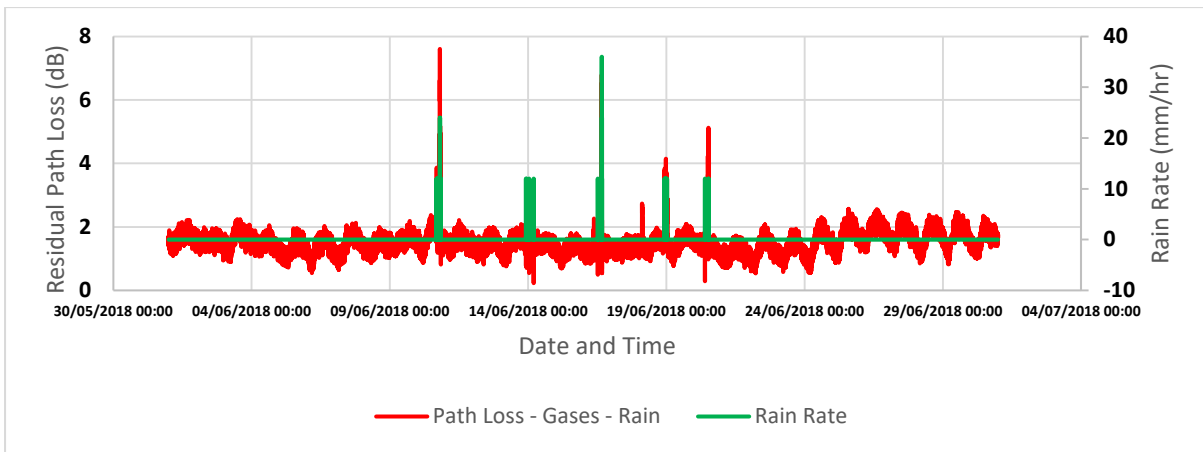
Figure 6.1.10.2 Residual Path Loss (dB) plotted against Rain rate (mm/hr) for June 2018

7 STATISTICAL ANALYSIS

7.1 Availability

60GHz Link Availability:

Link availability is typically expressed as "n-nines" where n is "five" for 99.999% availability (< 5.3 minutes of outage per year), "four" for 99.99% availability (< 53 minutes of outage per year), etc. Note that an "outage" may not actually mean that data is no longer delivered by the link, but rather indicates that the data bit error rate (BER) is elevated above a specified level (which varies by manufacturer). We quote link availability based on when the BER exceeds one error per trillion bits (10^{-12} BER). However, other manufacturers routinely specify link availability based on less stringent BER limits. The main factors in determining the availability of 60GHz links are heavy rainfall probabilities and distance.

For this research, the outages are calculated based on a threshold when the received packets are less than (one) 1 Mbps availability. By adding all he times when the received packets are less than 1 Mbps we have the total outages for each month. The table below shows the monthly availability in seconds. Figure 7.1.1 shows a graphical representation of the periods of unavailability on a monthly basis in seconds.
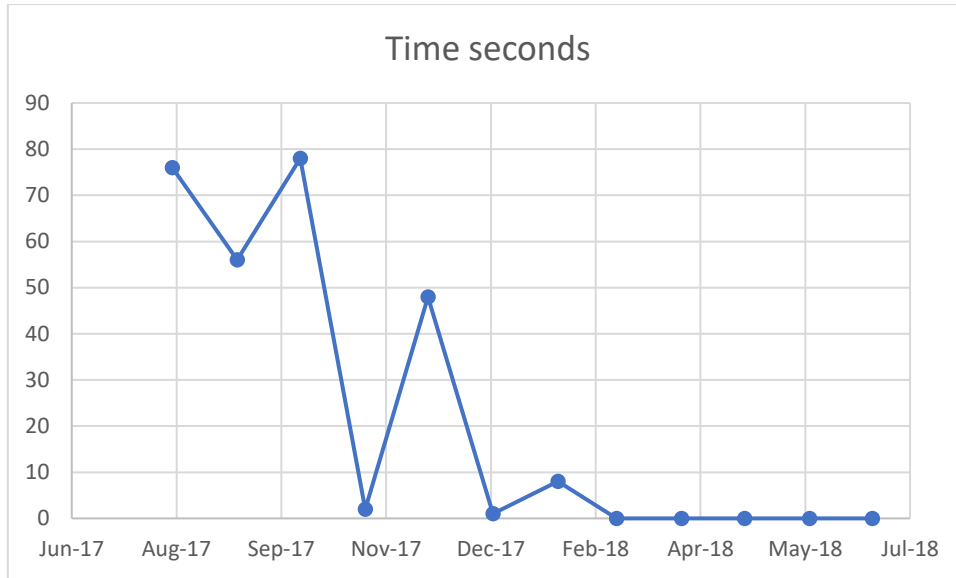
Figure 6.1.10.1 Link availability per month

Table 7.1.1 Link Availability

Month	Availability (seconds)
August 2017	76
September 2017	56
October 2017	78
November 2017	2
December 2017	48
January 2018	1
February 2018	8
March 2018	0
April 2018	0
May 2018	0
June 2018	0
July 2018	0
Total Availability	269 = 4.48 mins

The link availability calculated for this research is 4.48 mins as shown in table 7.1.1.

This time of outages corresponds to "5-nines'' because the total time of outages during the year was less than 5.3 minutes. Therefore, this system has 99.999% availability (< 5.3 minutes of outage per year).

7.2 **Statistical Analysis**

Statistical analysis is the process of generating statistics from stored data and analysing the results to deduce or infer meaning about the underlying dataset or the reality that it attempts to describe. Statistics is defined as "…the study of the collection, analysis, interpretation, presentation, and organization of data." (Diggle, 2015).

Statistical analysis may be used to:

Present key findings revealed by a dataset.

Summarize information.

Calculate measures of cohesiveness, relevance, or diversity in data.

Make future predictions based on previously recorded data.

Test experimental predictions.

One of the most common techniques used for summarising is graphs. Descriptive analysis is an important first step for conducting statistical analyses (Mertler & Reinhart, 2016). It helps describe and understand the features of a specific data set by giving short summaries about the sample and measures of the data. It gives an idea of the data distribution, it also helps detect outliers and typos, and enable you identify associations among variables.

The best approach for conducting descriptive analyses is to first decide about the types of variables and then use approaches for descriptive analyses based on variable types.

Descriptive statistics are used to repurpose hard-to-understand quantitative insights across a large data set into bite-sized descriptions. All descriptive statistics are either measures of central tendency or measures of variability, also known as measures of dispersion.

Measures of central tendency focus on the average or middle values of data sets; whereas, measures of variability focus on the dispersion of data. These two measures use graphs, tables, and general discussions to help people understand the meaning of the analysed data.

Measures of central tendency describe the centre position of a distribution for a data set. A person analyses the frequency of each data point in the distribution and describes it using the mean, median, or mode, which measures the most common patterns of the analysed data set.

Measures of variability, or the measures of spread, aid in analysing how spread-out the distribution is for a set of data. Measures of variability help communicate this by describing the shape and spread of the data set. Range, quartiles, absolute deviation, and variance are all examples of measures of variability.

7.2.1   *Mean, Variance, and Standard Deviation*

In order to examine the distribution of data samples, the descriptive statistics plots are commonly used. The approximation of standard deviation is done from input data samples. Let $X_1, X_2, ..., X_n$ be n observations of a random variable X. We wish to measure the average of $X_1, X_2, ..., X_n$ in some sense. One of the most commonly used statistics is the mean, μ_X, defined by the formula

$$\mu_X = \bar{X} = \frac{1}{n} \sum_{i=1}^{n} X_i$$

Next, we wish to obtain some measure of the variability of the data. The statistics most often used are the variance and the standard deviation $\sigma_X = \sqrt{\sigma_X^2}$. We have

$$\sigma_X = \sqrt{\frac{1}{n}\left\{ \sum_{i=1}^{n} X_i^2 - \frac{1}{n}\left(\sum_{i=1}^{n} X_i \right)^2 \right\}}$$

It is easy to show that the variance is simply the mean squared deviation from the mean.

Table 7.2.1 Descriptive statistics

	Mean Path Loss	Path Loss Std. Dev	Path Loss Variance	Rain Mean	Rain Std. Deviation	Rain Variance	RPL Mean	RPL Std. Deviat	RPL Variance	RPL Max
Aug-17	116.2325	0.51112	0.261	0.1139	1.28501	1.651	1.4969	0.47595	0.227	7.31
Sep-17	116.3375	0.62481	0.39	0.165	1.506	2.268	1.4241	0.63658	0.405	8.88
Oct-17	116.3267	0.61236	0.375	0.16	1.464	2.143	1.3077	0.6402	0.41	8.06
Nov-17	116.4452	0.49769	0.248	0.1265	1.26	1.588	0.8222	0.62695	0.393	6.63
Dec-17	116.5131	0.53351	0.285	0.17	1.417	2.009	0.6584	0.61671	0.38	6.85
Jan-18	116.4962	0.53936	0.291	0.1559	1.39334	1.941	0.783	0.66208	0.438	7.97
Feb-18	116.5115	0.4457	0.199	0.07	0.893	0.798	0.4013	0.59656	0.356	6.38
Mar-18										
Apr-18	116.3712	0.53988	0.291	0.1377	1.34462	1.808	1.0845	0.54875	0.301	5.25
May-18	116.2289	0.33972	0.115	0.04	0.705	0.497	1.3408	0.43097	0.186	6.51
Jun-18	116.1566	0.25126	0.063	0.0163	0.51326	0.263	1.5292	0.34011	0.116	7.61
Jul-18	116.1524	0.43697	0.19	0.03	0.626	0.391	1.7237	0.4377	0.192	6.07

In table 7.2.1 all the descriptive statistics are displayed.

7.2.1.1   Average (Mean)

Average is mostly the Mean. It has the advantage that it uses all the data values obtained and can be used for further statistical analysis. However, it can be skewed by 'outliers', values which are atypically large or small. The average gives you information about the size of the data, whether it is large or small. There are three measures of average: mean, median and mode.
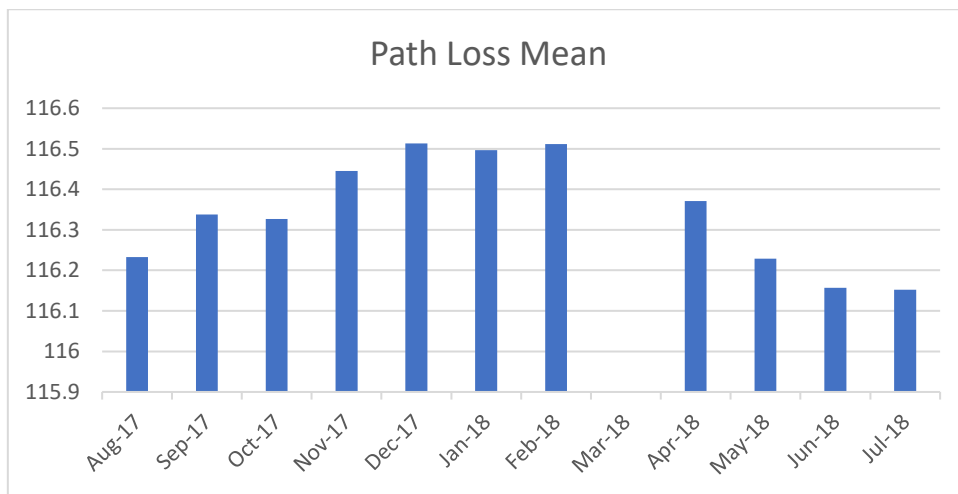
Figure 7.2.1.1 Mean Path-loss per month

Figure 7.2.1.1 shows the spread of average path loss for each month. December 2017 and February 2018 had the highest average path loss at 116.5dB, while, the lowest average path loss was recorded in June/July of 2018 at 116.1dB.
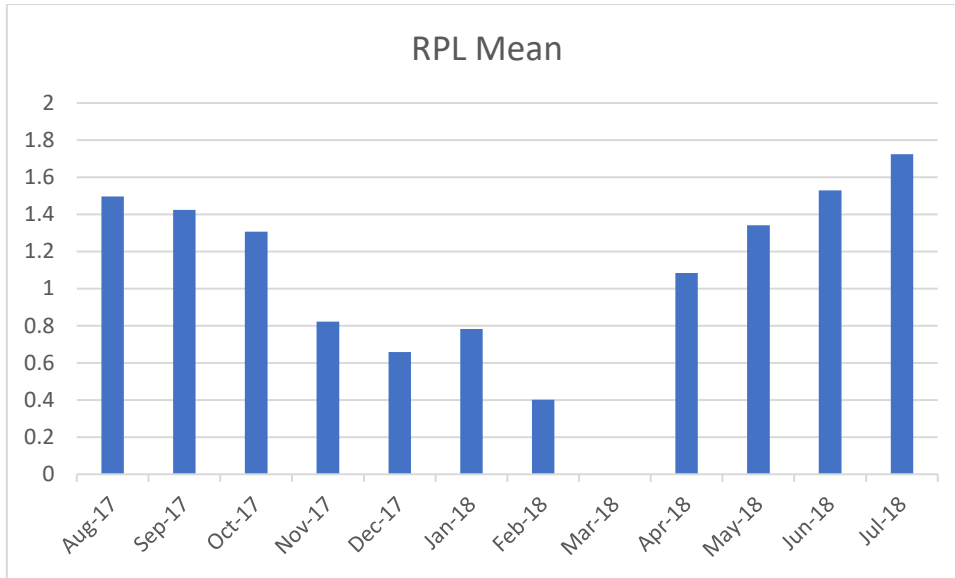
Figure 7.2.1.2 Mean Residual Path Loss per month
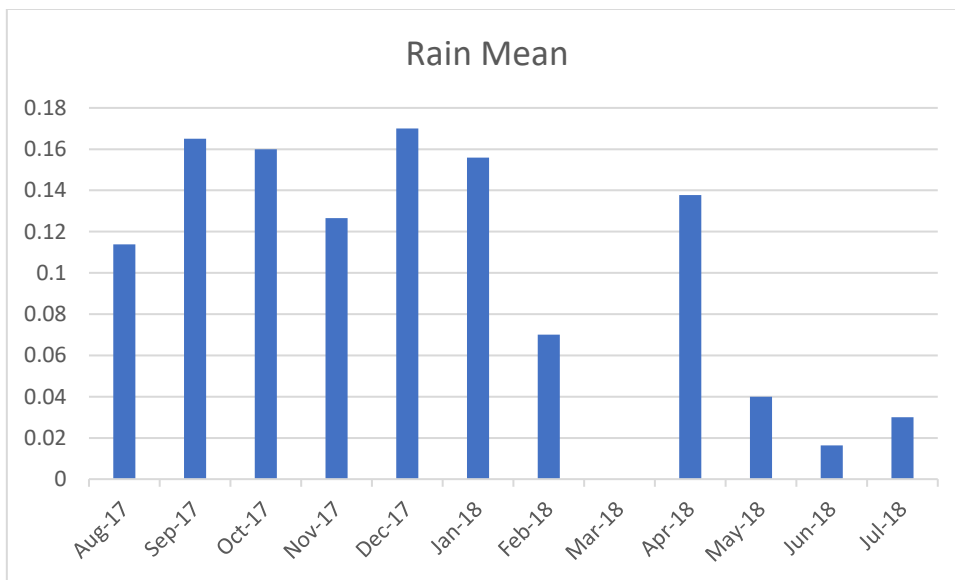
Figure 7.2.1.3 Mean Rain per month

In terms of rain, figure 7.2.1.3 shows the average rain for every month. December 2017 had the highest average rain rate at 0.17 mm/hr, while, June 2018 had the lowest average rain rate at 0.016 mm/hr. From figure 7.2.1.3 the months of May, June and July 2018 had very little rain.

7.2.1.2   Variance

Variance (σ2) in statistics is a measurement of the spread between numbers in a data set. That is, it measures how far each number in the set is from the mean and therefore from every other number in the set. Variance is calculated by taking the differences between each number in the data set and the mean, then squaring the differences to make them positive, and finally dividing the sum of the squares by the number of values in the data set.

The variance is the square of the standard deviation. They are calculated by:

calculating the difference of each value from the mean;

squaring each one (to eliminate any difference between those above and below the mean);

summing the squared differences;

dividing by the number of items minus one.

This gives the variance.
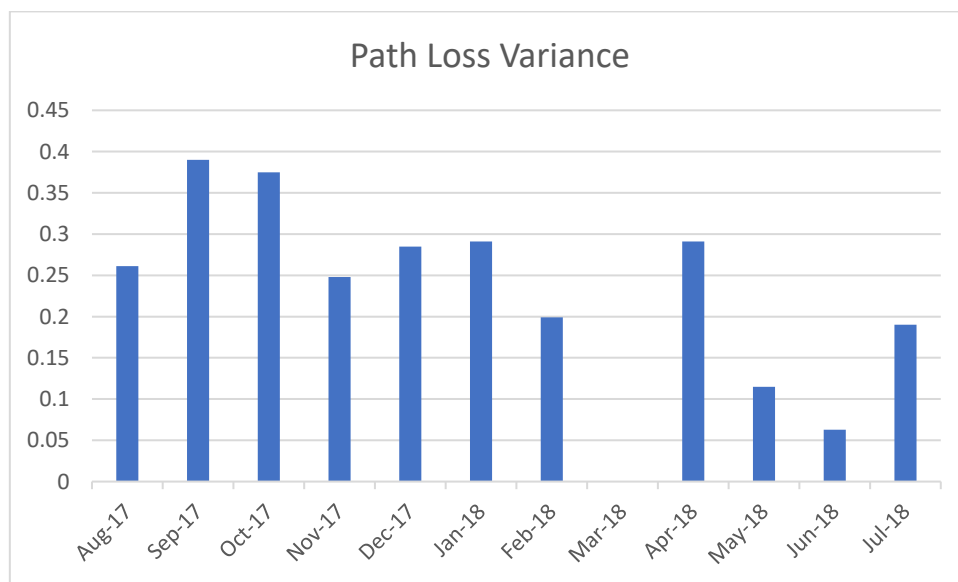
Figure 7.2.1.4 Variance of the Path-loss per month

The figure 7.2.1.4 shows variance of the Path Loss. June 2018 had the lowest variance in path loss at 0.063dB, while, September 2017 had the highest variance in path loss at 0.39dB.
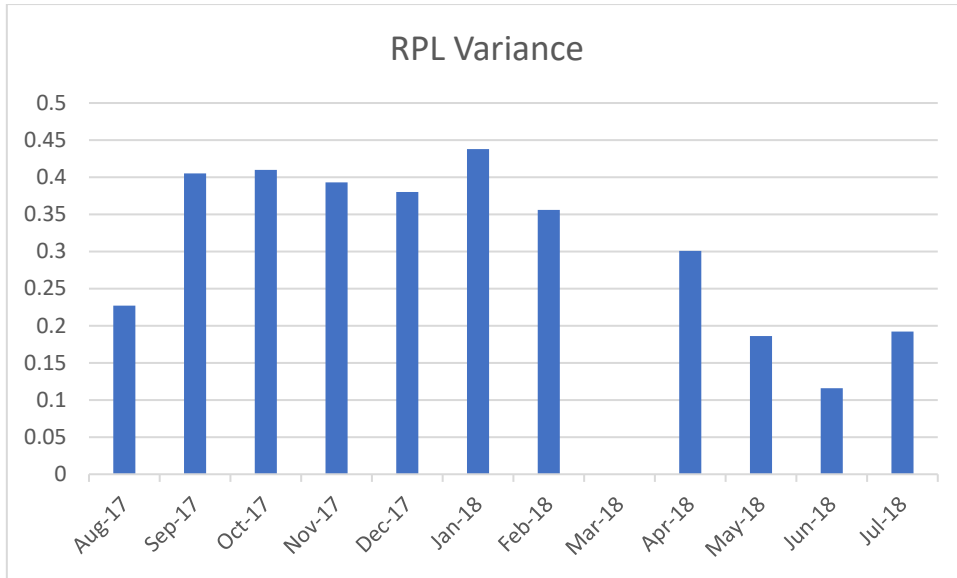
Figure 7.2.1.5 Variance of the Residual Path Loss per month

For the residual path loss, the variance as shown in figure 7.2.1.5 had January 2018 as the month with the highest RPL variance at 0.438dB, while the lowest RPL variance was in June 2018 at 0.116dB.
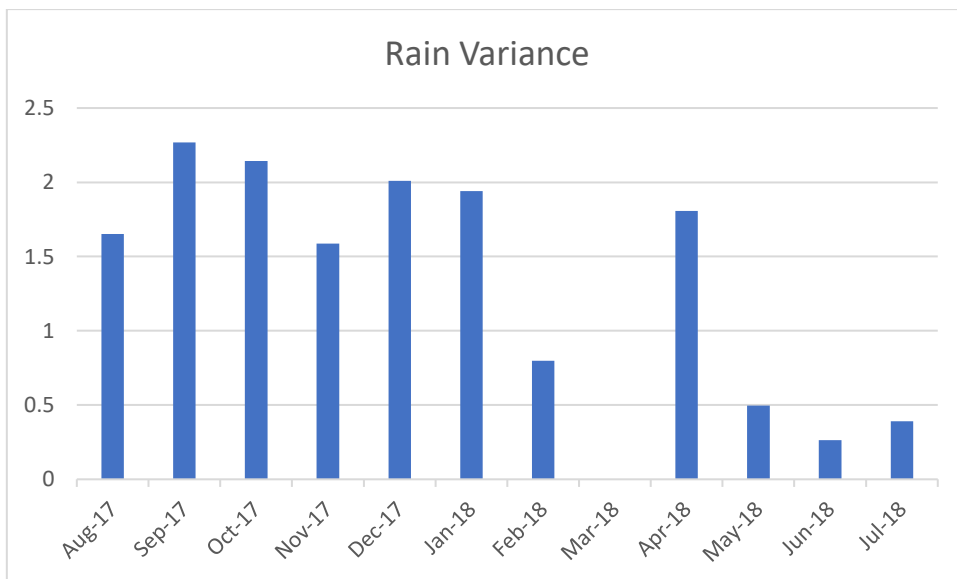
Figure 7.2.1.6 Variance of the Rain per month

in figure 7.2.1.6, the rain variance was low for the months of May, June and July 2018 because it was relatively dry periods with little or no rain, while august 2017 to January 2018 experienced high rainfall hence, high rain variance.

7.2.1.3 Standard Deviation

The standard deviation measures the average spread around the mean, and therefore gives a sense of the 'typical' distance from the mean. The standard deviation is a statistic that measures the dispersion of a dataset relative to its mean and is calculated as the square root of the variance. It is calculated as the square root of variance by determining the variation between each data point relative to the mean. If the data points are further from the mean, there is a higher deviation within the data set; thus, the more spread out the data, the higher the standard deviation.
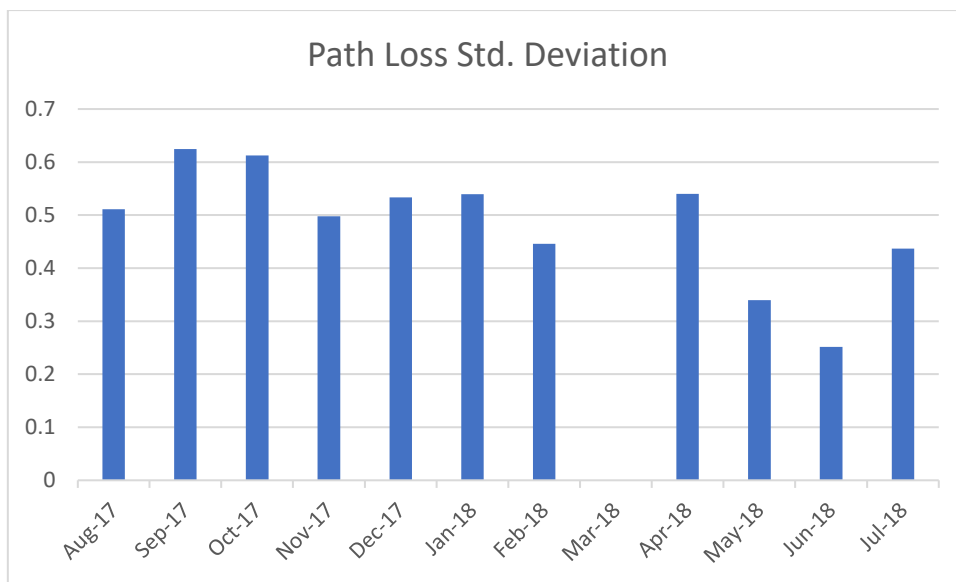
Figure 7.2.1.7 Standard Deviation of the Path-loss per month

From figure 7.2.1.7 the standard deviation for path loss is shown. September 2017 had the highest path loss standard deviation at 0.62dB, while 0.25dB standard deviation was the lowest recorded in June 2018.
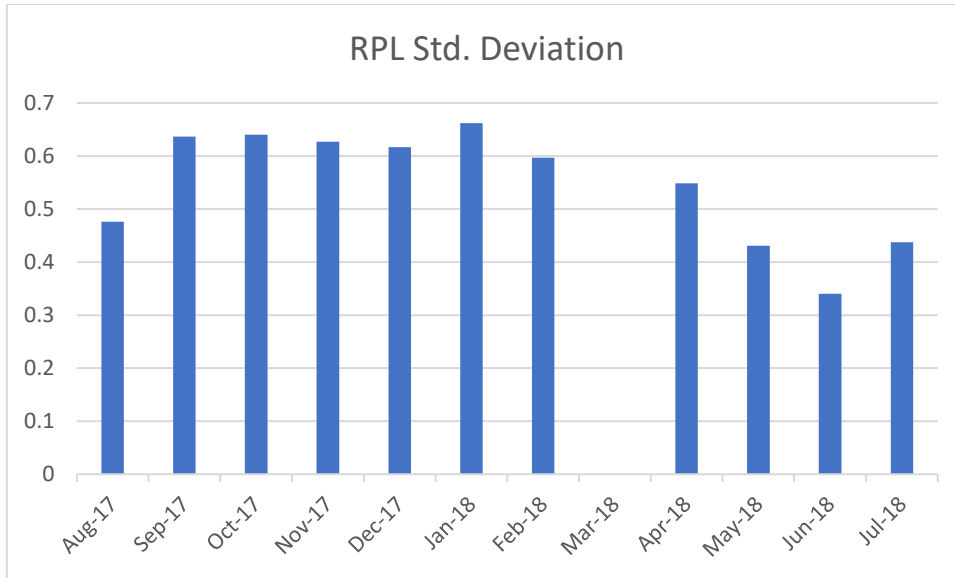
Figure 7.2.1.8 Standard Deviation of the Residual Path Loss per month

For the Residual Path Loss, the standard deviation is shown in figure 7.2.1.8. January 2018 had

the highest RPL standard deviation at 0.66dB, while June 2018 had the lowest RPL standard

deviation at 0.34dB.
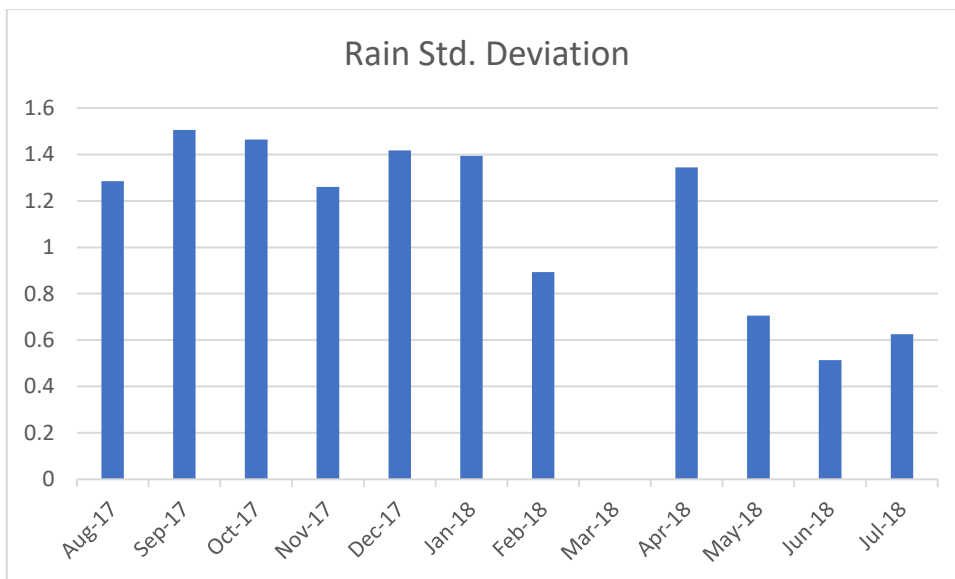
Figure 7.2.1.9 Standard Deviation of Rain per month

Figures 7.2.1.9 shows standard deviation for rain rate. The months with low rain rate such as

May, June and July 2018 had the lowest standard deviation. The months with high rain rates

such as August 2017 to January 2018 had the highest standard deviation.
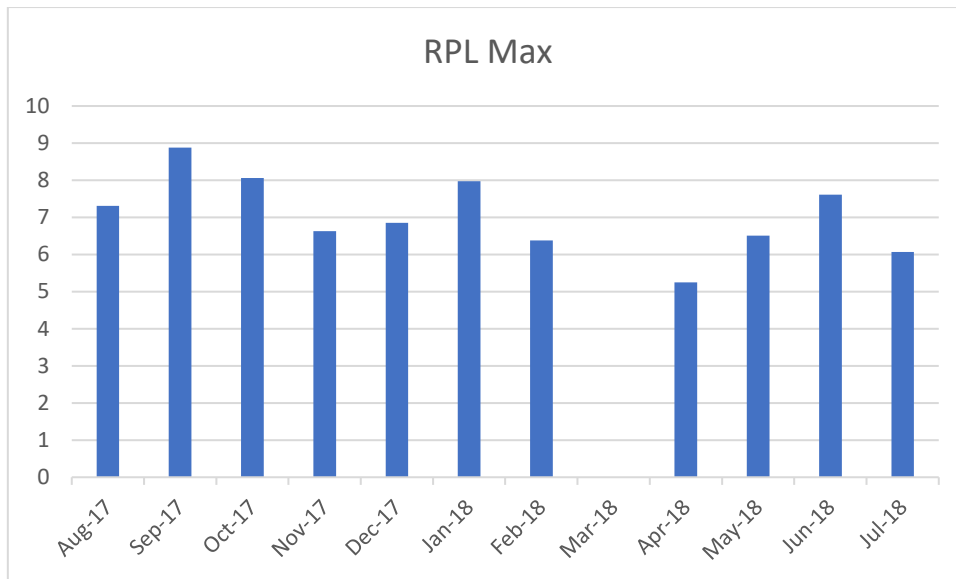
Figure 7.2.1.10 Maximum Residual Path Loss for every month

In figure 7.2.1.10 the maximum RPL shows the maximum residual path los that was observed for each month. September 2017 had the highest RPL at 8.88dB while, April 2018 had the lowest maximum RPL value at 5.25dB. This graph in figure 7.2.1.10 shows RPL never exceeded 9dB.

7.3 Summary

Variance is derived by taking the mean of the data points, subtracting the mean from each data point individually, squaring each of these results and then taking another mean of these squares. Standard deviation is the square root of the variance.

The variance helps determine the data's spread size when compared to the mean value. As the variance gets bigger, more variation in data values occurs, and there may be a larger gap between one data value and another. If the data values are all close together, the variance will be smaller. This is more difficult to grasp than are standard deviations, however, because variances represent a squared result that may not be meaningfully expressed on the same graph as the original dataset.

Standard deviations are usually easier to picture and apply. The standard deviation is expressed in the same unit of measurement as the data, which is not necessarily the case with the variance. Using the standard deviation, statisticians may determine if the data has a normal curve or other mathematical relationship. If the data behaves in a normal curve, then 68% of the data points will fall within one standard deviation of the average, or mean data point. Bigger variances cause more data points to fall outside the standard deviation. Smaller variances result in more data that is close to average.

8   CONCLUSIONS

8.1   **Summary**

This thesis has presented measurements obtained from a trial to evaluate the weather resilience of a 60GHz point-to-point link operating over 210m. This chapter summarizes the main results and contributions of this work and outlines for future work. There is significant interest in the adoption of 60GHz as a potential candidate for back-haul connectivity in future 5G ultra-dense network architectures. However, it is important for operators to understand how such links perform across a range of weather conditions and to appreciate what configuration is required to ensure network reliability.

This research work is a collaboration between University of Salford, NEC Europe, EE and British Telecommunications BT, which installed short (210 m) terrestrial links operating at 60 GHz and connecting two building rooftops in the university main campus. The radio equipment installation in 2016 is the starting point of this trial. However, there were hardware and software adjustments performed to optimize the system to increase the dynamic range available to quantify the atmospheric effects. Since July 2017, no changes have been applied to the equipment, which is therefore considered as the starting month for the collected propagation data on daily basis. The daily data collection only began in August 2017 and has since been collecting daily data comprising parameters of link performance such as transmit and receive power levels, bit error rate, packets sent and received etc. Besides the propagation, data derived from the link transceivers, the atmospheric conditions are monitored by a nearby weather station installed at a building rooftop adjacent to the radio link. Received and transmit power levels data are processed to identify and isolate different events and quantify the path loss induced by the events, the results point out the higher prediction accuracy achieved by

116

exploiting the information on rain rate, rain duration and the rate of change of atmospheric pressure around the oxygen lines.

All data are centralized to a PC and the following pre-processing steps are performed:

I. Time –UTC) The time stamps of the samples are accurately synchronized (Coordinated Universal

II. Outliers such as blanks erased in pairs.

8.2 Conclusions

The thesis is based on the propagation characteristics of 60GHz V-Band radio against varying weather conditions in a university environment. The experiment is a point-to-point link set between two building rooftops with 210m and a clear line of sight.

There are two different sets of data being measured, the propagation data such as power levels coming from the radio equipment and the weather data from the nearby weather monitoring station. These measurements are synchronised in a single time granularity and the results of path loss compared to the theoretical predictions of the ITU–P series models. There is a clear relationship between link path loss and rainfall at 60GHz. Generally, there is a residue of 1dB to 2dB across every month all through the experiment. This extra residual of the path loss of 1dB to 2dB is very consistent. But there are the high peaks in residue with losses ranging from 3dB to 9dB. These high residual losses can be correlated to periods of sustained rainfall.

Whilst these measurements have shown the well-understood impact of atmospheric gases and rain at 60GHz, the results obtained also suggest that other factors are influencing the performance of the point-to-point link. Should this prove to be the case then it will be necessary to accommodate these impacts within any future analysis and deployment of systems operating at 60GHz.

The objective of this work was to study the propagation characteristics of 60GHz millimetre wave through the atmosphere in a university environment. Another aim of this research was to gather experimental data that will give engineers additional information on the suitability of millimetre wave for the design of communications systems along with a link in an urban environment. Success has been achieved in this experiment and the results can be summarised as follows.

It is difficult to arrive at a definite conclusion on an attenuation and rainfall coefficient for 60GHz because the effect of different parameters on attenuation rainfall measurements and the lack of homogeneity in rainfall intensity along the propagation path may contribute to a considerable discrepancy between the experimental measurement results and the theoretical predictions. Hence, it can be concluded that the theoretical predictions give quite a good estimate of rain-induced attenuations and can be useful in system design. Having considered impacts due to atmospheric gases and rain as per the ITU recommendations, there is a general residue of between 1dB and 2dB path loss throughout the month, interspersed by definite larger peaks ranging from 3dB to 9dB.

Although attenuations due to rainfall impose severe limitations on the reliability of a 60GHz. From the engineers' point of view, the reliability of this system is crucial. This 210m line of sight radio link at 60GHz frequency has been operated non-stop for over one year in Salford without any major link failures or drops in throughput.

In terms of availability, the total outages for the year was 4.48 minutes which give availability of 99.999 because its less than 5.3 mins. This means that the system had very good availability.

In summary, there is significant interest in the adoption of 60GHz as a potential candidate for back-haul connectivity in future 5G ultra-dense network architectures. Precise knowledge of the 60-GHz absorption parameters is required due to the importance of this band for 5G ultra-

dense networks, atmospheric research, wireless communication, remote sensing, etc. However, it is important for operators to understand how such links perform across a range of weather conditions and to appreciate what configuration is required to ensure network reliability. Most importantly, there is the need for a new path loss model that will capture the extra effect of rainfall and other atmospheric parameters for millimetre wave frequencies.

8.3   Future work

The research for understanding and characterizing the propagation effects of 60GHz millimetre wave through the atmosphere is in its early stages. Although this thesis examines the effects of rainfall and changes in barometric pressure on a point-to-point radio signal in the 60 GHz band, avenues for research still exist. There is a need for improvement in the methodology of data collection and processing.

An experiment to determine the amount of water present in the atmosphere is crucial to give a comprehensive understanding of the exact contributions to path loss of the various parameters in the atmosphere. It is obvious that rain determines link feasibility for outdoor links at millimetre wave frequencies, but knowledge of other forms of water present in the atmosphere need to be measured and studied.

This experiment only considers the link on a horizontal path but makes no mention of the atmospheric effects on a slant path etc. it would be interesting to observe how 60GHz signals perform at different altitudes and elevation angles.

The major difficulty faced by engineers planning links at 60GHz is how to compensate for attenuation issues and balance the huge bandwidth available. It is important for engineers to allocate the proper fade margin on the link budget required to perform. There is also the

suggestion to understand the effects of oxygen at 60GHz. There is a need for research that will create an understanding of the properties of the oxygen molecule in the atmosphere. It is also important to understand how to compensate for oxygen properties as barometric pressure changes regularly. The equipment used in this research is unable to make measurements of the Oxygen lines due to pressure change at 60GHz hence restricting our study of these effects in details. An accurate measurement of pressure broadening and line shifts at 60GHz is essential.

Clearly, from this experiment results, there are about 3dB to 9dB of residual losses due to rainfall duration and other atmospheric parameters. These losses and others need to be studied intensively to build a new path loss model for millimetre wave that will capture most of the attenuations due to atmospheric effects for 5G infrastructure.

REFERENCES

1. Adhikari, P., 2008. Understanding millimetre wave wireless communication. VP of Business Development for Network Solutions, Loea Corporation, San Diego.

2. Ali, I., 2013. Bit-error-rate (BER) simulation using MATLAB. International Journal of Engineering Research and Applications, 3(1), pp.706-711.

3. Alrabadi, O.N., Perruisseau-Carrier, J. and Kalis, A., 2012. MIMO transmission using a single RF source: theory and antenna design. *IEEE Transactions on antennas and propagation*, *60*(2), pp.654-664.

4. Alade, M.O., 2013. Investigation of the Effect of Ground and Air Temperature on Very High Frequency Radio Signals. *Journal of Information Engineering and Applications www.iiste.org Vol*, *3*.

5. Aragon-Zavala, A., 2008. Antennas and propagation for wireless communication systems. John Wiley & Sons.

6. Annemalla, H. and Kumari, C.U., 2015. Estimation of Bit Error Rate and Mean Square Error in 4G Wireless Networks.

7. Ayanoglu, E., Gitlin, R.D., La Porta, T.F., Paul, S. and Sabnani, K.K., Lucent Technologies Inc., 1997. Adaptive forward error correction system. U.S. Patent 5,600,663.

8. Baldemair, R., Irnich, T., Balachandran, K., Dahlman, E., Mildh, G., Selen, Y. Osseriran, A. (2015). Ultra-dense networks in millimetre-wave frequencies. IEEE Communications Magazine, 53(1), 202-208.

9. Bandyopadhyay, L.K., Chaulya, S.K. and Mishra, P.K., 2009. *Wireless communication in underground mines: RFID-based sensor networking*. Springer Science & Business Media.

10. Baranger, M., 1958. Problem of overlapping lines in the theory of pressure broadening. *Physical Review*, *111*(2), p.494.

11. Baranger, M., 1958. Simplified quantum-mechanical theory of pressure broadening. *Physical Review*, *111*(2), p.481.

12. Barclay, L. ed., 2003. Propagation of radio waves (Vol. 502). Iet.

13. Belcher, R.W., 1990. Extremely High Frequency (EHF) Low Probability of Intercept (LPI) communication applications (Doctoral dissertation, Monterey, California: Naval Postgraduate School).

14. Bhatia, A. and Sharma, P., 2014. Analysis of Different Modulation Techniques In LTE SC-FDMA Uplink.

15. Bhawna, M.A., 2015. Analysis & Review Equalization & Channel Estimation for OFDM & CDMA.

16. Bloom, S., Korevaar, E., Schuster, J. and Willebrand, H., 2003. Understanding the performance of free-space optics. *Journal of optical Networking*, *2*(6), pp.178-200.

17. Bowers, N, 2014. Riding on the back of millimetre waves retrieved on 10th august 2017 from http://wireless.electronicspecifier.com/rf-microwave/riding-on-the-back-of-millimetre-waves

18. CableFree "Introduction to Millimetre Wave Technology for V-Band" retrieved on 10th August 2017 from http://www.cablefree.net/wirelesstechnology/millimeter-wave-technology/v-band-MMW-technology/

19. Caetano, L. and Li, S., 2005. Benefits of 60 GHz: right frequency, right time. White paper, SiBEAM.

20. Chambers D, 2013. 60GHz point-to-point microwave for small cell backhaul. Retrieved on 20th June 2017 from https://www.thinksmallcell.com/Backhaul/60ghz-point-to-point-microwave-for-small-cell-backhaul.html

21. Choi, S.N., Kim, J., Kim, I.G. and Kim, D.J., 2014. Development of millimeter-wave communication modem for mobile wireless backhaul in mobile hotspot network. *IEIE Transactions on Smart Processing & Computing*, *3*(4), pp.212-220.

22. Clark, I., Burges, A. and Porter-OciusB, G., 2006. Radio Systems at 60GHz and Above.

23. Coldrey, M., 2015. Maturity and field proven experience of millimetre wave transmission. *ETSI White Paper*, (10).

24. Damm, W., 2010. Signal to Noise, Carrier to Noise, Eb/No on Signal Quality Ratios.

25. Dehos, C., González, J.L., De Domenico, A., Ktenas, D. and Dussopt, L., 2014. Millimetre-wave access and backhauling: the solution to the exponential data traffic

increase in 5G mobile communications systems? *IEEE Communications Magazine*, *52*(9), pp.88-95.

26. Diggle, P.J., 2015. Statistics: a data science for the 21st century. *Journal of the Royal Statistical Society: Series A (Statistics in Society)*, *178*(4), pp.793-813.

27. Dipert B, 2009. The Origins of 60GHz: How Does It Work? Retrieved on 15th July 2017 from https://www.edn.com/Home/PrintView?contentItemId=4306116

28. Doan, C.H., Emami, S., Niknejad, A.M. and Brodersen, R.W., 2005. Millimetre-wave CMOS design. *IEEE Journal of solid-state circuits*, *40*(1), pp.144-155.

29. Duck, M. and Read, R., 2003. Data Communications and Computer Networks. Prentice-Hall, Englewood Cliffs, NJ.

30. Duck M; Bishop P; Read R., 1996 Data Communications for Engineers. Addison Wesley Publishing Company

31. Ericsson, A.B., 2015. Delivering high capacity and cost-efficient backhaul for broadBand networks today and in the future.

32. ETSI, E., 302 217-4-2 V1. 5.1 (2010-01). Harmonized European Standard (Telecommunications series).

33. European Computer Manufacturers Association (ECMA) High Rate 60 GHz PHY, MAC and PALs standard, ECMA-387 2nd Edition December 2010, retrieved on 10th august 2017 from https://www.ecma-international.org/publications/files/ECMA-ST/ECMA-387.pdf

34. European Telecommunications Standards Institute. (2015). White Paper no.9 E-Band and V-Band - Survey on status of worldwide regulation. France: ETSI.

35. Fano, U., 1963. Pressure broadening as a prototype of relaxation. *Physical Review*, *131*(1), p.259.

36. FCC Regulation 15.255. Part 15 Rules for Unlicensed Operation in the 57-64 GHz Band retrieved on 14th August 2017 from http://www.gpo.gov/fdsys/pkg/CFR-2013-title47-vol1/pdf/CFR-2013-title47-vol1-sec15-255.pdf

37. FCC, "Millimetre wave Propagation: Spectrum Management Implications," Office of Eng. and Tech., Bulletin no. 70, July 1997.

38. Feldhake, G., 1997. Estimating the attenuation due to combined atmospheric effects on modern earth-space paths. IEEE Antennas and Propagation Magazine, 39(4), pp.26-34.

39. Frenkiel, R., 2002. A brief history of mobile communications. *IEEE Vehicular Technology Society News*, *49*(2), pp.4-7.

40. Frenzel, L., 2013. Millimetre waves will expand the wireless future. Electron. Des. Mag, 61(4), pp.30-36.

41. Gao, Z., Dai, L., Mi, D., Wang, Z., Imran, M.A. and Shakir, M.Z., 2015. MMWave massive-MIMO-based wireless backhaul for the 5G ultra-dense network. *IEEE Wireless Communications*, *22*(5), pp.13-21.

42. Ge, X., Cheng, H., Guizani, M. and Han, T., 2014. 5G wireless backhaul networks: Challenges and research advances. *IEEE Network*, *28*(6), pp.6-11.

43. Ge, X., Tu, S., Mao, G., Wang, M.C. & Han, T. (2016). 5G Ultra-Dense Cellular Networks. IEEE Wireless Communications, 23(1), 72-79.

44. Green, H.E., 2004. Propagation impairment on Ka-band SATCOM links in tropical and equatorial regions. *IEEE Antennas and Propagation Magazine*, *46*(2), pp.31-45.

45. Hakusui, S., 2001. Fixed wireless communications at 60GHz unique oxygen absorption properties. *Disponible [Internet]: http://www.rfglobalnet.com/doc/fixedwireless-communicationsat-60ghz-unique-0001*.

46. Hansryd, J. and Edstam, J., 2011. Microwave capacity evolution. *Ericsson review*, *1*, pp.22-27.

47. Harris Corporation, RF Communications Division, "Radio Communications in the Digital Age", Volume One: HF Technology, Edition 2, © Harris Corporation 2005. Retrieved on 10th July 2017 from http://rf.harris.com/media/Radio%20Comms%20in%20the%20Digital%20Age%20-%201_tcm26-12947.pdf

48. Hettak, K., Delisle, G.Y., Morin, G.A. and Stubbs, M.G., 2009, June. A new type of array antennas fed by cpw for 60 ghz ism applications. In *Antennas and Propagation Society International Symposium, 2009. APSURSI'09. IEEE* (pp. 1-4). IEEE.

49. Hole, K.J. and Oien, G.E., 2001. Adaptive coding and modulation: A key to bandwidth-efficient multimedia communications in future wireless systems. *Telektronikk*, *97*(1), pp.49-57.

50. Houghton, A., 2001. Introduction. In Error Coding for Engineers (pp. 1-14). Springer US.

51. ITU-R P.840-3, 1999. Attenuation due to clouds and fog. ITU-R P.840- 3 Geneva (Switzerland): International Telecommunication Union.

52. ITU-R Recommendation P.837-5, Characteristic of precipitation for propagation modelling, 2007

53. ITU (International Telecommunications Union). (2017). Recommendation ITU-R P.1411-9 Propagation data and prediction methods for the planning of short-range outdoor radio communication systems and radio local area networks in the frequency range 300MHz to 100GHz. Geneva: ITU

54. ITU (International Telecommunications Union). (2016). Recommendation ITU-R P.676-11 Attenuation by atmospheric gases. Geneva: ITU

55. ITU (International Telecommunications Union). (2015). Recommendation ITU-R P.530-16 Propagation data and prediction methods required for the design of terrestrial line-of-sight systems. Geneva: ITU

56. ITU (International Telecommunications Union). (2005). Recommendation ITU-R P.838-3 Specific attenuation model for rain for use in prediction methods. Geneva: ITU

57. IWPC International Wireless Industry Consortium, 2014. Evolutionary and disruptive visions towards ultra-high capacity networks. White paper, Version, 1.

58. Jones, D., 1998. Navy Electricity and Electronics Training Series. Module 10-Introduction to Wave Propagation, Transmission Lines, and Antennas

59. Keusgen, W., Weiler, R.J., Peter, M., Wisotzki, M. and Göktepe, B., 2014, September. Propagation measurements and simulations for millimeter-wave mobile access in a busy urban environment. *The 39th International Conference on Infrared, Millimeter, and Terahertz waves (IRMMW-THz)* (pp. 1-3). IEEE.

60. Kaushal, H. and Kaddoum, G., 2017. Optical communication in space: Challenges and mitigation techniques. *IEEE Communications Surveys & Tutorials*, *19*(1), pp.57-96.

61. Kestwal, M.C., Joshi, S. and Garia, L.S., 2014. Prediction of rain attenuation and impact of rain in wave propagation at microwave frequency for tropical region (Uttarakhand, India). *International Journal of Microwave Science and Technology*, *2014*.

62. Kishore, K., 2009. *Antenna and wave propagation*. IK International Pvt Ltd.

63. Koh, C., 2004. The benefits of 60 GHz unlicensed wireless communications. YDI Wireless Whitepaper.

64. Liebe, H.J., Rosenkranz, P.W. and Hufford, G.A., 1992. Atmospheric 60-GHz oxygen spectrum: New laboratory measurements and line parameters. *Journal of quantitative spectroscopy and radiative transfer*, *48*(5-6), pp.629-643.

65. Lim, J., 2015. Is BER the bit error ratio or the bit error rate? EDN. Retrieved, pp.02-16.

66. Maher, R., Alvarado, A., Lavery, D. and Bayvel, P., 2016. Increasing the information rates of optical communications via coded modulation: a study of transceiver performance. *Scientific reports*, *6*.

67. Marcus, M. and Pattan, B., 2005. Millimetre wave propagation: spectrum management implications. *IEEE Microwave Magazine*, *6*(2), pp.54-62.

68. Markham, A., Trigoni, N. and Ellwood, S., 2010, July. Effect of rainfall on link quality in an outdoor forest deployment. In Wireless Information Networks and Systems (WINSYS), Proceedings of the 2010 International Conference on (pp. 1-6). IEEE.

69. Maruhashi, K., Ito, M., Desclos, L., Ikuina, K., Senba, N., Takahashi, N. and Ohata, K., 2000, February. Low-cost 60 GHz-band antenna-integrated transmitter/receiver modules utilizing multi-layer low-temperature co-fired ceramic technology. In *Solid-State Circuits Conference, 2000. Digest of Technical Papers. ISSCC. 2000 IEEE International* (pp. 324-325). IEEE.

70. McDonald, P.W. and Bowman, C.W., Remec BroadBand Wireless Llc, 2014. Transmission system of digital radio information using repeaters while minimizing data transfer latency. U.S. Patent 8,731,030.

71. Mertler, C.A. and Reinhart, R.V., 2016. *Advanced and multivariate statistical methods: Practical application and interpretation*. Routledge.

72. Mitra, M., 2005. Satellite Communication. PHI Learning Pvt. Ltd.

73. MiWaveS [Online] retrieved on 10th July from http://www.miwaves.eublue.

74. Miya, K (KDD, Japan). KDD Engineering & Consulting Inc., Tokyo, Japan, 1982. No. of pages: 442. *International Journal of Satellite Communications*, *1*(1), pp.60-60.

75. Newcombe, E.A. and Pasupathy, S., 1982. Error rate monitoring for digital communications. Proceedings of the IEEE, 70(8), pp.805-828.

76. Nie, S., MacCartney, G.R., Sun, S. and Rappaport, T.S., 2014, June. 28 GHz and 73 GHz signal outage study for millimeter wave cellular and backhaul communications. In *Communications (ICC), 2014 IEEE International Conference on* (pp. 4856-4861). IEEE.

77. Niu, Y., Gao, C., Li, Y., Su, L., Jin, D. and Vasilakos, A.V., 2015. Exploiting device-to-device communications in joint scheduling of access and backhaul for MMWave small cells. *IEEE Journal on Selected Areas in Communications*, *33*(10), pp.2052-2069.

78. OFCOM 2009, Release of the 59 – 64 GHz band retrieved on 14th August from https://www.ofcom.org.uk/__data/assets/pdf_file/0016/40516/statement.pdf

79. Proakis J, and Massoud S, 2007. Digital Communications, McGraw-Hill Education

80. Poole, I., 2006. *Cellular communications explained: from basics to 3G*. Elsevier.

81. Purkayastha, B.B. and Sarma, K.K., 2015. *A digital phase locked loop based signal and symbol recovery system for wireless channel*. Springer. Page 67

82. Rappaport, T.S., 1996. *Wireless communications: principles and practice* (Vol. 2). New Jersey: prentice hall PTR.

83. Rappaport, T.S, Rangan, S., and Erkip, E., 2014. Millimetre-wave cellular wireless networks: Potentials and challenges. *Proceedings of the IEEE*, *102*(3), pp.366-385

84. Recommendation, E.C.C., ECC/REC/(09)01. Use of the 57-64 GHz frequency band for point-to-point fixed wireless systems.

85. Rosenkranz, P., 1975. Shape of the 5 mm oxygen band in the atmosphere. *IEEE Transactions on Antennas and Propagation*, *23*(4), pp.498-506.

86. Sabri, N.H., Umar, R., Shafie, M.M., Zafar, S.N.A.S., Mat, R., Ahmad, S. and Ibrahim, Z.A., 2017. Correlation Analysis of Tropical Rainforest Climate Effect on Radio Signal Strength at KUSZA Observatory, Terengganu. *Advanced Science Letters*, *23*(2), pp.1268-1271.

87. Shannon, C.E., 1948. A mathematical theory of communication Reprinted with corrections from The Bell System Technical Journal, Vol. 27, pp. 379–423, 623–656

88. Simon, M.K., Hinedi, S.M. and Lindsey, W.C., 1995. *Digital communication techniques: signal design and detection*. Prentice Hall PTR.

89. Singh, S., Mudumbai, R. and Madhow, U., 2011. Interference analysis for highly directional 60-GHz mesh networks: The case for rethinking medium access control. IEEE/ACM Transactions on Networking (TON), 19(5), pp.1513-1527.

90. Simmons, L.D. and Ace, F.L., 1995. Electronics Technician, Volume 7-Antennas and Wave Propagation. *Pensacola, Florida: Naval Education and training Professional Development and Technology Centre*.

91. Sizun, H. and de Fornel, P., 2005. Radio wave propagation for telecommunication applications. Heidelberg: Springer.

92. Smith, E.W., 1981. Absorption and dispersion in the O2 microwave spectrum at atmospheric pressures. *The Journal of Chemical Physics*, *74*(12), pp.6658-6673.

93. Steele, R. and Webb, W.T., 1991. Variable rate QAM for data transmissions over Rayleigh fading channels.

94. Sutton A, 2016; Millimetre Wave Radio Systems - The Next Frontier. 46th European Microwave Conference

95. Sutton A, 2015; Microwave and millimetre-wave radio systems. The Journal Volume 9, part 2.

96. Titterton, D.H., 2015. Military laser technology and systems. Artech House.

97. Trivedi, S., Raeen, M.S. and Pawar, S.S., 2012. BER analysis of MIMO-OFDM system using BPSK modulation scheme. Channels, 7(8), p.9.

98. Van Vleck, J.H., 1934. Magnetic dipole radiation and the atmospheric absorption bands of oxygen. *The Astrophysical Journal*, *80*, p.161.

99. Van Vleck, J.H. and Weisskopf, V.F., 1945. On the shape of collision-broadened lines. *Reviews of Modern Physics*, *17*(2-3), p.227.

100.   Vihriala J, Ermolova N, Lahetkangas E, Tirkkonen O, Pajukoski K. On the waveforms for 5G mobile broadBand communications. In Vehicular Technology Conference (VTC Spring), 2015 IEEE 81st 2015 May 11 (pp. 1-5). IEEE.

101.   Wang, P., Li, Y., Song, L. and Vucetic, B., 2015. Multi-gigabit millimeter wave wireless communications for 5G: From fixed access to cellular networks. *IEEE Communications Magazine*, *53*(1), pp.168-178.

102.   Webb, W.T., 1992. QAM: the modulation scheme for future mobile radio communications. *Electronics & Communication Engineering Journal*, *4*(4), pp.167-176.

103.   Webb, W.T. and Steele, R., 1995. Variable rate QAM for mobile radio. *IEEE Transactions on Communications*, *43*(7), pp.2223-2230.

104.   Weiler, R.J., Peter, M., Keusgen, W., Calvanese-Strinati, E., De Domenico, A., Filippini, I., Capone, A., Siaud, I., Ulmer-Moll, A.M., Maltsev, A. and Haustein, T., 2014, June. Enabling 5G backhaul and access with millimeter-waves. In Networks and Communications (EuCNC), 2014 European Conference on (pp. 1-5). IEEE.

105.   Wells, J., 2009. Faster than fibre: The future of multi-G/s wireless. *IEEE microwave magazine*, *10*(3).

106.   Yang-Su, K. Jong-Ho, L. Joo-Hwan, and C. Yong-Seok, "Pathloss Measurement at 60Hz," retrieved on 20 September 2017 from https://www.researchgate.net/publication/265077134_PATHLOSS_MEASUREMENT_at_60_GHz

107.   Yong, S.K., Xia, P. and Valdes-Garcia, A., 2011. *60GHz Technology for Gbps WLAN and WPAN: from Theory to Practice*. John Wiley & Sons.

108.   Zheng, K., Zhao, L., Mei, J., Dohler, M., Xiang, W. and Peng, Y., 2015. 10 Gb/s hetsnets with millimeter-wave communications: access and networking-challenges and protocols. *IEEE Communications Magazine*, *53*(1), pp.222-231.

109.   Zhu, Y., Zhang, Z., Marzi, Z., Nelson, C., Madhow, U., Zhao, B.Y. and Zheng, H., 2014, September. Demystifying 60GHz outdoor picocells. In *Proceedings of the 20th annual international conference on Mobile computing and networking* (pp. 5-16). ACM.

110.   Ziemer, R. and Tranter, W.H., 2006. Principles of communications: system modulation and noise. John Wiley & Sons.

APPENDIX

Theoretical link design summary

Path Clearance

The link Path is very short and line-of-sight operation has been verified on site.

Propagation Performance

The radio hop will operate at a frequency close to a peak of atmospheric attenuation at 60GHz. However, the hop length is only 210m, so the additional atmospheric attenuation is quite low – less than 3dB. Preliminary calculations indicate that the link should function satisfactorily at modulation levels up to 256QAM. Hop fade margin for each modulation level is as follows:

256QAM:	12dB fade margin
128QAM:	15dB fade margin
64QAM:	19dB fade margin
32QAM:	21dB fade margin
16QAM:	24dB fade margin
4QAM:	35dB fade margin

Note* increased transmitter power in addition to improved receiver sensitivity at 4QAM.

General Equipment Performance

ITEM	SPECIFICATION
Frequency Range	59 ~ 63 GHz
Channel Spacing	50 MHz
T/R Spacing	2 GHz
Capacity	
LAN Throughput*	QSPK : 100 Mbps
	16QAM : 200 Mbps
*Note: Maximum throughput at 64-byte VLAN tagged frame passed rate base.	32QAM : 250 Mbps
	64QAM : 300 Mbps
	128QAM : 350 Mbps
	256QAM : 400 Mbps
DATA INTERFACES	
Ethernet	Option#1 : GbE/FE port (100/1000 Base-T(X)) 2 ports
	Option#2 : GbE/FE port (100/1000 Base-T(X)) 1 port
	SFP (1000Base-SX/LX) 1 port
	LCT: 10/100Base-T(X) 1 port
ENVIRONMENTAL	
Temperature, Operational	-33 C to +50 C (-40 C to +55 C workable)
Humidity, Operational	100% all-weather (IP-66)
Transportation / Storage	-40 C to + 70 C (ETSI EN300019-1-2 class2.3)
	-40 C to + 70 C (ETSI EN300019-1-1 class1.3)
EMC	EN300489-1, EN301489-4 classB
SAFETY	EN60950-1, EN60950-22, IEC6095022, UL60950 EN62479
POWER REQUIREMENT	
Input Voltage	PoE (802.3at type2)
Power Consumption	25 watts typ.
MECHANICAL	
Dimensions (W x H x D)	230 x 230 x 104mm
Weight	Approx. 5kg

Predicted Propagation Performance

256QAM Modulation (320Mbit/s radio transmission capacity)

	Salford Site 1	Salford Site 2	
Elevation (m)	32.11	38.39	
Latitude	53 29 07.63 N	53 29 08.89 N	
Longitude	002 16 16.32 W	002 16 25.33 W	
True azimuth (°)	283.19	103.19	
Vertical angle (°)	2.11	-2.11	
Antenna model	iPasoSx Integral	iPasoSx Integral	
Antenna height (m)	10.00	10.00	
Antenna gain (dBi)	37.00	37.00	**37dBi Antenna**
Frequency (MHz)	60000.00		**60GHz band**
Polarization	Vertical		
Path length (km)	0.21		**210m hop**
Free space loss (dB)	112.67		
Atmospheric absorption loss (dB)	2.59		**2.5dB atmospheric attenuation**
Field margin (dB)	3.00		
Net path loss (dB)	44.27	44.27	
Radio model	iPaso SX 256Q	iPaso SX 256Q	**iPasolinkSx - 4QAM Modulation**
TX power (watts)	6.31e-04	6.31e-04	
TX power (dBm)	-2.00	-2.00	
EIRP (dBm)	35.00	35.00	
RX threshold criteria	BER 1E-6	BER 1E-6	
RX threshold level (dBm)	-58.50	-58.50	
RX signal (dBm)	-46.27	-46.27	
Thermal fade margin (dB)	12.23	12.23	
Geoclimatic factor	5.32E-05		
Path inclination (mr)	36.76		
Fade occurrence factor (Po)	4.20E-09		
Average annual temperature (°C)	10.00		
Worst month - multipath (%)	100.00000	100.00000	
(sec)	6.59e-04	6.59e-04	
Annual - multipath (%)	100.00000	100.00000	
(sec)	1.98e-03	1.98e-03	

(% - sec)	100.00000 - 0.00	
0.01% rain rate (mm/hr)	34.00	
Flat fade margin - rain (dB)	12.23	**12dB flat fade margin**
Rain attenuation (dB)	12.23	
Annual rain (%-sec)	100.00000 - 0.76	
Annual multipath + rain (%-sec)	100.00000 - 0.76	

Average annual availability (rain and atmospheric multipath fading) - >99.995%

4QAM Modulation (80Mbit/s radio transmission capacity)

	Salford Site 1	Salford Site 2	
Elevation (m)	32.11	38.39	
Latitude	53 29 07.63 N	53 29 08.89 N	
Longitude	002 16 16.32 W	002 16 25.33 W	
True azimuth (°)	283.19	103.19	
Vertical angle (°)	2.11	-2.11	
Antenna model	iPasoSx Integral	iPasoSx Integral	
Antenna height (m)	10.00	10.00	
Antenna gain (dBi)	37.00	37.00	**37dBi Antenna**
Frequency (MHz)	60000.00		**60GHz band**
Polarization	Vertical		
Path length (km)	0.17		**170m hop**
Free space loss (dB)	112.67		
Atmospheric absorption loss (dB)	2.59		**2.5dB atmospheric attenuation**
Field margin (dB)	3.00		
Net path loss (dB)	44.27	44.27	
Radio model	iPaso SX 4Q	iPaso SX 4Q	**iPasolink Sx - 4QAM Modulation**
TX power (watts)	2.00e-03	2.00e-03	
TX power (dBm)	3.00	3.00	
EIRP (dBm)	40.00	40.00	
RX threshold criteria	BER 1E-6	BER 1E-6	
RX threshold level (dBm)	-76.50	-76.50	
RX signal (dBm)	-41.27	-41.27	

Thermal fade margin (dB)	35.23	35.23
Geoclimatic factor	5.32E-05	
Path inclination (mr)	36.76	
Fade occurrence factor (Po)	4.20E-09	
Average annual temperature (°C)	10.00	
Worst month - multipath (%)	100.00000	100.00000
(sec)	3.30e-06	3.30e-06
Annual - multipath (%)	100.00000	100.00000
(sec)	9.91e-06	9.91e-06
(% - sec)	100.00000 - 0.00	
0.01% rain rate (mm/hr)	34.00	
Flat fade margin - rain (dB)	35.23	**35dB flat fade margin**
Rain attenuation (dB)	35.23	
Annual rain (%-sec)	100.00000 - 0.00	
Annual multipath + rain (%-sec)	100.00000 - 0.00	

Average annual availability (rain and atmospheric multipath fading) - >99.995%

Capacity Menu

Channel Separation	50 MHz	50 MHz
Modulation Scheme	Throughput (Mbps)*	Radio Capacity (Mbps)
QSPK	100	80
16QAM	200	160
32QAM	250	200
64QAM	300	240
128QAM	350	280
256QAM	400	320

*Note: Maximum throughput at 64-byte VLAN tagged frame passed rate base.

Modulation Level (QAM)	Bit/Symbol	Increment Capacity Gain
4 QPSK	2	-
8	3	50%
16	4	33%
32	5	25%
64	6	20%
128	7	17%
256	8	14%

Modulation characteristics
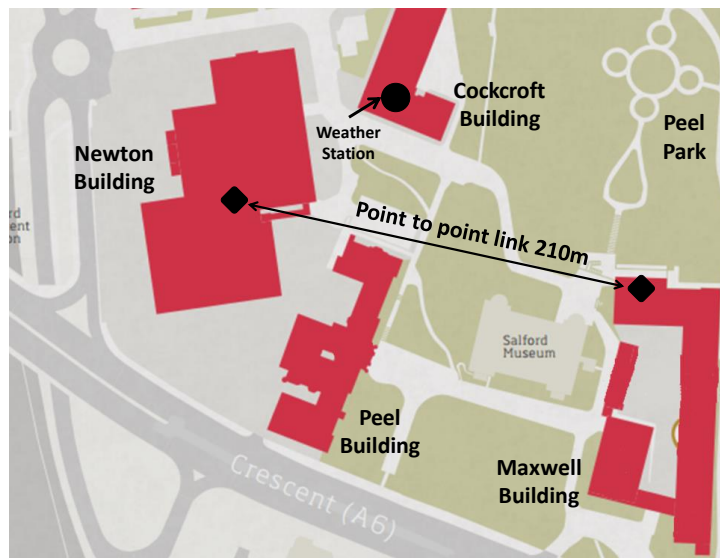
Figure 7.2.1.1 Link testbed site across the campus

Descriptive Statistics

	N	Range	Minimum	Maximum	Mean	Std. Deviation	Variance
RPL	44562	8.05	-.74	7.31	1.4969	.47595	.227
Rain Rate	44562	60.00	.00	60.00	.1139	1.28501	1.651
timestamp	44562	30 23:58:59	01-AUG-17	31-AUG-17	16-AUG-17	8 22:47:39.824	
Valid N (listwise)	44562						

Descriptive Statistics

	N	Range	Minimum	Maximum	Mean	Std. Deviation	Variance
timestamp	43095	29 23:59:00	01-SEP-17	30-SEP-17	16-SEP-17	8 15:53:22.232	
Path Loss	43095	8.10	115.50	123.60	116.3375	.62481	.390
Rain Rate	43095	60.0	.0	60.0	.165	1.5060	2.268
Valid N (listwise)	43095						

Descriptive Statistics

	N	Range	Minimum	Maximum	Mean	Std. Deviation	Variance
timestamp	43095	29 23:59:00	01-SEP-17	30-SEP-17	16-SEP-17	8 15:53:22.232	
RPL	43095	9.56	-.69	8.88	1.4241	.63658	.405
Rain Rate	43095	60.0	.0	60.0	.165	1.5060	2.268
Valid N (listwise)	43095						

Descriptive Statistics

	N	Range	Minimum	Maximum	Mean	Std. Deviation	Variance
timestamp	43588	30 22:59:00	01-OCT-17	31-OCT-17	16-OCT-17	9 00:38:28.727	
Path Loss	43588	7.50	115.60	123.10	116.3267	.61236	.375
Rain Rate	43588	48	0	48	.16	1.464	2.143
Valid N (listwise)	43588						

Descriptive Statistics

	N	Range	Minimum	Maximum	Mean	Std. Deviation	Variance
timestamp	43588	30 22:59:00	01-OCT-17	31-OCT-17	16-OCT-17	9 00:38:28.727	
RPL	43588	9.53	-1.47	8.06	1.3077	.64020	.410
Rain Rate	43588	48	0	48	.16	1.464	2.143
Valid N (listwise)	43588						

Descriptive Statistics

	N	Range	Minimum	Maximum	Mean	Std. Deviation	Variance
timestamp	40222	29 23:58:59	01-NOV-17	30-NOV-17	16-NOV-17	8 14:30:34.297	
Path Loss	40222	6.80	115.70	122.50	116.4452	.49769	.248
Rain Rate	40222	48.00	.00	48.00	.1265	1.26000	1.588
Valid N (listwise)	40222						

Descriptive Statistics

	N	Range	Minimum	Maximum	Mean	Std. Deviation	Variance
timestamp	40222	29 23:58:59	01-NOV-17	30-NOV-17	16-NOV-17	8 14:30:34.297	
RPL	40221	7.92	-1.29	6.63	.8222	.62695	.393
Rain Rate	40222	48.00	.00	48.00	.1265	1.26000	1.588
Valid N (listwise)	40221						

Descriptive Statistics

	N	Range	Minimum	Maximum	Mean	Std. Deviation	Variance

	N	Range	Minimum	Maximum	Mean	Std. Deviation	Variance
timestamp	44419	30 23:58:59	01-DEC-17	31-DEC-17	16-DEC-17	8 22:35:44.453	
Path Loss	44419	7.20	115.80	123.00	116.5131	.53351	.285
Rain (mm/hr)	44419	36	0	36	.17	1.417	2.009
Valid N (listwise)	44419						

Descriptive Statistics

	N	Range	Minimum	Maximum	Mean	Std. Deviation	Variance
timestamp	44419	30 23:58:59	01-DEC-17	31-DEC-17	16-DEC-17	8 22:35:44.453	
RPL	44419	8.17	-1.32	6.85	.6584	.61671	.380
Rain (mm/hr)	44419	36	0	36	.17	1.417	2.009
Valid N (listwise)	44419						

Descriptive Statistics

	N	Range	Minimum	Maximum	Mean	Std. Deviation	Variance
timestamp	39413	30 23:58:50	01-JAN-18	31-JAN-18	15-JAN-18	9 07:41:23.508	
Path Loss	39413	6.50	115.70	122.20	116.4962	.53936	.291
Rain Rate	39413	48.00	.00	48.00	.1559	1.39334	1.941
Valid N (listwise)	39413						

Descriptive Statistics

	N	Range	Minimum	Maximum	Mean	Std. Deviation	Variance
timestamp	39413	30 23:58:50	01-JAN-18	31-JAN-18	15-JAN-18	9 07:41:23.508	
RPL	39413	8.54	-.58	7.97	.7830	.66208	.438
Rain Rate	39413	48.00	.00	48.00	.1559	1.39334	1.941
Valid N (listwise)	39413						

Descriptive Statistics

	N	Range	Minimum	Maximum	Mean	Std. Deviation	Variance
timestamp	39501	27 13:03:00	01-FEB-18	28-FEB-18	14-FEB-18	7 22:41:24.168	
Path Loss	39501	7.00	115.70	122.70	116.5115	.44570	.199
Rain Rate	39501	12	0	12	.07	.893	.798
Valid N (listwise)	39501						

Descriptive Statistics

	N	Range	Minimum	Maximum	Mean	Std. Deviation	Variance
timestamp	39501	27 13:03:00	01-FEB-18	28-FEB-18	14-FEB-18	7 22:41:24.168	
RPL	39501	7.77	-1.39	6.38	.4013	.59656	.356
Rain Rate	39501	12	0	12	.07	.893	.798
Valid N (listwise)	39501						

Descriptive Statistics

	N	Range	Minimum	Maximum	Mean	Std. Deviation	Variance
timestamp	39655	29 23:59:00	01-APR-2018	30-APR-2018	16-APR-2018	8 17:48:29.106	
Path Loss	39655	6.30	115.50	121.80	116.3712	.53988	.291

	N	Range	Minimum	Maximum	Mean	Std. Deviation	Variance
Rain Rate mm/hr	39655	36.00	.00	36.00	.1377	1.34462	1.808
Valid N (listwise)	39655						

Descriptive Statistics

	N	Range	Minimum	Maximum	Mean	Std. Deviation	Variance
timestamp	39655	29 23:59:00	01-APR-2018	30-APR-2018	16-APR-2018	.106	
RPL	39655	5.95	-.70	5.25	1.0845	.54875	.301
Rain Rate mm/hr	39655	36.00	.00	36.00	.1377	1.34462	1.808
Valid N (listwise)	39655						

Descriptive Statistics

	N	Range	Minimum	Maximum	Mean	Std. Deviation	Variance
timestamp	44142	30 23:57:59	01-MAY-18	31-MAY-18	16-MAY-18	8 22:41:33.580	
Path Loss	44142	5.60	115.40	121.00	116.2289	.33972	.115
Rain Rate	44142	24	0	24	.04	.705	.497
Valid N (listwise)	44142						

Descriptive Statistics

	N	Range	Minimum	Maximum	Mean	Std. Deviation	Variance
timestamp	44142	30 23:57:59	01-MAY-18	31-MAY-18	16-MAY-18	8 22:41:33.580	
RPL	44142	6.81	-.29	6.51	1.3408	.43097	.186
Rain Rate	44142	24	0	24	.04	.705	.497
Valid N (listwise)	44142						

Descriptive Statistics

	N	Range	Minimum	Maximum	Mean	Std. Deviation	Variance
timestamp	42541	29 23:57:00	01-JUN-18	30-JUN-18	15-JUN-18	8 15:14:55.042	
Path Loss	42541	7.30	115.40	122.70	116.1566	.25126	.063
Rain Rate	42541	36.00	.00	36.00	.0163	.51326	.263
Valid N (listwise)	42541						

Descriptive Statistics

	N	Range	Minimum	Maximum	Mean	Std. Deviation	Variance
timestamp	42541	29 23:57:00	01-JUN-18	30-JUN-18	15-JUN-18	8 15:14:55.042	
RPL	42541	7.38	.23	7.61	1.5292	.34011	.116
Rain Rate	42541	36.00	.00	36.00	.0163	.51326	.263
Valid N (listwise)	42541						

	N	Range	Minimum	Maximum	Mean	Std. Deviation	Variance
Path Loss	44562	7.20	115.50	122.70	116.2325	.51112	.261
Rain Rate	44562	60.00	.00	60.00	.1139	1.28501	1.651
timestamp	44562	30 23:58:59	01-AUG-17	31-AUG-17	16-AUG-17	8 22:47:39.824	
Valid N (listwise)	44562						

Descriptive Statistics

	N	Range	Minimum	Maximum	Mean	Std. Deviation	Variance
timestamp	735	30 22:59:00	01-JUL-18	31-JUL-18	16-JUL-18	8 22:46:21.547	
Path Loss	735	5.20	115.50	120.70	116.1524	.43697	.191
Rain Rate mm/hr	735	12	0	12	.03	.626	.391
Valid N (listwise)	735						

Descriptive Statistics

	N	Range	Minimum	Maximum	Mean	Std. Deviation	Variance
timestamp	735	30 22:59:00	01-JUL-18	31-JUL-18	16-JUL-18	8 22:46:21.547	
RPL	735	5.15	.93	6.07	1.7237	.43770	.192
Rain Rate mm/hr	735	12	0	12	.03	.626	.391
Valid N (listwise)	735						